Tbx1 functions in pharyngeal arch and cardiovascular development

Thesis

Dr. Caprio Cinzia

Doctor of Philosophy in Human Genetics

Tbx1 functions in pharyngeal arch and cardiovascular development

The Open University, Milton Keynes (UK)

ARC: Telethon Institute of Genetics and Medicine (TIGEM), Naples (IT)

Director of Studies
Prof Brunella Franco

Supervisors
Prof Antonio Baldini
Dr Suzanne Dietrich

31 January 2014

DATE OF SUBMISSION: 30 JANUARY 2014
DATE OF AWARD: 8 JULY 2014

Alla mia famiglia...

جده مرحبا

TABLE OF CONTENTS

ABSTRACT Pag. 8

CHAPTER 1 – INTRODUCTION AND BACKGROUND Pag. 9

1.1) Genetic basis of the DiGeorge Syndrome Pag. 9

1.2) Mapping causative genes Pag. 12

1.3) Tbx1 and the T-box family Pag. 17

1.4) *Tbx1* expression pattern Pag. 18

1.5) The development of PAAs and their derivatives Pag. 20

1.6) The role of *Tbx1* gene during PAAs development Pag. 29

1.7) The development of the cardiac OFT Pag. 35

1.8) The role of *Tbx1* gene during cardiac OFT development Pag. 41

1.9) p53: not only a tumor suppressor Pag. 45

1.10) p53 and development in the context of other genetic deficiencies Pag. 46

CHAPTER 2 – AIM OF THE RESEARCH PROJECT Pag. 49

2.1) To establish the effect of *Tbx1* on the cell proliferation Pag. 49

2.2) Rescue strategies in a mouse model of DiGeorge syndrome Pag. 49

CHAPTER 3 – MATERIALS AND METHODS Pag. 51

3.1) Mouse mutant lines, breeding and genotyping Pag. 51

3.2) Culture and in vitro transfection of mES cells and C2C12 myoblasts Pag. 52

3.3) Culture and differentiation of P19CL6 cell line Pag. 52

3.4) Silencing of *Trp53* by siRNA Pag. 53

3.5) Cell cycle analysis and Proliferation assay Pag. 53

3.6) RNA extraction, reverse transcription and q real-time PCR Pag. 54

3.7) Ink injection and histological staining Pag. 55

3.8) Immunohistochemistry Pag. 56

3.9) Western blotting Pag. 57

3.10) Co-immunoprecipitation Pag. 57

3.11) Chromatin Immunoprecipitation (ChIP) Pag. 58

3.12) ChIP and Western blotting Pag. 60

3.13) Cloning, plasmids Pag. 60

3.14) Luciferase assay Pag. 61

CHAPTER 4 – RESULTS Pag. 62

4.1) Tbx1-enhanced cell proliferation is associated with down regulation of *p21* and *p27* expression in cultured cells Pag. 62

4.2) Epistatic genetic interaction between *Trp53* and *Tbx1* Pag. 66

4.3) p53 temporary pharmacological inhibition rescues the *Tbx1* haploinsufficiency phenotype Pag. 68

4.4) *Trp53* mutation modifies the hypomorphic but not the null *Tbx1* phenotype Pag. 69

4.5) *Trp53* ablation rescues the proliferation defect in a $Tbx1^{+/neo2}$ background Pag. 74

4.6) Tbx1 and p53 proteins co-occupy chromatin segments Pag. 75

4.7) The *Gbx2* gene is down regulated in *Tbx1*$^{+/-}$ embryos and rescued by *Trp53* mutation Pag. 77

4.8) A DNA fragment adjacent to the *Gbx2* gene is occupied by both Tbx1 and p53 transcription factors Pag. 80

4.9) The DNA fragment occupied by Tbx1 and p53 is sensitive to p53 dosage in a luciferase reporter assay Pag. 84

CHAPTER 5 – DISCUSSION Pag. 87

REFERENCES Pag. 97

ACKNOWLEDGMENTS Pag. 116

FIGURE INDEX

Fig. 1 *Human 22q11 deleted region.* Pag. 12

Fig. 2 *The mouse chromosome 16 region that is syntenic with 22q11.2.* Pag. 13

Fig. 3 *Cardiovascular defects in mutant embryos.* Pag. 14

Fig. 4 *Tbx1 expression in early mouse embryogenesis.* Pag. 16

Fig. 5 *Scanning electron microscopy (SEM) images of vascular casts of mouse embryos late in E8.5-E9 (12-somite stage, A) and early and late in E9-E9.5 (15-16-somite stage, B).* Pag. 21

Fig. 6 *SEM images of vascular casts of mouse embryos in the middle (25-somite stage, A) and late (27-somite stage, B) parts of E9.5-E10.* Pag. 22

Fig. 7 *SEM images of vascular casts of mouse embryos at E10 (32-somite stage, A-B; 34-somite stage, C).* Pag. 23

Fig. 8 *SEM images of vascular casts of mouse embryo at E11.* Pag. 25

Fig. 9 *SEM images of the vascular casts of mouse embryos at E11.5 (A) and E12 (B, C).* Pag. 26

Fig. 10 *SEM images of vascular casts of mouse embryos at E12.5 (A) and E13 (B,C).* Pag. 28

Fig. 11 *Tbx1 expression in the pharyngeal region.* Pag. 31

Fig. 12 *Topography of the second heart field.* Pag. 36

Fig. 13 *The regulation of second heart field development.* Pag. 38

Fig. 14 *A clinically relevant subdomain of the second heart field.* Pag. 40

Fig. 15 *Development of the ROSA-TET system and induction of expression in that.* Pag. 63

Fig. 16 *Tbx1 enhances cell cycle.* Pag. 64

Fig. 17 *Tbx1 enhances cell proliferation and suppresses cell cycle inhibitors expression in cultured cells.* Pag. 65

Fig. 18 *Trp53 deletion rescues the 4th PAA defects in Tbx1$^{+/-}$ embryos.* Pag. 68

Fig. 19 *Trp53 ablation in a Tbx1 null background causes severe cardiovascular abnormalities as in Tbx1$^{-/-}$ embryos.* Pag. 70

Fig. 20 *Trp53 deletion ameliorates the outflow tract phenotype in Tbx1 hypomorphic mutants.* Pag. 71

Fig. 21 *Trp53 deletion ameliorates the outflow tract phenotype in Tbx1 hypomorphic mutants at E18.5.* Pag. 73

Fig. 22 *Trp53 ablation rescues cardiac precursors proliferation defects in Tbx1$^{+/neo2}$ background.* Pag. 75

Fig. 23 *Molecular analyses of Trp53-Tbx1 interaction.* Pag. 76

Fig. 24 *Trp53 deletion rescues the Gbx2 expression down regulation in Tbx1$^{+/-}$ E8.5 embryos.* Pag. 79

Fig. 25 *p53 and Tbx1 occupy a DNA segment adjacent to the Gbx2 gene.* Pag. 81

Fig. 26 *Gbx2 expression during cardiomyocyte differentiation of P19CL6 cells.* Pag. 82

Fig. 27 *Trp53 knockdown during cardiomyocyte differentiation of P19CL6 cells.* Pag.84

Fig. 28 *Gbx2 has a conserved p53 binding element (p53BE) that is required for response to p53 in luciferase assays.* Pag. 86

Fig. 29 *Schematic model of Gbx2 regulation.* Pag. 95

LIST OF ABBREVIATIONS

AO Aorta

CHARGE Coloboma of the eye, Heart defects, Atresia of the choanae, Retardation of growth and/or development, Genital and/or urinary abnormalities, and Ear abnormalities and deafness

CHD Congenital heart defect

cNCCs Cardiac neural crest cells

DGS DiGeorge syndrome

DORV Double outlet right ventricle

E Embryonic day

IAA-B Interrupted aortic arch type B

LCR Low copy repeat

mESC Mouse embryonic stem cell

OFT Outflow tract

PAA Pharyngeal arch artery

PFT Pifithrin

PSE Pharyngeal surface ectoderm

PT Pulmonary trunk

PTA Persistent truncus arteriosus

RA Retinoic acid

RAR Retinoic acid receptor

RARE Retinoic acid responsive element

RSA Right subclavian artery

SHF Second heart field

TAC Truncus arteriosus communis

TBE T-box binding element

VSD Ventricular septal defect

ABSTRACT

Tbx1, a gene encoding a T-box transcription factor, is required for embryonic development in humans and mice. Half dosage of this gene causes most of the features of the DiGeorge or Velocardiofacial syndrome phenotypes, including aortic arch and cardiac outflow tract abnormalities. Here we show that genetic ablation of *Trp53* or pharmacological inhibition of its protein product p53 rescues almost completely aortic arch defects and significantly ameliorates outflow tract defects of *Tbx1* mouse mutants. *Trp53* deletion rescues the cell proliferation deficit in the second heart field of *Tbx1* mutants. In addition, and surprisingly, Tbx1 and p53 proteins can be found on neighboring sites on chromatin, suggesting that they share a set of target genes. In a search for shared targets, we found that the expression of *Gbx2*, a gene that interacts with *Tbx1* during development of the aortic arch arteries, is down regulated by *Tbx1* heterozygosity and rescued by *Trp53* heterozygosity. In addition, Tbx1 and p53 occupy the *Gbx2* gene, indicating that both contribute to its regulation.

Overall our data identify unexpected interactions between *Tbx1* and *Trp53* and provide a proof of principle that developmental defects associated with reduced dosage of *Tbx1* can be rescued pharmacologically.

1.1 *Genetic basis of the DiGeorge Syndrome*

The term "genomic disorders" refers to those diseases that are caused by chromosomal rearrangements involving large regions of one to several megabase pairs (Lupski 1998). Chromosomal rearrangements can result in interstitial or terminal deletions or duplications, as well as unbalanced translocations, and all of these consequences may subsequently result in imbalanced gene dosage. Each of these rearrangements occurs sporadically in the population and therefore represents the product of *de novo* mutations. Most of the rearrangements are associated with both congenital malformations and mental retardation. Therefore, genomic disorders have a large impact on human health.

The 22q11 region serves as a model for genomic disorders because it is particularly susceptible to chromosomal rearrangements, leading to three different congenital malformation syndromes.

In the late '60s, Angelo DiGeorge described a syndrome characterized by aberrant development of the thymus and parathyroid (DiGeorge AM, 1968). The phenotypic spectrum of DiGeorge syndrome (DGS) has since been extended to include many organs and clinical characteristics, including growth retardation, psychiatric disorders and congenital heart disease; the latter being the most dramatic feature and most common cause of death.

The 22q11.2 deletion has been identified in the majority of patients with DiGeorge syndrome (de la Chapelle, Herva et al. 1981; Kelley, Zackai et al. 1982; Scambler, Carey et al. 1991; Driscoll, Budarf et al. 1992), Velocardiofacial syndrome (Driscoll, Spinner et al. 1992; Driscoll, Salvin et al. 1993) and Conotruncal Anomaly Face syndrome (Burn, Takao et al. 1993; Matsuoka, Takao et al. 1994). Originally described as individual entities by a number of subspecialists who were concentrating on one particular area of interest, following the widespread use of fluorescence in situ hybridization (FISH), these syndromes are now

collectively referred to by their chromosomal etiology the 22q11.2 deletion syndrome (22q11.2DS) (McDonald-McGinn, Emanuel et al. 1996). The 22q11.2DS is the most common microdeletion syndrome with an estimated incidence of 1 in 4,000 live births. In most cases, the deletion occurs *de novo*, but in about 10% of cases it is inherited from a mildly affected parent (Scambler 2000), thus behaving as an autosomal-dominant trait.

22q11.2DS is caused by heterozygous deletions in the chromosome region 22q11.2. It has been proposed that deletion may result from aberrant homologous recombination between low copy repeat (LCR) sequences that flank the deleted region (Edelmann, Pandita et al. 1999; Shaikh, Kurahashi et al. 2000). LCRs might confer instability to the region by mediating aberrant homologous recombination and unequal crossing over events during meiosis due to high sequence similarity between the repeat segments, thereby generating chromosomal rearrangements of a uniform and predictable size (Shaikh, Kurahashi et al. 2000).

The majority of patients (85%) have a common 3 megabases (Mb) deletion encompassing 30 genes, and ≈8% has an 1.5 Mb nested deletion encompassing 24 genes (Fig. 1) (Lindsay, Goldberg et al. 1995; Shaikh, Kurahashi et al. 2000). 22q11.2DS can be associated with a broad phenotype, but the most characteristic features are congenital heart disease and thymic and parathyroid aplasia or hypoplasia. This syndrome is characterized by neonatal hypocalcemia, which may present as tetany or seizures, due to hypoplasia of the parathyroid glands, and susceptibility to infection due to a deficit of T cells. The immune deficit is caused by hypoplasia or aplasia of the thymus gland. A variety of cardiac malformations are seen in particular affecting the outflow tract; these include tetralogy of Fallot, type B interrupted aortic arch, truncus arteriosus, right aortic arch and aberrant right subclavian artery.

Other common findings are facial anomalies. In infancy, micrognathia may be present; the ears are typically low set and deficient in the vertical diameter with abnormal folding of the pinna; telecanthus with short palpebral fissures is seen; both upward and downward slanting eyes have been described; the philtrum is short and the mouth relatively small.

Short stature, renal anomalies, skeletal anomalies and variable mild to moderate learning difficulties are common. A variety of psychiatric disorders have been described in a small proportion of adult cases of velocardiofacial syndrome. These have included paranoid schizophrenia and major depressive illness. Clinical features seen more rarely include hypothyroidism, cleft lip, and deafness.

Most features show variable expressivity and penetrance. In addition to having physical malformations, most affected children have learning disabilities and behavioral disorders (Swillen, Devriendt et al. 1999). Adults with this syndrome develop major psychiatric illnesses, including schizophrenia and bipolar disorder (Chow, Bassett et al. 1994; Pulver, Nestadt et al. 1994; Papolos, Faedda et al. 1996; Murphy, Jones et al. 1999; Shprintzen 2000; Murphy and Owen 2001).

The prognosis for 22q11.2DS varies widely, depending largely on the nature and degree of involvement of different organs, and many adults live long and productive lives.

The most common cause of mortality in 22q11.2DS is a congenital heart defect and the second most common is severe immune deficiency. Mortality is higher in infancy because of the severity of these 2 conditions. Infants with thymus aplasia present with severe immunodeficiency and typically die of sepsis, which usually results from bacterial or fungal infections.

In a large European collaborative study, 558 patients with 22q11.2DS were evaluated using a questionnaire (Ryan, Goodship , et al. 1997). Eight percent of the patients died, with more than half of the deaths occurring within the first month of life and the majority happening within 6 months of birth. Of the patients who survived, 62% had only mild learning problems or were developmentally normal. All but one of the deaths was attributable to congenital heart disease.

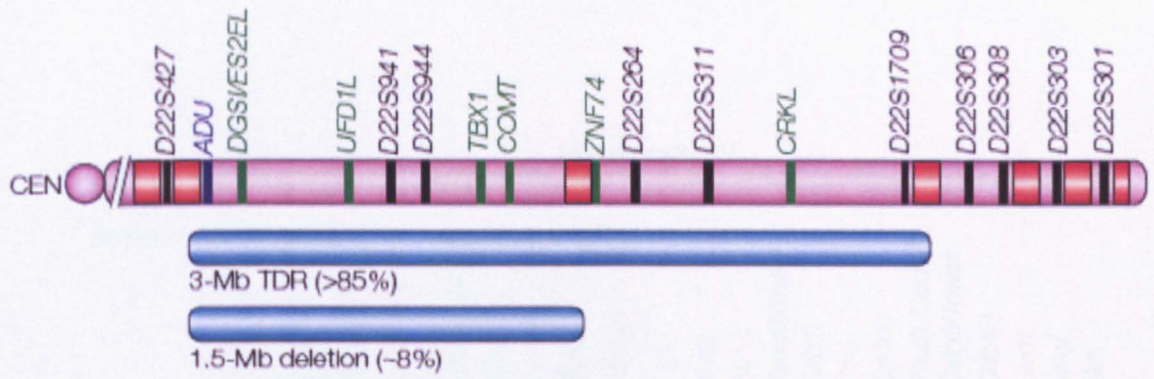

Figure 1: ***Human 22q11 deleted region.*** The 22q11 deleted region on human chromosome 22, on which selected genes (green) and molecular markers (black) that have been used to characterize patient deletions are shown. Red blocks represent low-copy repeats (LCRs). ADU (blue) is a patient with DiGeorge syndrome and a balanced chromosomal translocation. The common 3 Mb typically deleted region (TDR), which is present in more than 85% of 22q11 deleted patients and the 1.5 Mb deletion are shown (turquoise) (Lindsay 2001).

1.2 *Mapping causative genes*

Identifying the genes that underlie the pathogenesis of chromosome deletion and duplication syndromes is a challenge because the affected chromosomal segment can contain many genes. Creating chromosomal rearrangements that include or exclude given sets of genes in an experimental model is a way to resolve the genetics of these genomic disorders. This has been the strategy of several groups, whose research focuses on unravelling the molecular genetics of the 22q11.2DS.

Several researchers have used the mouse as a model to study the 22q11.2DS, since there is a strong homology between a region on mouse chromosome 16 and the region on human chromosome 22 (Fig. 2) (Scambler 2000). Using chromosome-engineering strategies, three research groups generated deletions in mice that encompassed subsets of the genes deleted in patients with 22q11.2DS (Lindsay, Botta et al. 1999).

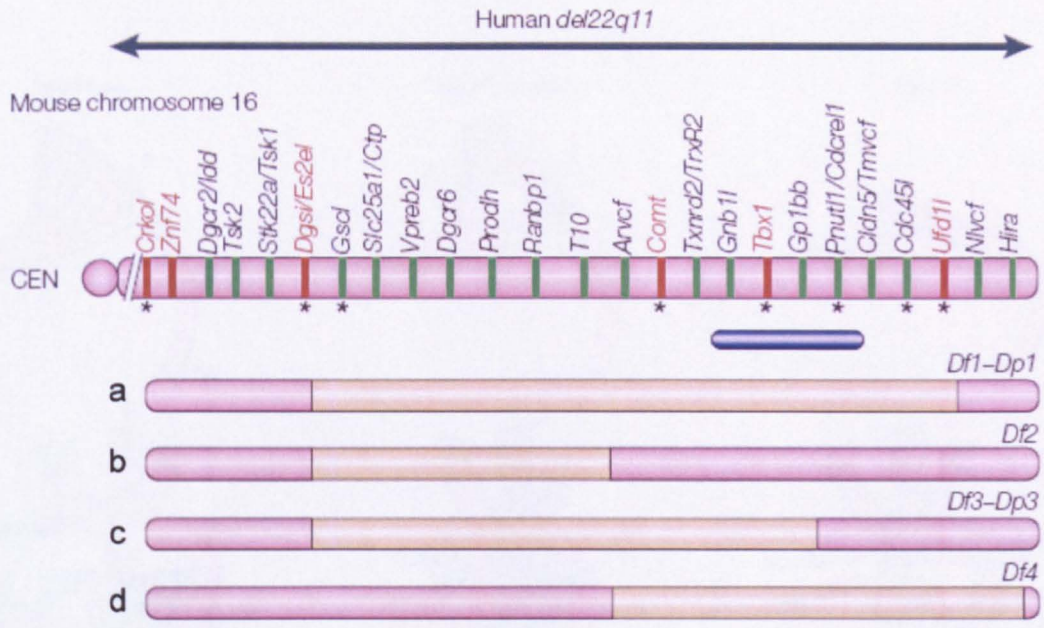

Figure 2: ***The mouse chromosome 16 region that is syntenic with 22q11.2.*** The gene content of the region deleted in 22q11.2DS patients is highly conserved in the mouse genome, although several ancestral rearrangements have led to changes in gene order between the two species. Mouse mutants have been reported for the genes that are marked with an asterisk. (a-d) Mouse chromosome 16 deletion mutants that have been made by different groups. Yellow indicates deleted or duplicated, and purple indicates non-deleted or non-duplicated, chromosome segments. The blue bar shows the extent of a transgene that rescues cardiovascular defects in *Df1/+* mutant(Lindsay 2001).

The first generated mouse deletion was named *Df1 (Lindsay, Botta et al. 1999)*, which encompassed mouse homologues of 18 out of the 24 genes that are deleted in patients with the 1.5 Mb deletion (Fig. 2). Mice carrying one copy of the deleted chromosome (*Df1/+)* had cardiovascular defects similar to those seen in human patients (Fig. 3). Furthermore, the cardiovascular defects could be corrected in mice that were bred to carry the *Df1* deletion on one chromosome 16, and a reciprocal duplication (*Dp1*) on the other, which restored normal

gene dosage. This genetic-rescue experiment showed that a gene(s) within the *Df1* region is involved in heart development and is haploinsufficient in these mutant mice.

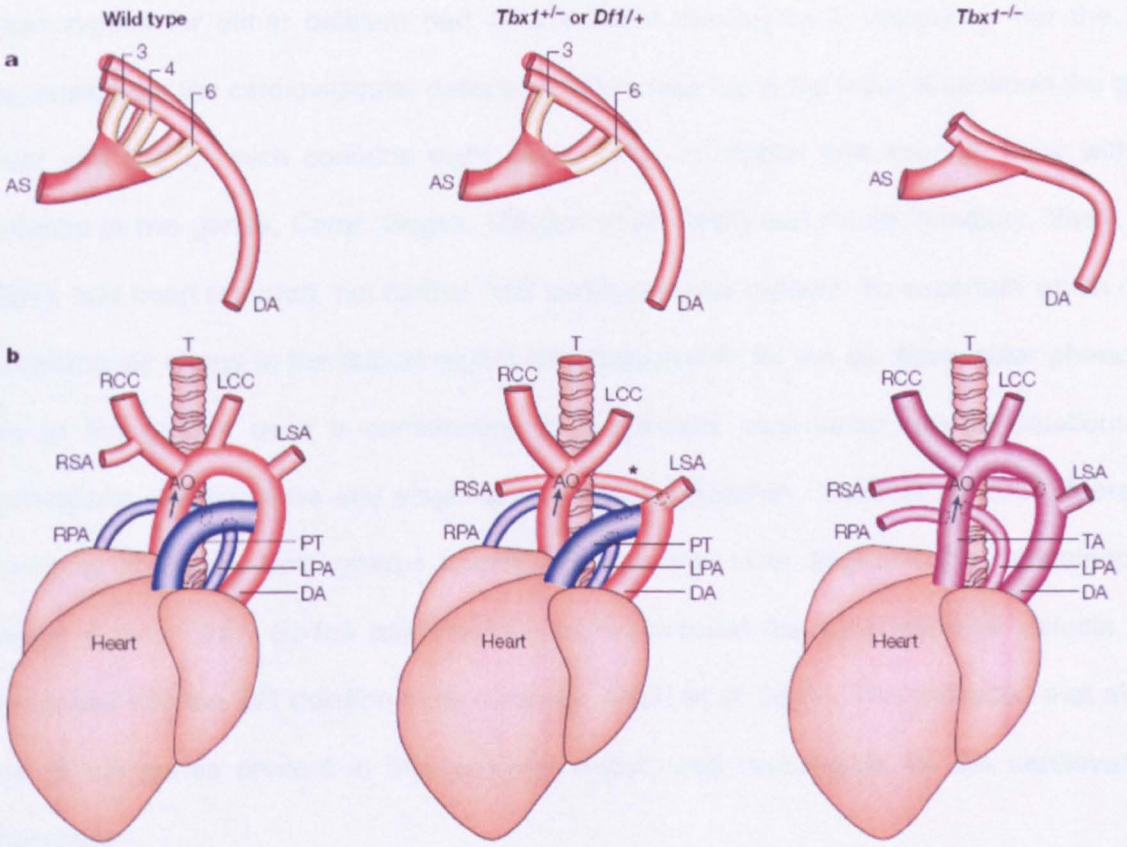

Figure 3: ***Cardiovascular defects in mutant embryos.*** (a) At embryonic day (E) 10.5, *Tbx1*$^{+/-}$ embryos and *Df1/+* embryos have abnormally small or absent fourth aortic-arch arteries. In *Tbx1*$^{-/-}$ embryos, there is no development of the pharyngeal apparatus distal to arch two. As a result, arch arteries three to six do not form, and the aortic sac (AS) connects directly with the dorsal aorta (DA). (b) In near-term embryos (E18.5), *Tbx1*$^{+/-}$ embryos and *Df1/+* embryos have abnormalities in the structures that derive from the fourth aortic-arch arteries, which are the root of the right common carotid (RCC) and a segment of the aortic arch. The resultant abnormalities include aberrant right subclavian artery (RSA), which originates from the aortic arch instead of from the RCC, and an interrupted aortic arch (asterisk). *Tbx1*$^{-/-}$ embryos have persistent truncus arteriosus (PTA), in which a single vessel exits the heart instead of the normal two, the aorta (AO) and pulmonary trunk (PT). Blue and red vessels indicate pulmonary and aortic arterial flow, respectively. Purple indicates that in the presence of the PTA abnormality, blood from both sides of the heart is mixed. Arrows indicate the direction of blood flow from the heart. (LCC, left common carotid; LPA, left pulmonary artery; LSA, left subclavian artery; RPA, right pulmonary artery; T, trachea; TA, truncus arteriosus) (Lindsay 2001).

Two other mouse deletions were subsequently reported (Fig. 2) that partially overlapped with the *Df1* deletion: the first deletion encompassed 7 genes (Df2) (Kimber, Hsieh et al. 1999), and the second encompassed 12 genes (Df3) (Puech, Saint-Jore et al. 2000). Mice that were heterozygous for either deletion had normal heart development, indicating that the gene responsible for the cardiovascular defects in *Df1/+* mice lay in the interval between the genes *Arvcf* and *Ufd1l*, which contains eight genes (Fig. 2). Within that interval, mice with null mutation in two genes, *Comt* (Gogos, Morgan et al. 1998) and *Pnutl1* (Lindsay, Vitelli et al. 2001), had been reported, but neither had cardiovascular defects. To ascertain which of the remaining six genes in the critical region was responsible for the cardiovascular phenotype, two of the groups used a combination of genetically engineered nested deletions and duplications, transgenesis and single-gene targeting (Lindsay, Vitelli et al. 2001; Merscher, Funke et al. 2001). Both groups identified a genomic DNA fragment that contained four genes: *Gnb1l*, *Tbx1*, *Gp1bb* and *Pnutl1*, which corrected the cardiovascular defects when introduced into the *Df1* deletion mice (Lindsay, Vitelli et al. 2001). This indicated that at least one of the genes present in this genomic region was responsible for the cardiovascular phenotype.

To identify the gene responsible for the cardiovascular phenotype, both groups took a candidate-gene approach, selecting to knock out *Tbx1* in the mouse. This gene is a member of the T-box family of genes, and was considered to be the strongest candidate because during embryonic development it is highly expressed in the pharyngeal apparatus (Chapman, Garvey et al. 1996) (Fig. 4), which gives rise to the structures that are most commonly affected in 22q11.2DS.

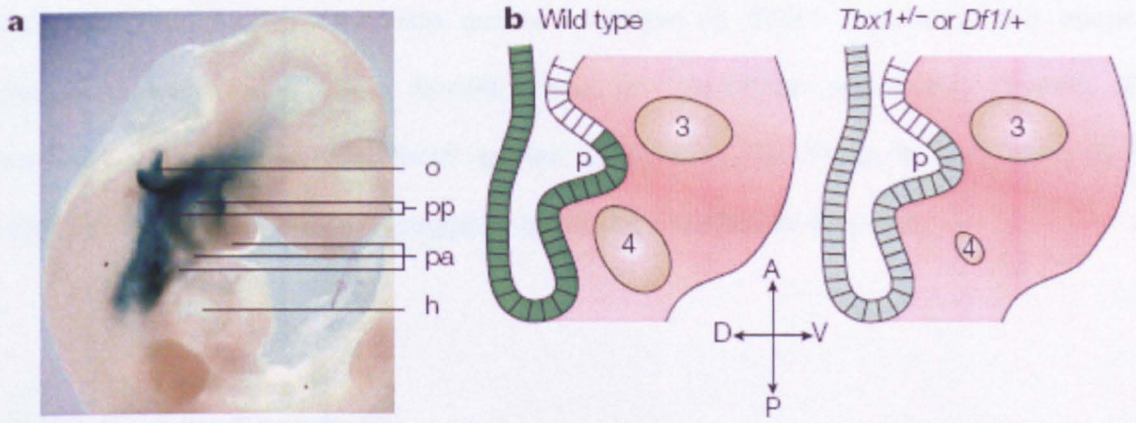

Figure 4: ***Tbx1 expression in early mouse embryogenesis.*** *Tbx1* expression shown by a lacZ reporter gene that has been inserted into the *Tbx1* locus. (a) On embryonic day (E) 10.5, *Tbx1* is expressed in the pharyngeal arches (pa), the pharyngeal pouches (pp) and in the otocyst (o), which will form the inner ear. (h, heart.) (b) At E10.5, *Tbx1* is strongly expressed in the pharyngeal endoderm (green, light shade in $Tbx1^{+/-}$ indicates 50% reduction of gene dosage), which lines the developing pharynx (p). The fourth pharyngealarch artery (4) is small or absent in $Tbx1^{+/-}$ and *Df1/+* embryos. 3, third pharyngeal-arch artery. (A, anterior; P, posterior; D, dorsal; V, ventral) (Lindsay 2001).

The finding of cardiovascular defects in $Tbx1^{+/-}$ mice that were identical to those found in *Df1/+* mice (Fig. 3), provided compelling evidence that *Tbx1* alone is responsible for that phenotype. The phenotype of *Tbx1*-null mice was remarkably reminiscent of severe forms of 22q11.2DS (Jerome and Papaioannou 2001), indicating that human TBX1 might be involved in both cardiovascular and non-cardiovascular aspects of the 22q11.2DS phenotype.

TBX1 was confirmed to be the major genetic determinant of 22q11.2DS in 2003, when the screening of 10 patients with DGS/VCFS without deletion, identified missense mutations in two patients with sporadic disease and one truncation mutation segregating in a family with the characteristic 22q11.2DS phenotype (Yagi, 2003). The truncation mutation was shown to result in loss of function due to the deletion of a C-terminal nuclear localization signal of TBX1 (Stoller, 2005). A C-terminal truncating mutation was identified in another family with the DGS/VCFS phenotype, but without the common deletion (Paylor, 2006). The third

missense mutation and the fifth overall mutation in TBX1 expanding the associated phenotype was found in a familial case of Shprintzen syndrome (Zweier, 2007), characterized by the typical facial gestalt of DGS/VCFS. Thus, to date, only 5 TBX1 mutations have been reported, suggesting that the mutation is very rare.

1.3 *Tbx1 and the T-box family*

Tbx1 encodes a member of an evolutionarily conserved T-box family of transcription factors, whose expression is precisely regulated during embryogenesis. *Brachyury* (*T*) is the founder member of the T-box gene family (Smith J, 1997). In 1994, Bollag et al. (Bollag, Siegfried et al. 1994) showed the existence of a family of *T*-related genes in the mouse genome, which was named T-box gene family. Members of this family are expressed in, and are required for, the development of multiple cell types in diverse organisms. The family has 18 members in mammals that can be divided into five major phylogenetic subfamilies based on overall sequence similarity and gene structure (Minguillon and Logan, 2003). The Tbx1 subfamily includes Tbx10, Tbx15, Tbx18, Tbx20 and Tbx22. The defining feature of the T-box gene family is a conserved domain that was first uncovered in the sequence of the mouse *T* locus; this homology domain encodes a polypeptide region that was named the T-box (Bollag, Siegfried et al. 1994). It is defined as the minimal region within the T-box protein that is both necessary and sufficient for sequence-specific DNA binding (Conlon, Fairclough et al. 2001; Papaioannou 2001). Despite the sequence variations within the T-box between family members, examination of downstream targets and binding-site selection experiments for a number of T-box proteins show that all members of the family so far examined bind to the DNA consensus sequence TCACACCT. T-box proteins have been demonstrated to function both as transcriptional activators and repressors. In all cases studied, the transcriptional regulation activity has been shown to require sequences located in the carboxy-terminal

portion of the protein (Conlon, Fairclough et al. 2001). Tbx1 has been shown to function as a transcriptional activator in several experimental systems. TBX1 is capable of activating an engineered CAT reporter construct with one copy of the typical palindromic Brachyury binding site in mammalian cells (Paylor, Glaser et al. 2006). Tbx1 was also found to be able to activate an Fgf10 promoter via a Tbx5 binding element in tissue culture (Xu, Morishima et al. 2004). Furthermore, Tbx1 has also been shown to function as a transcriptional repressor (Pane, Zhang et al. 2012). The T-box genes share two characteristics of interest to researchers studying cell specification and differentiation: they tend to be expressed in specific organs or cell types, especially during development, and they are generally required for the development of those tissues. These considerations, together with their DNA-binding and transcriptional activation/repression capacity, mean that T-box proteins are well placed to fulfill a wide array of important regulatory roles in development. This is supported by the observation that mutant alleles commonly give a phenotype even in heterozygotes (that is, they show haploinsufficiency), indicating that the level of a T-box protein is important for determining its function.

1.4 *Tbx1 expression pattern*

Tbx1 expression varies both spatially and temporally across tissues, and gene dosage studies in mice have shown that *Tbx1* expression during embryogenesis requires precise regulation (Xu, Cerrato et al. 2005); expression analyses have shown dynamic *Tbx1* expression in tissues that form the pharyngeal apparatus (including pharyngeal endoderm, mesodermal core of pharyngeal arches, head mesenchyme, the second heart field, the otocyst and sclerotome), which gives rise to the heart and face (Chapman, Garvey et al. 1996; Vitelli, Morishima et al. 2002; Xu, Morishima et al. 2004). *Tbx1* was not detected in the blastocyst, but in the 7.5 dpc egg cylinder expression was observed in the embryonic

mesoderm, and in no other tissues (Chapman, Garvey et al. 1996). In the 8.0 dpc *Tbx1* is expressed in the pharyngeal endoderm and in the mesodermal core of the 1st pharyngeal arch. In the mid-gestation, *Tbx1* expression revealed by both RNA *in situ* hybridization and a LacZ knock-in allele ($Tbx1^{lacZ}$) shows specific pattern in the pharyngeal region and otic vesicle. The strongest expression is observed in the endoderm lining the 3rd pouch and 3rd arch (Vitelli, Morishima et al. 2002). Expression in the pharyngeal region is both mesenchymal and epithelial: it is in the core mesenchyme of the 1st, 2nd and 3rd pharyngeal arches, and in the epithelium of the 1st, 2nd and 3rd pharyngeal pouches. Expression in the otic vesicle is predominantly in the caudal half, but includes both the epithelium and the surrounding mesenchyme. In 10.5 dpc embryos, when the pharynx has grown to include the 4th arch, 4th pouch and 6th arch, *Tbx1* in the endoderm is again expressed most strongly in the posterior segments. In addition to this anteroposterior gradient of expression, we observed higher expression towards the dorsolateral folds of the pharynx. At 11.5 dpc, endodermal expression persists almost exclusively in the 4th pouch. Hence *Tbx1* is expressed following anterior-posterior and medial-to-lateral gradients. These are also the directions of growth of the pharynx, suggesting that Tbx1 may be involved in the growth process (Vitelli, Morishima et al. 2002). By 12.5 dpc, expression is still evident in the otic vesicle epithelium. There is also expression in the mesenchyme surrounding the cochlear duct and the Eustachian tube epithelium. By 12.5 dpc, with organogenesis well underway, several additional sites of *Tbx1* expression are evident. They are the myogenic core of the tongue, the incisor tooth buds, the mesenchyme surrounding Rathke's pouch and the branching lung epithelium (Chapman, Garvey et al. 1996). At pre-term stage, a $Tbx1^{lacZ}$ allele reveals new expression domain in blood vessels of brain surface and parenchyma and this brain expression increases steadily from E17.5 to 12 weeks by real-time PCR (Paylor, Glaser et al. 2006).

1.5 *The development of PAAs and their derivatives*

The mature aortic arch and great vessels derive from the embryonic pharyngeal arch arteries (PAAs) and the aortic sac. The PAAs are components of the pharyngeal apparatus, a vertebrate-specific structure comprising alternating bulges (arches) and indentations (pouches and clefts) that develops sequentially along the body axis in a head-to-tail direction. The pharyngeal arches are overlaid by surface ectoderm and lined by endoderm, which were referred to together as the pharyngeal epithelia. Between the epithelial layers of the pharyngeal apparatus there is mesenchyme of mesodermal origin that is later infiltrated by ectomesenchyme of neural crest origin. The endothelial cells of the PAAs are mesodermally derived and the surrounding tissue layers (pericytes and smooth muscle cells) develop from neural crest derived cells. The PAAs, which connect the aortic sac with the dorsal aortae, and which pass through the core of the arches, initially form as five pairs of symmetrical vessels. Beginning around embryonic day (E) 11.5 of mouse development, the caudal PAAs and the aortic sac remodel extensively to form the mature asymmetric aortic arch and great vessels. Proper remodeling of the PAAs into the aortic arch system is a complex process, requiring intercellular signaling events and correct spatiotemporal gene expression in multiple cell types. Migration and differentiation of neural crest-derived cells as well as growth and apoptosis of the developing vessels within a biomechanically active environment is a prerequisite of normal PAA transformation (Hutson and Kirby 2007; Snider, Olaopa et al. 2007).

In 12-somite embryos in the late part of the period E8.5-9, the pharyngeal arch artery system was not yet apparent, and the arterial trunk projecting from the endocardiac tube of the heart bifurcated into paired ventral aortae. The ventral aortae connected with the dorsal aortae through a loop (Fig. 5A), which, together with the ventral aortae, is generally called the 1st pharyngeal arch artery. Until 15-somite stage, the ventral and dorsal aortae were still connected solely by the first PAA and the 2nd PAA was observed only as signs of sprouting

at the sides of the aortic sac and dorsal aorta (arrows in Fig. 5B). In the 16-somite embryo, the 2nd PAA with a lumen, which was still thin, was established. By early in E9.5-10 embryo (21-23 somites), the 2nd PAA had grown until its diameter approached that of the 1st PAA.

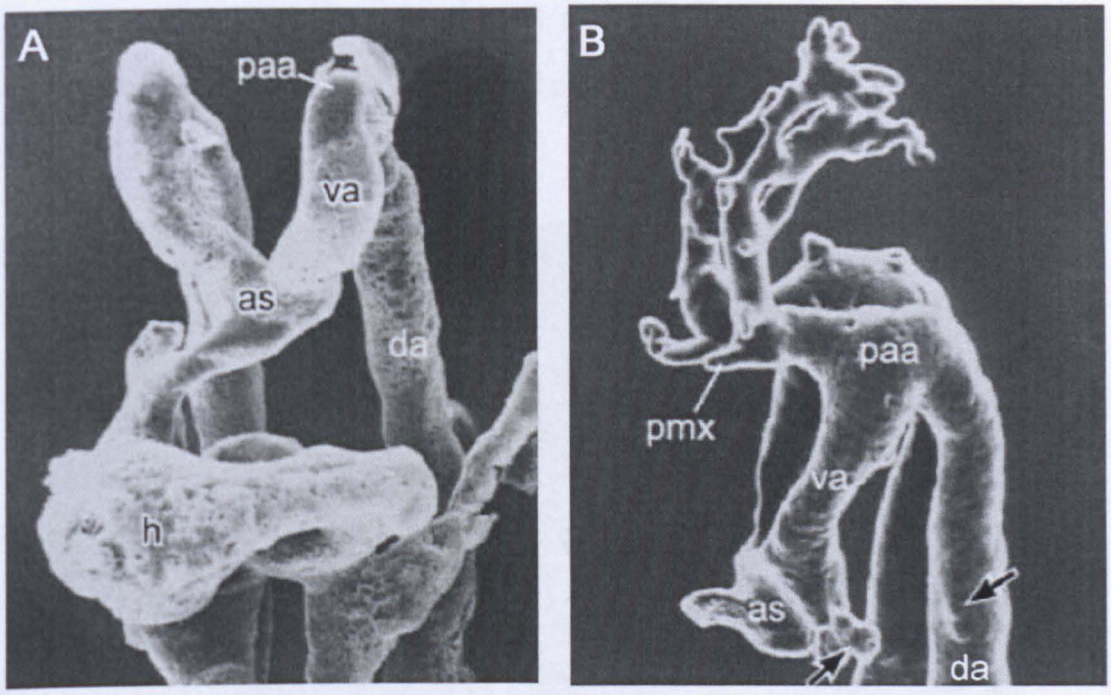

Figure 5: ***Scanning electron microscopy (SEM) images of vascular casts of mouse embryos late in E8.5-E9 (12-somite stage, A) and early and late in E9-E9.5 (15-16-somite stage, B).*** (A) Ventral view. The primitive intra-embryonic arterial system is seen. (B) Left side view. The sprouting indications of the 2nd PAA can just be recognized (arrows) (Hiruma, Nakajima et al. 2002). paa: pharyngeal arch artery, va: ventral aorta, as: aortic sac, da: dorsal aorta, h: heart. Scale bar = 100 μm.

The 3rd PAA was first recognized at the 22-somite stage, but it was very thin and consisted of a network connecting the aortic sac to the dorsal aorta in the caudal part of the second pharyngeal pouch. In the middle part of E9.5-10 (24-26 somites), three paired PAAs were clearly observed (Fig. 6A). The 1st PAA was thin, the 2nd PAA was the thickest, and the 3rd PAA gradually thickened as the stage of development increased. Late in E9.5-10 (27-29

somites), the 1st PAA had dwindled further, and it gave off numerous fine branches into the first pharyngeal pouch; the 3rd PAA came to be thickest, and a very thin 4th PAA was forming just caudal to the 3rd (arrow in Fig. 6B). At E10 (31-34 somites), the 1st PAA was interrupted, and its distal part was transformed into the mandibular artery; this gave off many branches into the maxillary process. In addition, the 2nd PAA was now much thinner, becoming transformed into a thin capillary plexus.

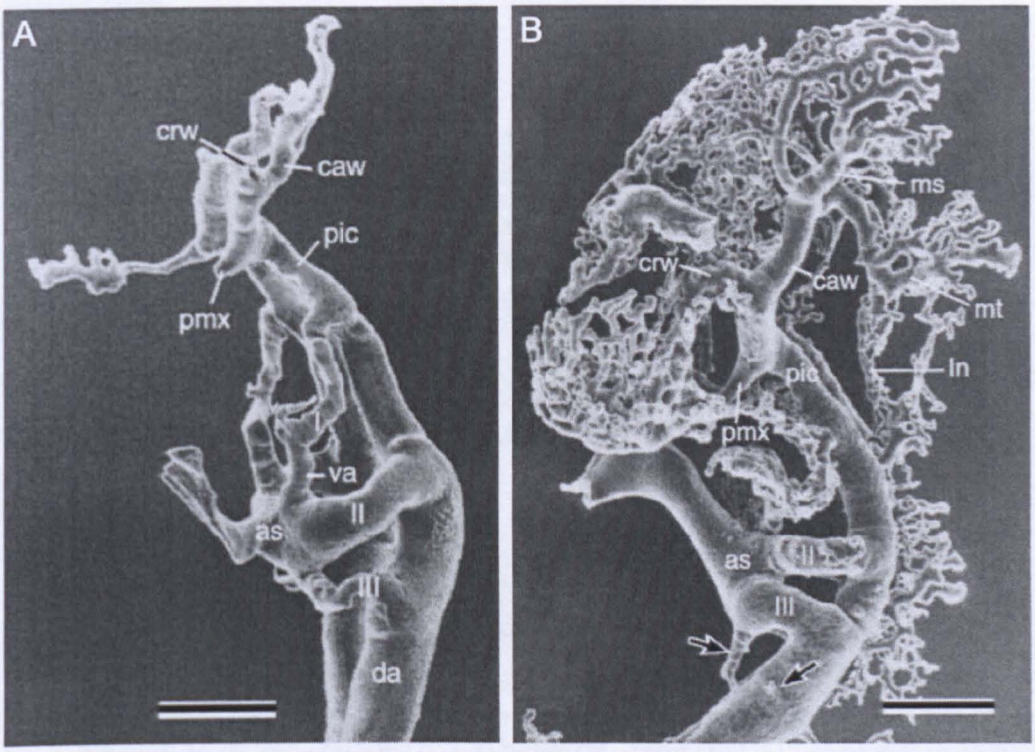

Figure 6: ***SEM images of vascular casts of mouse embryos in the middle (25-somite stage, A) and late (27-somite stage, B) parts of E9.5-E10.*** (A) Three PAAs (I, II, III) are seen, of which the 2nd is the thickest. (B) The cephalic vascular system is well developed. The primordial of the 4th PAA are present between the aortic sac and dorsal aorta (arrows) (Hiruma, Nakajima et al. 2002). pic: primitive internal carotid artery, va: ventral aorta, as: aortic sac, da: dorsal aorta. Scale bar = 250 μm.

The 3rd PAA was the thickest, the 4th PAA was becoming thicker as the stage advanced from 32 to 34 somite stage (Fig. 7A,B), and the very thin 6th PAA appeared, at a position

cadal to the 4th PAA, connected the aortic sac to the dorsal aorta (Fig. 7C). The primordium of the pulmonary artery was first observed at this time, and in the 32- and 34-somite embryos it arose from the proximal part of the 6th PAA and run straight in the caudal direction, parallel to the dorsal aorta (Fig. 7C). At E10.5 and E11, the mandibular artery had grown in size and gave off many branches to the jaw region; at this time, the 2nd PAA was interrupted and its distal part was transformed into the very thin hyoid artery. The proximal part, on the other hand, fused with the proximal part of the 1st PAA to form the primordium of the external carotid artery.

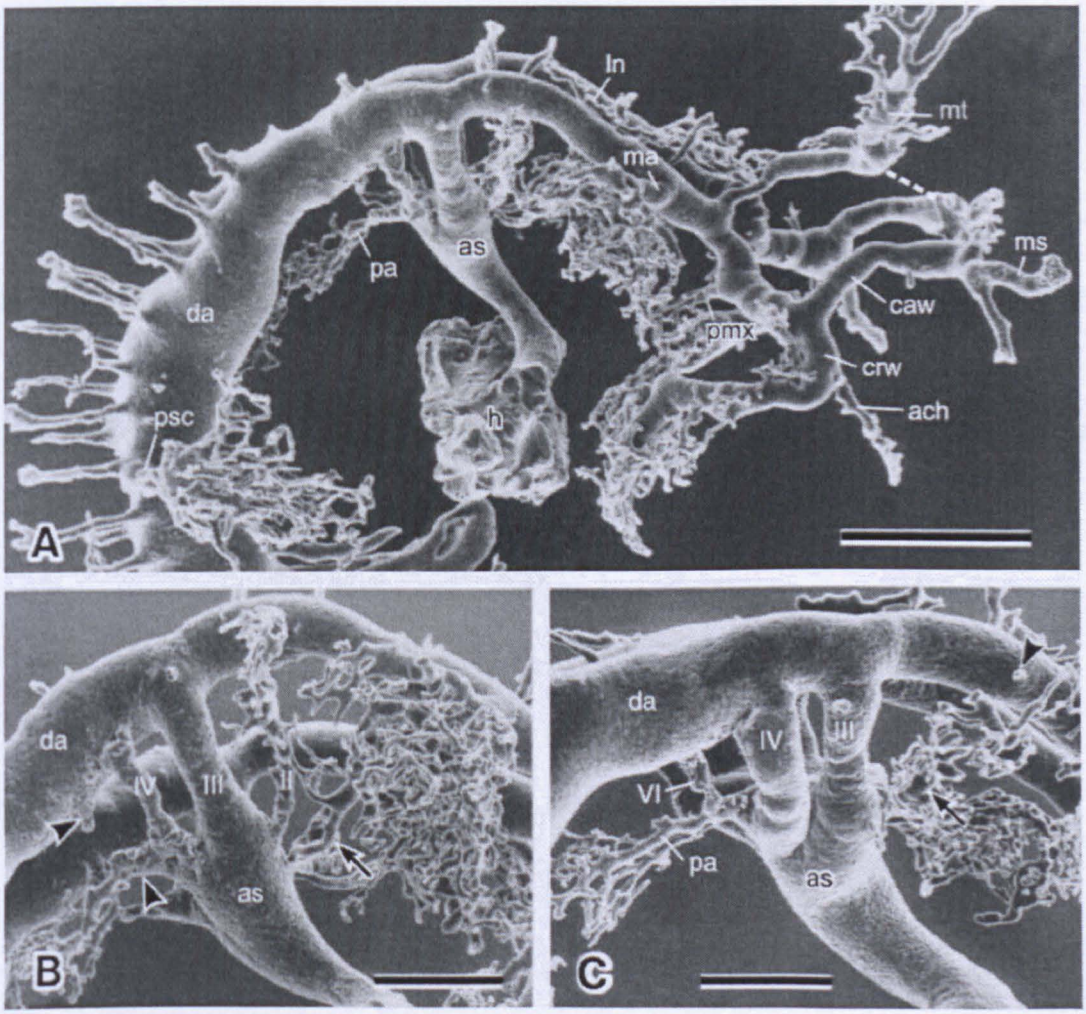

Figure 7: ***SEM images of vascular casts of mouse embryos at E10 (32-somite stage, A-B; 34-somite stage, C).*** All show right side view. (A) The interrupted line (top right) indicates the posterior part of the cranial division of the circle of Willis, which was broken during

preparation of the cast. (B) The remnants of the ventral aorta and the proximal portion of the 1st PAA (arrow) as well as the ventral primordial of the 6th PAA (arrowheads) can be discriminated. (C) The arrow points to the proximal portion of the 2nd PAA, and the arrowhead points to its distal portion. (Hiruma, Nakajima et al. 2002). as: aortic sac, h: heart, pa: pulmonary artery, da: dorsal aorta, psc: primitive subclavian artery. Scale bar in A = 500 μm; B-C = 250 μm

At this stage, the 3rd, the 4th and the 6th PAAs were all well developed, and of almost equal thickness, and they formed connections between the aortic sac and the dorsal aorta (Fig. 8). Until E11, the pharyngeal arch artery system was bilaterally symmetrical. From E11 to E11.5, the portion between the basal parts of the 3rd, the 4th and the 6th PAA became elongated, and the vascular organization around the aortic sac changed (Fig. 9A).

At E11.5, the aortic sac could be seen to be T-shaped, with right and left horns, and its proximal part was divided into the aortic trunk and pulmonary trunk (Fig. 9B). The pharyngeal arch artery system became asymmetrical at this stage. The dorsal aorta was small in diameter between the 3rd and the 4th PAAs; this is commonly called the carotid duct (arrow in Fig. 9C).

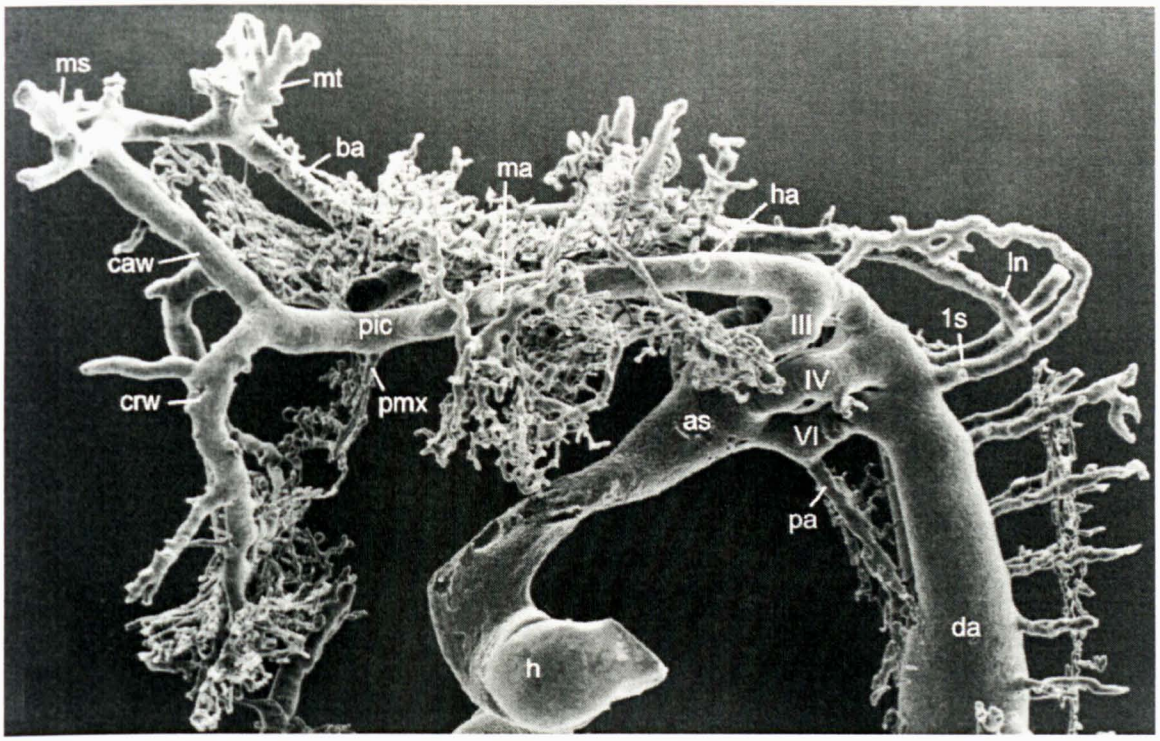

Figure 8: ***SEM images of vascular casts of mouse embryo at E11.*** Left side view. The hyoid artery, which was broken during preparation of the cast, remains only at its origin. The pulmonary artery branches from the mid-point of the 6th PAA, and the primitive subclavian artery originates from the single dorsal aorta (Hiruma, Nakajima et al. 2002). pic: primitive internal carotid artery, ha: hyoid artery, as: aortic sac, h: heart, pa: pulmonary artery, da: dorsal aorta. Scale bar 500 μm.

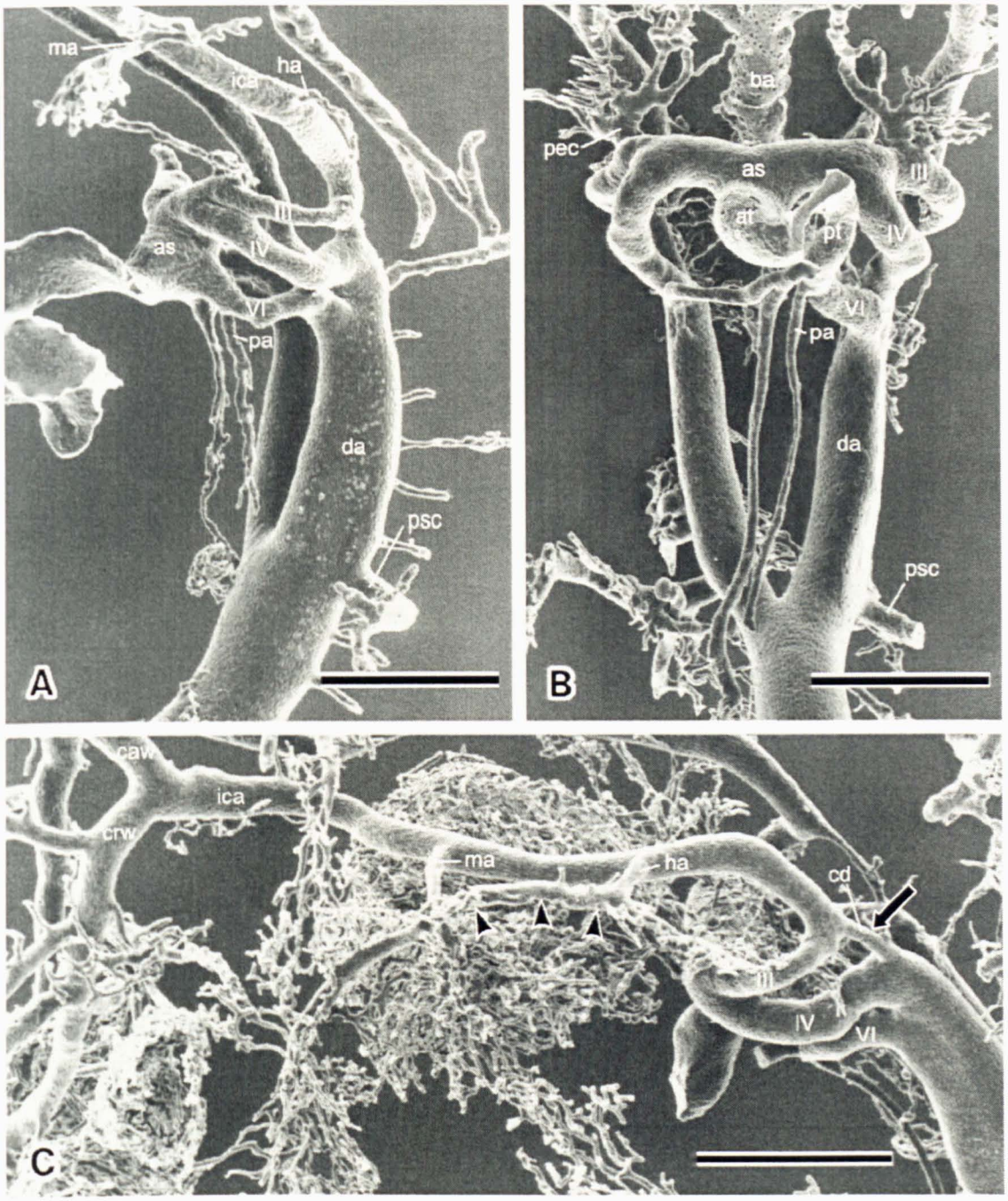

Figure 9: ***SEM images of the vascular casts of mouse embryos at E11.5 (A) and E12 (B, C).*** (A) Left side view. Origin of the 4th PAA from the aortic sac is separated from that of the 6th PAA. The pulmonary arteries originate from the proximal part of the 6th PAA (compare with Fig. 8A). The primitive subclavian artery is given off from the boundary between the paired and single portion of the dorsal aorta. (B) Ventral view. The proximal portion of the aortic sac is divided into the aortic trunk and the pulmonary trunk. The primitive subclavian artery branches from the paired dorsal aorta. (C) Left side view. A vessel (arrowheads) is seen connecting the mandibular artery and hyoid artery. The carotid duct (arrow) is indicated. as: aortic sac, pa: pulmonary artery, da: dorsal aorta, psc: primitive subclavian artery, pec: primitive external carotid artery, at: aortic trunk, pt: pulmonary trunk, cd: carotid duct (Hiruma, Nakajima et al. 2002). Scale bar = 500 μm.

At E13, the 3rd PAA had become both the common carotid artery (CCA) and the proximal part of the internal carotid artery (ICA), since the carotid duct had disappeared (Fig. 10A). By then, the right dorsal aorta, which had been situated between the right subclavian artery (RSA) and the left dorsal aorta, had completely disappeared. As a result, the aortic-arch system had become bilaterally asymmetrical, and almost the same as in the adult (Fig. 10B,C); that is to say, the right horn of the T-shaped aortic sac was transformed into the so called "innominate" artery or right brachiocephalic artery, while the left horn together with the left 4th PAA comprise the definitive aortic arch (AA). The right 4th PAA formed the proximal part of the subclavian artery, and the left became a distal division of the aortic arch. The left 6th PAA persisted as the arterial duct between the pulmonary artery and the aortic sac.

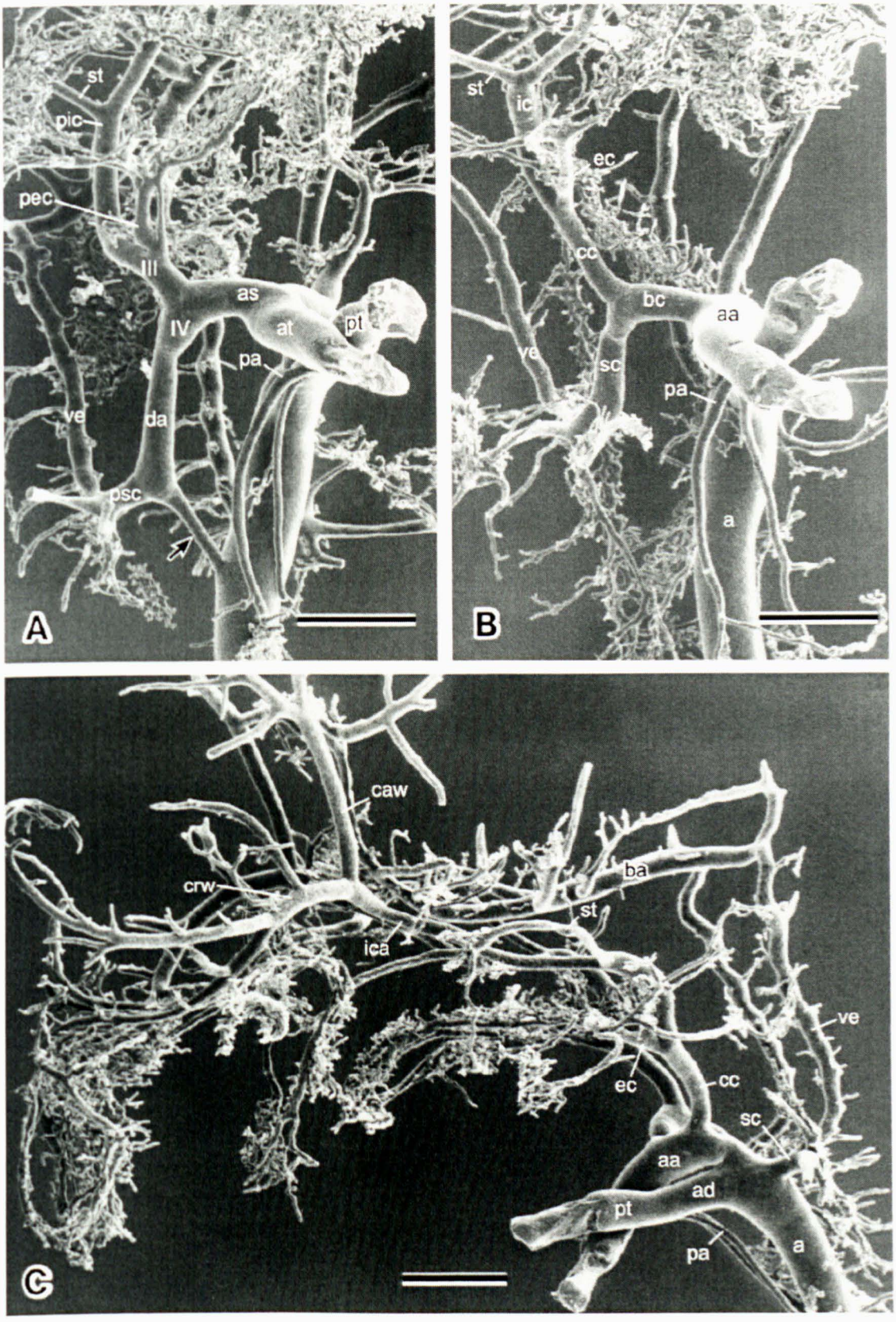

Figure 10: ***SEM images of vascular casts of mouse embryos at E12.5 (A) and E13 (B,C).*** (A) Ventral view. The right dorsal aorta is slender compared to the left. (B) Ventral view. The

particularly thin portion of the right dorsal aorta seen in A (arrow) has disappeared. (C) Left side view. The aortic arch system is quite similar to that seem in the adult (Hiruma, Nakajima et al. 2002). pic: primitive internal carotid artery, pec: primitive external carotid artery, as: aortic sac, at: aortic trunk, pt: pulmonary trunk, pa: pulmonary artery, da: dorsal aorta, psc: primitive subclavian artery, ic: definitive internal carotid artery, ec: definitive external carotid artery, cc: common carotid artery, bc: brachiocephalic artery, aa: definitive aortic arch, sc: definitive subclavian artery, a: definitive aorta, ad: arterial duct. Scale bar = 500 μm.

1.6 *The role of Tbx1 gene during PAAs development*

The main cause of death in 22q11.2DS patients is congenital heart defects (CHDs), which affects the following tissues: the cardiac outflow tract (OFT; resulting in Tetralogy of Fallot and persistent truncus arteriosus); the fourth pharyngeal arch artery (PAA; resulting in interrupted aortic arch type B, IAA-B); and the right subcavian artery (resulting in aberrant origin of the right subcavian artery, ARSA) (McDonald-McGinn and Sullivan 2011). Moreover, most 22q11.2DS phenotypes, including CHDs, are caused by defects in development of the pharyngeal apparatus during early embryogenesis, and *Tbx1* is a gene required for the development of this apparatus.

The primary embryological defect underlying most of the cardiovascular abnormalities observed in $Tbx1^{+/-}$ embryos is defective development of the fourth pharyngeal arch arteries (PAAs) (Lindsay et al. 2001). Instead, $Tbx1^{-/-}$ mutants revealed severe disruption of the PAA system. In these embryos the third, fourth and sixth PAAs are absent and the dorsal aortae connected directly with the aortic sac, suggesting a severe developmental impairment of the pharyngeal arches. Thus *Tbx1* is a dosage-sensitive gene, which when haploid results in fourth PAA abnormalities and loss of function of *Tbx1* leads to disruption of PAAs 3-6. Great artery defects involving third and sixth PAA derivatives are almost never seen in 22q11.2DS patients, suggesting that the haploinsufficiency models reflect more closely the aortic arch defects than do the homoxygous mutations.

In order to understand the mechanism by which *Tbx1* dosage reduction affects fourth PAA development, it is important to determine where Tbx1 is required for this function. However, *Tbx1* is expressed in many tissues that could contribute to fourth PAA development. So it has been considered the Cre-driver strategy to be an effective way to address systematically the tissue requirement for Tbx1 in fourth PAA development.

In mice, *Tbx1* is required for fourth PAA formation and growth. 100% of $Tbx1^{+/-}$ embryos have hypoplastic fourth PAAs at E10.5, whereas, at term, 30-50% have fourth PAA-derived cardiovascular defects (specifically, IAA-B, RAA and ARSA), according to whether the left, right, or both fourth PAAs are affected (Lindsay and Baldini 2001). The penetrance of these defects in E10.5 and term embryos varies with genetic background (Zhang, Cerrato et al. 2005). When the fourth PAA forms at around E9.75, *Tbx1* is most highly expressed in the endoderm of the fourth arch and pouch. However, *Tbx1* is expressed in many tissues potentially involved in the development of these arteries.

To understand the developmental and genetic mechanisms governing the formation, growth and remodeling of the fourth PAAs, it is necessary to understand the role of the individual tissues. This can be approached using tissue-specific, gene-dosage reduction. To this end, a panel of Cre drivers that induce recombination in different tissues of the pharyngeal apparatus have been used to delete one copy of the *Tbx1* gene. Results clearly indicate that the critical tissue for early fourth PAA development is the pharyngeal epithelia (Zhang, Cerrato et al. 2005).

Tbx1 expression in the pharyngeal region was first seen at embryonic stage E8 in the surface ectoderm overlying the pharynx, in the pharyngeal endoderm and mesoderm (Fig. 11 A,A'), and in the head mesenchyme. At E9, expression in the surface ectoderm extended over the presumptive caudal arches (Fig. 11B,B'), whereas after E9.5, ectodermal expression was no longer detectable. Thus, *Tbx1* expression in surface ectoderm precedes the formation of the fourth PAA at E9.75, suggesting that it may contribute to this process. Hence, both endoderm and ectoderm express *Tbx1* in a region relevant to fourth PAA

formation. *Fgf8* is also expressed in surface ectoderm at E9 and its expression in that tissue is required for fourth PAA development (Macatee, Hammond et al. 2003). Thus, it is possible that the reported genetic interaction between *Tbx1* and *Fgf8* (Vitelli, Taddei et al. 2002) operates through transcriptional regulation of the *Fgf8* gene by Tbx1 in ectoderm. *Fgf8* expression has been analyzed in $Tbx1^{-/-}$ embryos between E9 and E10 and found it to be robustly expressed in surface ectoderm, although it was not expressed in the pharyngeal endoderm of these mutants. Thus, it is unlikely that Tbx1 regulates *Fgf8* expression in pharyngeal ectoderm to PAAs development.

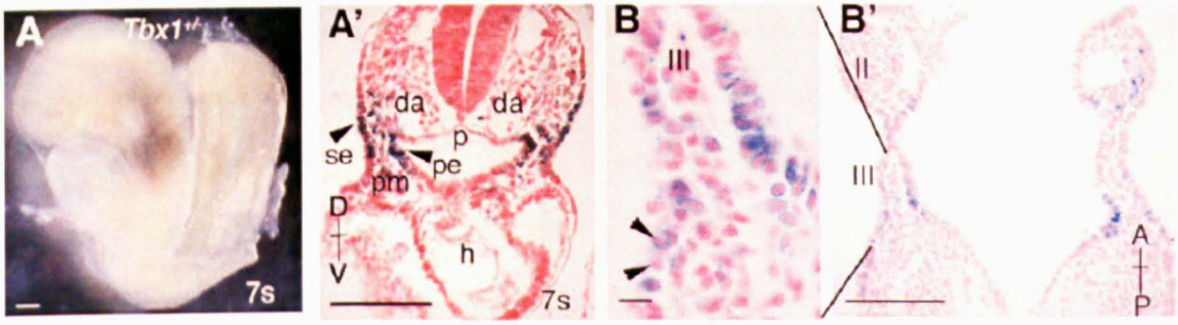

Figure 11: ***Tbx1 expression in the pharyngeal region.*** (A,A') X-gal staining pattern generated by a *Tbx1- lacZ* knock-in allele ($Tbx1^{+/-}$) at E8 (A), and in a transverse section through the pharynx of the same embryo (A'). D, dorsal; V, ventral; da, dorsal aorta; se, surface ectoderm; pe, pharyngeal endoderm; pm, pharyngeal mesoderm; p, pharynx; h, heart. (B,B') *Tbx1* expression in surface ectoderm overlying the presumptive caudal arches (arrowheads) at E9. (From Zhang Z. et al., 2005). A, anterior; P, posterior; II, III, second and third pharyngeal arch.

In order to achieve recombination in pharyngeal mesoderm, another tissue in which *Tbx1* is expressed by E8, a $Mesp1^{Cre}$ driver was used. $Mesp1^{Cre}$ induces recombination in mesoderm-derived tissues (Saga, Hata et al. 1996), but rigorously spares pharyngeal epithelia. In gastrulating embryos, *Mesp1* is expressed by all mesodermal cells as they exit

the primitive streak between E6.5 and E7. As a result, *Mesp1*^{Cre} induces extensive recombination in a sub-population of mesoderm-derived tissues that include core arch mesoderm, pharyngeal mesoderm and vascular endothelium. *Mesp1*$^{Cre/+}$ mutants were bread with *Tbx1*$^{flox/flox}$ mutants and none of the embryos tested had fourth PAA defects, suggesting that the role of Tbx1 in fourth PAA development is not mediated by mesodermal expression (Zhang, Cerrato et al. 2005).

Foxg1^{Cre} induces recombination in pharyngeal epithelia and in pharyngeal mesoderm, including the core arch mesoderm and second heart field. *Foxg1*$^{cre/+}$ mutants were bread with *Tbx1*$^{flox/flox}$ mutants and results shown that the forty-two percent of *Foxg1*^{Cre} conditional mutant embryos had hypoplasia of one or both fourth PAAs. Thus, *Tbx1* gene-dosage reduction in *Foxg1*^{Cre}-expressing cells, or daughter cells, is sufficient to cause fourth PAA hypoplasia. The reduced penetrance of the fourth PAA phenotype may be do to the late activation (E8.5) of Cre-induced recombination of the *Tbx1*-floxed allele in some cells.

To dissect further the tissue requirement of Tbx1 in fourth PAA development a transgenic Fgf15Cre driver line that is specific for pharyngeal ectoderm and endoderm was used (Zhang, Cerrato et al. 2005). As no recombination was seen in the core arch mesoderm or arch mesenchyme, it has been concluded that recombination is epithelial specific. *TgFgf15*^{Cre}; *Tbx1*$^{flox/+}$ conditional mutants had hypoplasia of one or both fourth PAAs, indicating that *Tbx1* dosage reduction in pharyngeal epithelia is sufficient to cause fourth PAA hypoplasia (Zhang, Cerrato et al. 2005).

To map over time the role of *Tbx1* gene in the development of pharyngeal derivatives and cardiovascular system, a time-course deletion on *Tbx1* during embryogenesis was used. Results shown distinct time windows in which *Tbx1* is required for different organs and structures. A drug-induced Cre-mediated recombination of a *Tbx1* conditional allele (*Tbx1*^{flox}), in which the exon 5, encoding part of the T-box domain, is flanked by *LoxP* sites (Xu, Morishima et al. 2004), was used. Cre-induced recombination of this allele generates the allele *Tbx1*$^{\Delta E5}$, which is functionally null. To drive Cre recombinase expression, a transgenic

mouse line (Tg-CAGG-CreER^{TM}) expressing ubiquitously a tamoxifen-inducible Cre^{ERTM} protein (Hayashi and McMahon 2002) was used. Tg-CAGG-CreER^{TM}; *Tbx1*$^{flox/+}$ embryos exposed to tamoxifen at E7.5 demonstrated that heterozygous deletion of *Tbx1* at this time point causes fourth PAAs defects. Exposure to tamoxifen at E8.5 of embryos with the same genotype results in normal or only mildly hypoplastic fourth PAA (Xu, Cerrato et al. 2005). Thus, the fourth PAA haploinsufficiency phenotype is due to an early requirement for Tbx1 that precedes the morphological appearance of the arteries, which occurs after E9.5.

Retinoic acid (RA), the active derivative of vitamin A (retinol), is a modifier of the PAA phenotype of *Tbx1* mutants. In the developing PAs of the chick embryo, both the application of exogenous RA and reduction of RA levels repress *Tbx1* gene expression (Roberts, Ivins et al. 2005).

RA acts as a ligand for nuclear receptors (RARs), which exist as three distinct isotypes (RARα, -β, -γ) and bind as heterodimers with retinoid X receptors to regulatory DNA sequences known as RA responsive elements (RAREs). Two enzymatic reactions convert retinol into RA. The retinaldehyde (Ral) to RA conversion can be carried out by three members of the aldheyde dehydrogenase family, the retinaldehyde dehydrogenases (RALDH) 1, 2 and 3 (Mic, Molotkov et al. 2000). Among these, RALDH2 is expressed from gastrulation onward. Homozygous disruption of the mouse *Raldh2* gene is early (around E10.5) embryonic lethal, because of defects in heart morphogenesis (Niederreither, Vermot et al. 2001), whereas RA-supplemented *Raldh2*$^{-/-}$ embryos display OFT defects and impaired development of posterior (3rd to 6th) PAAs. Consistent with these findings, *Raldh2*-null mice were found to exhibit DGS-like aortic arch defects (Vermot, Niederreither et al. 2003). Tbx1 has also been implicated in the repression of RA signaling in experiments involving the down-regulation of *Raldh2* (Ryckebusch, Bertrand et al. 2010). Interestingly, in *Tbx1*$^{+/-}$ mice with decreased RA levels, the penetrance of fourth PAA defects was reduced (Ryckebusch, Bertrand et al. 2010). Thus, it appears that a precise balance between *Tbx1* expression and RA signaling is crucial for PAA development.

Chromatin modifiers also contribute to *Tbx1* regulation during PAA development. A genetic interaction has been found between *Tbx1* and the gene encoding the chromatin remodeling protein chromodomain helicase DNA-binding protein 7 (*Chd7*), which is mutated in CHARGE syndrome, that is a recognizable (genetic) pattern of birth defects which occurs in about one in every 9-10,000 births worldwide. It is an extremely complex syndrome, involving extensive medical and physical difficulties that differ from child to child. Babies with CHARGE syndrome are often born with life-threatening birth defects, including complex heart defects. *Tbx1* and *Chd7* are both required in the pharyngeal ectoderm for the growth and remodeling of the fourth PAAs. Both *Tbx1* and *Chd7* act cell-non-autonomously in this context, signaling to the mesenchymal cells that populate the PAs (Randall, McCue et al. 2009).

Neuroepithelium-derived cardiac neural crest cells (cNCCs) are needed for proper septation of the OFT into the aorta and pulmonary trunk. cNCCs migrate through the PAs and differentiate into the vascular smooth muscle (VSM) layer through which the PAA pass (Hutson and Kirby 2007). Various signaling pathways play roles in the migration, proliferation and differentiation of these cells. Although, *Tbx1* is not expressed in these cNCCs, it regulates their migration in a non-cell-autonomous manner, probably by activating expression of the homeobox-containing gene *Gbx2* in the pharyngeal surface epithelium (Calmont, Ivins et al. 2009). *Gbx2* encodes a homeobox trancription factor important for both development of the fourth PAA and proper cNCC migration into the PAs; cNCC patterning defects in mouse embryos lacking this gene lead to aortic arch defects such as IAA-B and also cardiac OFT defects, including double outlet right ventricle (DORV) and overriding aorta (Byrd and Meyers 2005).

1.7 *The development of the cardiac OFT*

The cardiac OFT is a structure of the arterial pole of the heart connecting the embryonic ventricles with the aortic sac. The OFT forms during heart looping from cardiac progenitor cells in pharyngeal mesoderm. At its maximal extension the OFT is a torsioned myocardial cylinder lined with endocardial cells; then, it is subsequently remodeled, concomitant with ventricular septation, during which process the OFT wall rotates and divides to generate the base of the ascending aorta and pulmonary trunk. Since the 1970s, studies revealed that cardiac growth occurs by addition of cells lying outside the early heart (de la Cruz, Sanchez Gomez et al. 1977). About ten years ago, a population of cardiac progenitor cells was identified in pharyngeal mesoderm that give rise to a major part of the heart. These multipotent progenitor cells, termed the second heart field (SHF), contribute progressively to the poles of the elongated heart tube during looping morphogenesis, giving rise to myocardium, smooth muscle, and endothelial cells. SHF cells originate in medial splanchnic mesoderm in the anterior region of the embryo, adjacent to pharyngeal endoderm (Fig. 12). Immediately contiguous lateral splanchnic mesoderm gives rise to the cardiac crescent and early heart tube (from Schoenwolf, Bleyl et al., 2009). The SHF is also patterned along the anterior-posterior embryonic axis. Anterior-SHF cells give rise to the right ventricle and OFT at the arterial pole, while the posterior component of the SHF contributes to atrial, atrial septal, and venous pole myocardium. The linear heart tube is thought to give rise predominantly to the left ventricle (Buckingham, Meilhac et al. 2005).

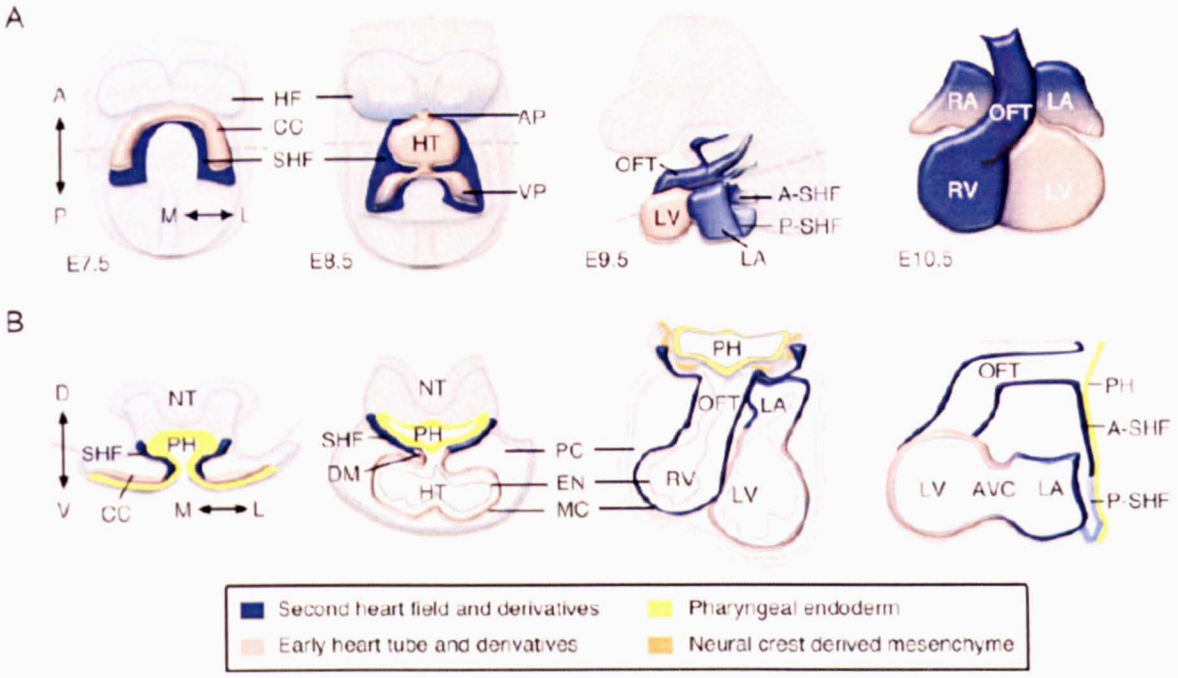

Figure 12: ***Topography of the second heart field.*** (A) Cartoons showing the stages of mouse heart development during which second heart field progenitors are added to the heart. From left to right: embryonic day (E) 7.5 (cardiac crescent, ventral view), E8.5 (early heart tube, ventral view), E9.5 (looped heart, left lateral view), and E10.5 (ventral view). Second heart heart field progenitor cells and their contribution to the heart are shown in dark blue and the early heart tube giving rise to the left ventricle in pink. Anterior (A) posterior (P) and medial (M) lateral (L) embryonic axes are indicated. (B) Schematized histological sections showing the location of second heart field cells and their myocardial derivatives (dark blue) at the stages shown in (A) relative to pharyngeal endoderm (yellow), myocytes derived from the early heart tube (pink), and neural crest-derived mesenchyme (orange). The first three panels show transverse sections at the levels indicated by the dotted lines in (A). The right hand panel shows a mid-saggital E9.5 section. Dorsal (D) ventral (V) and medial (M) lateral (L) embryonic axes are indicated (from Kelly, RG 2012). CC, cardiac crescent; SHF, second heart field; HF, head fold; HT, heart tube, AP, arterial pole; VP, venous pole; OFT, outflow tract; LV, left ventricle; LA, left atrium; RV, right ventricle; RA, right atrium; A-SHF, anterior component of the second heart field; P-SHF, posterior component of the second heart field; NT, neural tube; PH, pharynx; PC, pericardial cavity; DM, dorsal mesocardium; EN, enodcardium; MC, myocardium.

The SHF cells differ from cells giving rise to the linear heart tube by two defining properties: continued proliferation and differentiation delay (Rochais, Mesbah et al. 2009). These properties allow the progressive increase of SHF cells during heart tube elongation and are controlled by the dynamic pharyngeal signaling environment and the distinct pharyngeal mesodermal transcriptional program of the SHF. *Fgf10* was identified as the first molecular

marker of the SHF (Kelly, Brown et al. 2001). SHF cells are also characterized by expression of genes encoding *Fgf8* and the transcription factors *Isl1*, *Tbx1*, *Prdm1*, and *Six1* (reviewed in (Buckingham, Meilhac et al. 2005). Expression of these genes is downregulated upon differentiation, and regulators of cardiac specification, such as Nkx2.5, Gata4, and Mef2c, are activated as progenitor cells approach the heart tube (Waldo, Kumiski et al. 2001). The properties of continued proliferation and differentiation delay that define cardiac progenitor cells in the SHF are regulated by a complex network of intercellular signals that collectively describe the niche of the SHF in the caudal pharyngeal region. These signals both regulate and are regulated by transcription factors in pharyngeal mesoderm and adjacent cell types, including pharyngeal epithelia and neural crest-derived cells, as well as autocrine signals from pharyngeal mesoderm itself (Fig. 13) (Vincent and Buckingham 2010; Rochais, Mesbah et al. 2009). Other signals include bone morphogenetic protein (BMP), fibroblast growth factor (FGF), and canonical and noncanonical Wnt signaling (Evans, Yelon et al. 2010). These signals induce *Mesp1* positive mesodermal progenitor cells to activate cardiac transcription factors, including *Isl1*, *Tbx5*, *Nkx2.5*, *Baf60c*, and *Gata4* that combinatorially drive cardiomyogenesis (van Weerd, Koshiba-Takeuchi et al. 2011; Bruneau, Nemer et al. 2001). As the cardiac crescent and linear heart tube form, SHF cells in medial splanchnic mesoderm remain in contact with pharyngeal endoderm and their continued proliferation and delayed differentiation is regulated by canonical Wnt, FGF, and Hedgehog (Hh) signaling pathways (Fig. 13). So, pro-proliferation and pro-differentiation signaling appear to identify core antagonistic signaling pathways regulating progressive addition of SHF cells to the heart tube (Hutson, Zeng et al. 2010). The balance between these two pathways is influenced by neural crest cell invasion of the caudal pharyngeal region that plays a critical role in braking the proliferative effect of FGF signaling on SHF cells, in addition to a direct later role in OFT septation (Hutson, Zhang et al. 2006).

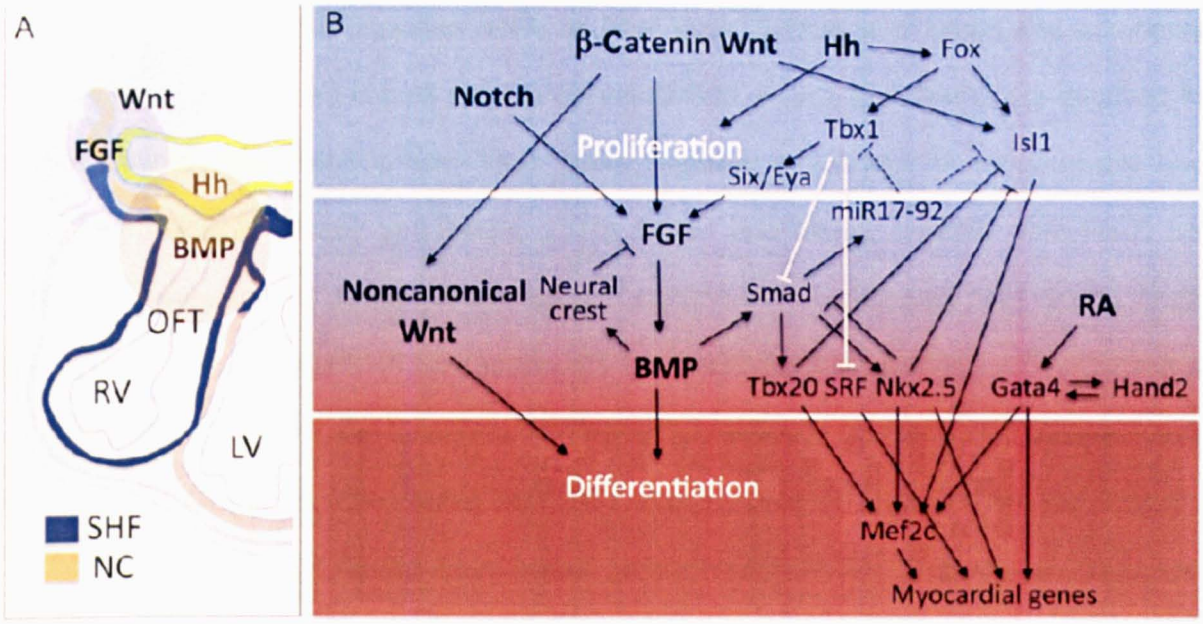

Figure 13: ***The regulation of second heart field development.*** (A) Cartoon showing zones of Wnt, fibroblast growth factor (FGF), Hedgehog (Hh), and bone morphogenetic protein (BMP) signaling at the arterial pole of the mouse heart. LV, left ventricle; RV, right ventricle; OFT, outflow tract; SHF, second heart field; NC, neural crest-derived cells. (B) Schema showing the network of major signaling pathways and regulatory genes impacting on progressive second heart field development during the transition from proliferating progenitor cell (top) to differentiated cardiomyocyte (bottom). Note the central position of Isl1 and Tbx1 in regulating the proliferative progenitor cell state (top), the pivotal position of FGF/BMP antagonism in controlling the balance between proliferation and differentiation (middle), and the activation of the cardiomyogenic program by a network of interacting transcription factors (bottom). Gray lines, direct protein interactions; dotted lines, microRNA silencing (from Kelly, RG 2012).

Transcription factors such as *Isl1* and *Tbx1* play central roles in integrating the output of different signaling pathways during SHF development (Fig. 13B). *Isl1* is required for development beyond the linear heart tube stage and regulates signaling pathways ligand and receptor gene expression in the pharyngeal region (Cai, Liang et al. 2003). Recent data from ES cell studies implicates *Isl1*, together with *Mesp1*, in driving early cardiac specification (Bondue, Tannler et al. 2011). A growing number of additional transcription factors from diverse families, including forkhead, homeobox, T-box, Gata, Zinc-finger, and bHLH factors,

have been found to play important roles in SHF development and single and compound mutations in these genes impact on SHF development. Foxc1 and Foxc2 are required for arterial pole development and have been found, together with Foxa2, to transactivate *Tbx1* regulatory elements (Zhang and Baldini 2010). Foxc1 and Foxc2, together with Foxf1 and Gata4, also regulate *Isl1* through a downstream enhancer (Kang, Nathan et al. 2009). *Mef2c* expression in the anterior-SHF is regulated by Isl1 and Gata4 as well as by Tbx20 (Dodou, Verzi et al. 2004). Finally, the homeodomain transcription factor Six1 and its coactivator Eya1 are required for proliferation within the SHF and survival of adjacent tissues including pharyngeal epithelia and neural crest-derived mesenchyme. Promoter analysis and genetic interaction studies, position Six/Eya transcriptional complex downstream of *Tbx1* and directly upstream of *Fgf8* expresson (Guo, Sun et al. 2011).

Direct or indirect perturbation of SHF development results in congenital heart defects. Loss of function of *Isl1* or early ablation of key regulatory genes such as *Fgf8* results in severe heart tube elongation defects and midgestation lethality (Cai, Liang et al. 2003; Park, Watanabe et al. 2008). Milder defects in heart tube elongation results in alignment defects and failure to separate systemic and pulmonary circulations at birth, corresponding to a variety of common congenital heart anomalies seen in human patients. These include conotruncal defects resulting from OFT hypoplasia and failure of ascending aorta to make the right connection with the left ventricle, such as ventricular septal defects, common arterial trunk, tetralogy of Fallot, and double outlet right ventricle. In the mouse, hypomorphic alleles of genes required for normal SHF development, such as *Tbx1*, can results in a similar spectrum of conotruncal defects (Zhang and Baldini 2008). However, specific subpopulations of SHF cells contributing to the terminal stages of SHF development appear to be particularly relevant with respect to the etiology of common congenital heart defects. *Cre*-labeling experiments have shown that *Tbx1* is expressed in a subpopulation of SHF cells giving rise to the inferior and lateral wall of the midgestation OFT and later to myocardium at the base of the pulmonary trunk (Huynh, Chen et al. 2007). Underdevelopment of the myocardium at the

base of the pulmonary trunk is considered to be the primary cause of OFT alignment defects. Studies have confirmed that this subpopulation of SHF cells is affected in *Tbx1* null hearts (Fig. 14) (Parisot, Mesbah et al. 2011).

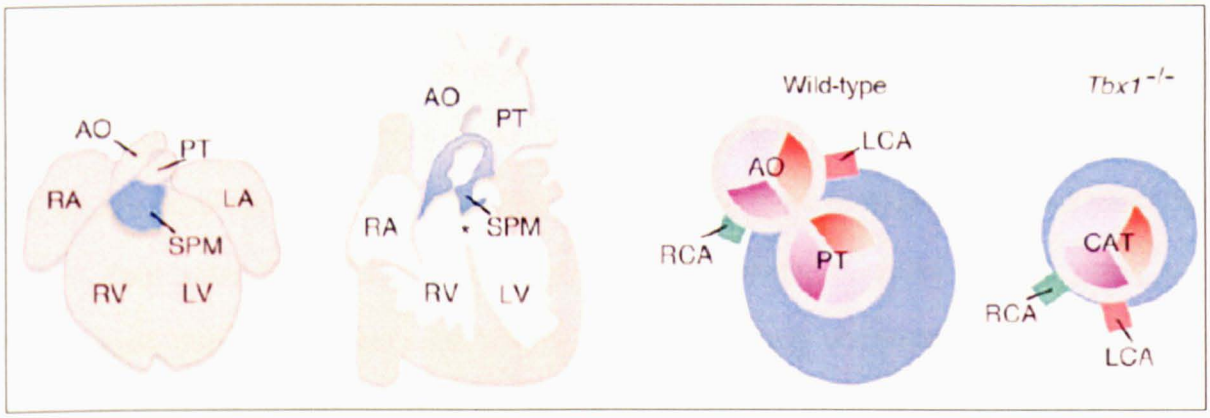

Figure 14: ***A clinically relevant subdomain of the second heart field.*** Subpulmonary myocardium at the base of the outlet of the right ventricle (blue) in a mouse heart at E14.5 and a human heart with tetralogy of Fallot; note the hypoplastic right ventricular outlet and ventricular septal defect (asterisk). Subpulmonary myocardium is severely reduced in the common arterial trunk of *Tbx1* mutant hearts (from Kelly RG, 2012). AO, aorta; PT, pulmonary trunk; RA, right atrium; RV, right ventricle; LA, left atrium; LV, left ventricle; SPM, subpulmonary myocardium; RCA, right coronary artery; LCA, left coronary artery; CAT, common arterial trunk.

1.8 *The role of Tbx1 gene during cardiac OFT development*

Tetralogy of Fallot and persistent truncus arteryosus are defects of the cardiac OFT that occur in 22q11.2DS patients. Formation of the OFT is a complex process that requires precisely regulated spatiotemporal expression of various genes in several cell types. To provide a sufficient number of cells to the developing heart (which grows by addition of cells and by proliferation of resident cells), second heart field (SHF) cells, that are cardiac precursors cells resident in the pharyngeal mesoderm, must proliferate at a sufficient rate before they enter the OFT of the heart and differentiate, because at that point, their proliferation rate will decrease substantially. A possible way to understand the mechanism by which this process is maintained is to identify genes and proteins expressed in the SHF but not in the OFT of the heart. *Tbx1* is required for growth, alignment and septation of the OFT in mice.

Prior to E11.5, there is a common outflow tract, the truncus arteriosus, which connects the heart to the systemic circulation. Subsequently, the outflow undergoes septation to separate aortic and pulmonary flows. Formally, the septum is divided into three components (from distal to proximal, relative to the heart): the aortico-pulmunary (AP) septum, the truncal septum and the conal septum (intracardiac), which is also important for the closure of the interventricular foramen. *Tbx1* homozygous mutation causes disruption of all three components, leading to truncus arteriosus communis (TAC). The most proximal component of the outflow septum, the conal septum, is also severely affected in *Tbx1* homozygous mutants. In these mutants at term, the single arterial orifice is connected exclusively to the right ventricle, while the left ventricle communicates to the right ventricle through a large ventricular septal defect (VSD) (Vitelli, Taddei et al. 2002). Despite the severity of the OFT phenotype in *Tbx1* mutants, Tbx1 protein is not found in SHF-derived cells of the OFT but only in the SHF (Chen, Fulcoli et al. 2009). Reports of *Tbx1* gene expression in the OFT myocardium were mostly based on the visualization of β-galactosidase activity from a

Tbx1^{LacZ} reporter (Vitelli, Taddei et al. 2002), thus probably biased by the stability of the β-galactosidase protein. Tbx1 is also expressed in endothelial cells and in a subpopulation of α-sma-positive cells of the outer wall of the OFT (Vitelli, Taddei et al. 2002). Endothelial cells in the conal OFT, transform into mesenchymal cells of the outflow ridges (van den Hoff, Moorman et al. 1999), thus, these cells may be important for septation. *Tbx1* conditional mutation in the endothelial cell and their precursors (using Tie2:Cre;*Tbx1*+/- mice bred with *Tbx1*$^{flox/flox}$ mice) resulted in no cardiovascular defects other than aortic arch defects associated with *Tbx1* haploinsufficiency (Xu, Morishima et al. 2004). Similarly, *Tbx1* conditional mutation driver by an αMHC:Cre resulted in normal cardiovascular phenotype, apart from the aortic arch abnormalities characteristic of *Tbx1* haploinsufficiency (Xu, Morishima et al. 2004).

Therefore, Tbx1 is not required in resident, differentiated OFT cells, but being expressed in SHF cells, conditional deletion of *Tbx1* in cardiac precursors cells, using *Nkx2.5*$^{Cre/+}$ mice, is sufficient to recapitulate the OFT abnormalities found in *Tbx1*$^{-/-}$ mutants (Xu, Morishima et al. 2004).

As Nkx2.5Cre induced recombination in pharyngeal mesoderm, as well as in pharyngeal endoderm and ectoderm, conditional deletion of *Tbx1* specifically in restricted tissues was addressed to identify the tissue(s) in which Tbx1 is required for cardiac OFT development. Mesodermal deletion of *Tbx1*, using *Mesp1*^{Cre}, causes a cardiovascular phenotype very similar to that observed in *Tbx1*$^{-/-}$ embryos. In particular, conditional mutants at term had TAC, VSD, as well as aortic arch defects. At E10.5, conditional embryos presented with hypoplasia of the 2nd pharyngeal arches, loss of the 3rd, 4th and 6th pharyngeal arches and PAAs, and severe hypoplasia of the pharynx. RNA in situ hybridization with a marker of pharyngeal pouch endoderm, showed no labeling of the 2nd and 3rd pharyngeal pouches of conditional mutants, suggesting that Tbx1 in the mesoderm regulates a signaling pathway required for pharyngeal endoderm development (Zhang, Huynh et al. 2006). To confirm that *Tbx1* mesodermal expression is necessary for a correct development of the cardiac OFT,

Tbx1 expression was restored in this tissue and its reactivation rescued completely the OFT defects, the formation and remodeling of the 3rd and 6th PAAs, the hypoplasia of the 2nd pharyngeal arch, and the 2nd and 3rd pharyngeal pouches, but did not rescue the 4th pharyngeal arch and the 4th PAA aplasia (Zhang, Huynh et al. 2006). The crucial time requirement for *Tbx1* in mesoderm, in the development of the cardiac OFT is between E8.5 and E9.5, as demonstrated by timed fate mapping of *Tbx1*-expressing cells (Xu, Cerrato et al. 2005). This relatively late and narrow time-window is not consistent with a crucial role in the early SHF cell populations located medially to the cardiac crescent; rather, these findings are consistent with a crucial role of Tbx1 in regions that provide precursors destined to the OFT at a later stage, such as the splanchnic mesoderm (Kelly, Brown et al. 2001).

To understand the earliest molecular consequences of *Tbx1* loss of function in the mesoderm, conditional mutants (showed above) were examined for cell proliferation at a stage shown to be crucial for Tbx1 function in cardiac OFT development, i.e. E8.5. A strong reduction in cell proliferation was found in the region of the SHF and adjacent splanchnic mesoderm that normally expresses *Tbx1* (Zhang, Huynh et al. 2006; Chen, Fulcoli et al. 2009). Such reduced proliferation explained the strongly reduced cellularity in the pharyngeal arches and the cardiac OFT defects. The Tbx1 pro-proliferative activity was affected, at least in part, by regulating FGF signaling in a cell-autonomous manner, positively modulating the expression of *fibroblast growth factor 8* (*Fgf8*), *Fgf10* and *Fgf receptor 1* (*Fgfr1*). *Fgf8* and *Fgf10* both drive SHF proliferation (Watanabe, Zaffran et al. 2012; Park, Ogden et al. 2006), and Tbx1 positively modulates *Fgf8* and *Fgf10* expression in the SHF mesoderm (Hu, Yamagishi et al. 2004). Studies have shown that Tbx1 binds to the first intron of *Fgf10* to regulate its expression in the SHF (Watanabe, Zaffran et al. 2012). The loss of *Tbx1* disrupts the expression of *Fgfr1* (Park, Ogden et al. 2006), and Crkl1 interacts with Fgfr1 to mediate Fgf8 signaling (Moon, Guris et al. 2006).

SHF cells maintain an undifferentiated precursor state until they migrate into the heart (Cai, Liang et al. 2003). Therefore, it is important to maintain a proliferating as well as an

undifferentiated progenitor cell pool in the SHF for appropriate OFT development. In addition to regulating cardiac precursors proliferation, Tbx1, similarly, controls the differentiation of these cells, keeping theme in an undifferentiated precursor state. For this end, *Tbx1* supports the expression of several genes to maintain a balance between proliferation and differentiation of progenitor cells in the SHF.

Tbx1 maintain the undifferentiated cardiac precursors state in different manners. Studies have shown that Bmp signaling promotes cardiac OFT differentiation (Wang, Greene et al. 2010). Smad1, a member of the Bmp pathway, is a critical negative regulator of SHF proliferation in vivo, and its ablation in the SHF enhances cell proliferation (Prall, Menon et al. 2007). Tbx1 binds to Smad1 and negatively modulates the Bmp-Smad signaling pathway by interfering with the Smad1-Smad4 interaction (Fulcoli, Huynh et al. 2009). This regulation by Tbx1 is necessary to maintain the cardiac progenitor population in the SHF, and to prevent the premature myocardial differentiation.

Tbx1 inhibits SHF differentiation by antagonizing not only the Bmp pathway but also the activities of Mef2c and serum response factor (Srf). Mef2c is key transcription factor in OFT myocardial differentiation (Pane, Zhang et al. 2012), and Srf is a myogenic transcription factor that regulates muscle differentiation. Tbx1 did not regulate *Srf* transcriptionally, but it interacts with Srf protein, decreasing its stability and increasing proteasome-mediated degradation of Srf protein levels (Chen, Fulcoli et al. 2009). Together, these findings indicate that *Tbx1* is precisely regulated in the SHF, and that it maintains the balance between the cardiac progenitor population and differentiating cardiac cells by interacting with pro-proliferation and pro-differentiation factors during development of the OFT.

Recent studies identified a novel function of Tbx1, to interact with chromatin modifiers during development of the cardiac OFT. Baf60a, a component of the SWI-SNF-like BAF chromatin-remodeling complex, is a key cofactor for Tbx1 function in the cardiac progenitors. *Wnt5a* has been found to be a novel and important transcriptional target of Tbx1, whose regulation is mediated by the recruiting of Baf60a and histone modifier Setd7 to the gene. *Wnt5a*

encodes a ligand of the non-canonical Wnt pathway, whose mutation leads to defects in OFT development. Combined loss of *Tbx1* and *Wnt5a* genes caused a severe hypoplasia of the SHF-derived heart segments, leading to a much more severe phenotype than that caused by loss of the individual genes (Chen, Fulcoli et al. 2012). These findings demonstrated that Tbx1 is able to regulate OFT development by interacting with chromatin modifiers.

1.9 *p53: not only a tumor suppressor*

Since its discovery in 1979, the role of the p53 protein in cancer has been studied intensively (Levine and Oren 2009). p53 is a crucial tumor suppressor, implicated in the control of cell proliferation and tumor progression. Allelic losses and mutations in the *Trp53* genes are frequently observed in many types of tumors. Unequivocal confirmation of the crucial role for p53 in tumor suppression was demonstrated by the completely penetrant cancer phenotype of *Trp53* null mice (Kenzelmann Broz and Attardi 2010).

Although research on p53 has focused on cancer for many years, it is now appreciated that p53 has a much more pleiotropic role as a stress sensor, and that p53 has functions in various physiological and pathological processes (Vousden and Lane 2007).

Most mice missing both functional copies of *Trp53* exhibit normal prenatal and postnatal development (Donehower, Harvey et al. 1992). The developmental viability of *Trp53* null mice was initially surprising, given the importance of p53 as a known cell-cycle checkpoint control protein and its high levels of expression in early phases of embryonic development (Schmid, Lorenz et al. 1991). The *Trp53* null mice were developmentally normal in every measurable way, except that they were predisposed to early tumor development (primarily lymphomas and sarcomas). An initial indication that p53 has functions that extend beyond tumor suppression came from the observation that a fraction of *Trp53*$^{-/-}$ mouse embryos display developmental aberrations, including prominent defects in neural-tube closure and

consequent exencephaly (Armstrong, Kaufman et al. 1995; Sah, Attardi et al. 1995). Further examination of *Trp53*$^{-/-}$ adult mice recently revealed a role for p53 in embryo implantation, indicated by the dramatically low fertility rates observed in female *Trp53*$^{-/-}$ mice (Hu, Feng et al. 2007). Additional abnormalities have been described in the *Trp53* null embryos, including upper incisor fusion, ocular abnormalities and polydactyly of the hindlimbs (Armstrong, Kaufman et al. 1995). The incomplete penetrance might be due to the interaction of genetic and environmental factors. Sah et al. (Sah, Attardi et al. 1995) demonstrated that 129/Sv *Trp53* null embryos had a higher rate of exencephaly than null embryos of mixed 129/Sv-C57BL/6 background, suggesting that strain-specific modifier genes may influence the degree of penetrance. The discovery that an absence of p53 activity can lead to a fatal defect in a significant fraction of embryos clearly implicates p53 as an important factor in development.

In addition to its role in development and aging, recent studies have elaborated newly identified functions of p53 in several other physiological contexts. p53 is involved in restricting the self-renewal of several types of stem cells, including neural stem cells and hematopoietic stem cells (Meletis, Wirta et al. 2006; Cicalese, Bonizzi et al. 2009). Furthermore, several groups have reported enhanced efficiency of cellular reprogramming of somatic cells to induce pluripotent stem (iPS) cells in the absence of p53, implicating p53 in the maintenance of a differentiated state (Krizhanovsky and Lowe 2009).

1.10 *p53 and development in the context of other genetic deficiencies*

As a transcription factor, p53 has been demonstrated to regulate a number of genes involved in cell-cycle control, apoptosis, and checkpoint function (Gottlieb and Oren 1996; Ko and Prives 1996; Levine 1997). Moreover, p53 appears to bind an amazingly large number of proteins involved in growth control, DNA repair and transcriptional regulation. Given the

many molecular functions and interactions mediated by p53, it is perhaps not surprising that in the last few years it has been shown to influence developmental processes in the context of other genetically deficient knockout mice. Usually, this interaction takes the form of partial or complete rescue of an embryonic lethal phenotype following crosses of *Trp53*-deficient mice to a mouse deficient in a growth regulatory or DNA repair-related gene. Such crosses have provided important new insights into the interactions of *Trp53* and other genes during differentiation, development, DNA repair and growth control.

The most dramatic example of phenotype rescue by *Trp53* -deficiency was observed when *Mdm2* -deficient mice were crossed to *Trp53* -deficient mice (Jones, Roe et al. 1995; Montes de Oca Luna, Wagner et al. 1995). The *Mdm2* gene encodes a protein which directly binds to p53 and inhibits its normal transcriptional activation and tumor suppressor functions at least in part through p53 degradation. It has been found that *Mdm2* nullizygosity resulted in early embryonic lethality at roughly 6.5 days gestation (Jones, Roe et al. 1995; Montes de Oca Luna, Wagner et al. 1995). However, after crosses of *Trp53* -deficient mice to *Mdm2* heterozygous mice, double null *Trp53* and *Mdm2* mice were found to be completely viable with no obvious developmental abnormalities. Interestingly, rescue of the *Mdm2* null embryonic lethality could not be achieved by substituting *p21WAF1/CIP1* nullizygosity for *Trp53* nullizygosity, suggesting that abrogation of the G1 arrest checkpoint function of p53 was not involved in the (Montes de Oca Luna, Amelse et al. 1997)).

Another example of rescue by *Trp53*-deficiency was illustrated in the *Rad51- Trp53* knockout mouse crosses (Lim and Hasty 1996).

Nullizygous embryos deficient in the *Brca1* and *Brca2* tumour suppressors have also been partially rescued by the absence of p53 (Hakem, de la Pompa et al. 1997; Ludwig, Chapman et al. 1997).

Tissue-specific partial rescue by p53 deficiency was observed in *ATM*-null mice, the genetic model for the human disorder ataxia telangiectasia, characterized by various neurological malfunctions, infertility and increased tumour susceptibility (Barlow, Liyanage et al. 1997)

Trp53 deficiency, caused by germ-line mutation or by pifithrin-α, a p53 inhibitor, rescues neural tube defects in *Pax-3*-deficient *Splotch* (*Sp/Sp*) embryos (Pani, Horal et al. 2002) and prevented the defective cardiac neural crest migration and apoptosis in *Pax3*-deficient embryos, restoring proper development of cardiac outflow tract (Morgan, Lee et al. 2008). Inhibition of p53 also prevents cyclin G1-driven apoptotic elimination of neural crest cells while rescuing the craniofacial abnormalities associated with mutations in *Tcof1* (Jones, Lynn et al. 2008).

Together, these findings underscore the importance of p53 in diverse pathological states and indicate that p53 inhibitors might be promising therapeutics for these diseases.

2.1 *To establish the effect of Tbx1 on the cell proliferation*

Tbx1 has a critical role in splanchnic mesoderm of the Second Heart Field (SHF), which gives cardiomyocyte progenitor cells of the OFT and right ventricle. It was further observed that the loss of function of *Tbx1* in the SHF is associated with a reduction of cell proliferation. The reduced cell proliferation in the SHF is associated with reduced contribution of cells to the OFT and, consequently, to a reduced number of muscle cells.

To understand the functional and molecular basis of Tbx1 action to promote cell proliferation I analyzed cell proliferation and more specifically cell cycle, modulating *Tbx1* expression, and I analyzed molecular markers that are direct or indirect *Tbx1* targets, necessary to promote cell proliferation.

2.2 *Rescue strategies in a mouse model of DiGeorge syndrome.*

Deletion 22q11.2 syndrome is the most frequent known microdeletion syndrome and is associated with a highly variable phenotype. This syndrome constitutes a major cause of congenital heart disease (CHD), accounting for about the 5% of all CHD cases among live births. Of the about 30 commonly deleted genes, *Tbx1* is the only gene that, after an extensive functional analysis in the mouse, has been found to be haploinsufficient with a convincingly similar phenotype to the human syndrome. So it is a very frequent and complicated syndrome, and although there have been many studies related to the role of *Tbx1* during development, they do not yet arrived to the identification of drugs that could

rescue the mutant phenotype. I therefore, searched for genetic and pharmacologically strategies that could counteract the effects of reduced dosage of *Tbx1*.

The transcription factor p53, which is encoded by the *Trp53* gene, has pro-differentiation and anti-proliferation activities in stem cells, and its loss of function facilitates reprogramming of differentiated cells. Therefore, we asked whether *Tbx1* and *Trp53* interact during cardiovascular development.

3.1 Mouse mutant lines

Lines *Tbx1*^{lacZ} (here referred to as *Tbx1*$^{-}$) (Lindsay, Vitelli et al. 2001), *Tbx1*^{neo2} (Zhang, Huynh et al. 2006) and *Trp53*$^{-}$ mutant (Jacks, Remington et al. 1994) where maintained in our SPF colony in a mixed C57Bl6/129SvEv background and genotyped according to the original reports. For timed crosses, developmental stage was evaluated by considering the morning of vaginal plug as E0.5. Pifithrin-α (Enzo Life Sciences, #BML-GR325) was diluted in PBS and injected at 2.2 mg/kg body weight. Injections were carried out intraperitoneally at E7.5, E8.5, and E9.5. Controls were injected with the same amount of carrier, but without drug.

Mouse were genotyped by PCR using DNA extracted from tail biopsies, using following primer pairs:

Tbx1^{lacZ}: Tbx1WT-F (5'-AGTCTGGGGACTCTGGAAGG-3')
Tbx1WT-R (5'-AAGGCAGATCCTGCTACACC-3')
Tbx1 Tar2R (5'-TCGACTAGAGCTTGCGGAAC-3')

Tbx1^{Neo2}: Tbx1Neo2-F (5'- GACTAGAGACAGGGGCATGG-3')
Tbx1Neo2-TF (5'- GCCAGAGGCCACTTGTGTAG-3')
Tbx1Neo2-R (5'- AGGCTGGGATTCCAAAAGAC-3')

Trp53: Trp53 WT-F: (5'-ACAGCGTGGTGGTACCTTAT-3')
Trp53 Mut-F: (5'-CTATCAGGACATAGCGTTGG-3')
Trp53 WT-R: (5'-TATACTCAGAGCCGGCCT-3')

PCR products have been separated on 2% agarose gels.

3.2 Culture and in vitro transfection of mES cells and C2C12 myoblasts

mES cells were culture in Glasgow minimal essential medium (GMEM) supplemented with 15% fetal bovine serum (FBS), 1mM sodium pyruvate, 1X non-essential amino acids (NEAA), 1 : 500 b-mercaptoethanol (BME) and 1000 U/mL leukemia inhibitory factor (mLIF), on gelatin-coated dishes. For *Tbx1* over-expression, I used the Amaxa nucleofector (using the standard protocol for stem cells); cells were collected 24 h after transfection for RNA extraction.

Mouse C2C12 myoblasts were cultured in DMEM supplemented with 10% FBS and 10^5 cells were plated in 6 wells plate. The next day, cells were transiently transfected using Lipofectamine 2000 according to the manufacturer's instructions; cells were collected 24 h after transfection for RNA extraction.

3.3 Culture and differentiation of P19CL6 cell line

P19CL6 cells were grown in MEM Eagle Alpha Modification (Sigma Aldrich, #M4526) supplemented with 10% FBS. To induce cardiomyocyte differentiation, I used a published protocol (Mueller, Kobayashi et al. 2010). Briefly, $3x10^6$ P19CL6 cells were plated on a 100 mm tissue culture dish. The next day (day 0 of differentiation), cells were treated with 10 μmol/L 5-Azacytidine (Sigma Aldrich, #A2385) for 24h, and subsequently, cells were incubated with 1% DMSO.

3.4 Silencing of *Trp53* by siRNA

For *Trp53* silencing, P19CL6 cells were differentiated as described above. At day 0 of differentiation, cells were transfected with anti-p53 siRNA (Sigma, 5'-CCACUUGAUGGAGAGUAUU-3') to knockdown p53 expression, using Lipofectamine RNAiMAX Reagent (Invitrogen, #13778-150) following the standard protocol. Non-targeting siRNA (5'- GUCGUAACGUCGAUUAUAG-3') was used for control transfections. 24 h after transfection, cells were transfected again at the same conditions and collected 24 h after the second transfection (day 2 of differentiation). mRNA expression was evaluated by quantitative real-time PCR and protein expression by western blotting.

3.5 Cell cycle analysis and Proliferation assay

For cell cycle analysis I used an inducible (*Tbx1*-TetOFF) system, in which the presence of Tetracycline (Tc) in the culture medium turns off expression of a transgenic construct, while the removal of Tc from culture medium, induces *Tbx1* expression.
In this experiment, *Tbx1* expression was induced for 5 and 24h, cells were collected and 1.2 x 10^6 cells were fixed with 70% Ethanol on ice for 30 minutes. Samples were treated with RNase A, 100 μg/mL, and then stained with a DNA dye, 20 μg/mL propidium iodide (PI), and after at least 30 minutes, they were analyzed by flow cytometry (Becton Dickinson FACSAria) to measure DNA content.

For proliferation assay, C2C12 cells were labeled with 10 μmol/L 5-(and-6)-Carboxyfluorescein Diacetate, Succinimidyl Ester (5(6)-CFDA, SE; CFSE), (Life Technologies, # C1157) and 10^5 cells were plated in 6 wells plate, grown in Dulbecco's Modified Eagle Medium (Sigma, #D5671) supplemented with 10% fetal bovine serum. The next day, cells were transfected with a *Tbx1* expression vector or with empty vector (with

Lipofectamine 2000, Invitrogen #11668-019, using the standard protocol). Cells where collected after 24h and analyzed by flow cytometry.

3.6 RNA extraction, reverse transcription and q real-time PCR

RNA was isolated from whole E8.5 WT, *Tbx1*$^{+/-}$, *Trp53*$^{+/-}$ and *Tbx1*$^{+/-}$;*Trp53*$^{+/-}$ embryos, from C2C12 cells or from P19CL6 cells (Mueller, Kobayashi et al. 2010) using Trizol reagent (Invitrogen, #15596018). Prior to procede to reverse transcription, RNA samples were treated with DNAse I (Invitrogen). First strand cDNA synthesis was performed on 300 ng of RNA from E8.5 embryos and 1 μg of RNA from cultured cells using the High-Capacity cDNA Reverse Transcrition Kit, with oligo (dT)12-18 and random primers (Applied Biosystems, #4368814). mRNA expression was evaluated by quantitative real-time PCR carried out using FastStart Universal SYBR Green (Roche, #04913850001), on a 7900HT Fast Real-Time PCR System (Applied Biosystem). All samples were run in triplicates, by using 2 μl of cDNA (diluited 1:10 in water) in 20 μl reaction volumes. The cycle threshold (Ct) was determined during the geometric phase of the PCR amplification plots, as recommended by the manufacturer. Relative differences in transcript levels were quantified using the ΔΔCt method and normalized to Gapdh expression reference. All PCR were performed using primers that amplify across an intron. The following primer sequences were used:

Cdkn1a-F: 5'-CTGCCCAAGGTCTACCTGAG-3'

Cdkn1a-R: 5'-TGCAGAAGACCAATCTGCGC-3'

Cdkn1b-F: 5'-GGAGCAGTGTCCAGGGATGAGG-3'

Cdkn1b-R: 5'-GGCCCTTTTGTTTTGCGAAG-3'

Gapdh-F: 5'-TGCACCACCAACTGCTTAGC-3'

Gapdh-R: 5'-TCTTCTGGGTGGCAGTGATG-3'

Gbx2-F: 5'-GCTGCTCGCTTTCTCTGC-3'

Gbx2-R: 5'-GCTGTAATCCACATCGCTCTC-3'

Smad7-F: 5'-AACGAGAGTCAGCACTGCCA-3'

Smad7-R: 5'-GAAGGTGGTGCCCACTTTCA-3'

Tbx1-F: 5'-CTGACCAATAACCTGCTGGATGA-3'

Tbx1-R: 5'-GGCTGATATCTGTGCATGGAGTT-3'

Trp53-F: 5'- GCAACTATGGCTTCCACCTG-3'

Trp53-R: 5'-TTATTGAGGGGAGGAGAGTACG-3'

Wnt5a-F: 5'-CTCCTTCGCCCAGGTTGTTATAG-3'

Wnt5a-R: 5'-TGTCTTCGCACCTTCTCCAATG-3'

3.7 Ink injection and histological staining

Ink injection was performed on E10.5 embryos, which were collected and injected intracardially with India ink, and fixed in 4% paraformaldehyde. Embryos were then dehydrated and cleared in 1:1 benzyl benzoate:methyl salicylate.

Hearts collected from E18.5 embryos were fixed in 4% paraformaldehyde over night at 4°C, embedded in paraffin and cut into 10 μm sections. Histological staining was

performed using eosin and counterstaining was performed using Nuclear Fast Red (Vector Lab., #H-3403).

3.8 Immunohistochemistry

For proliferation studies, E9.5 embryos were fixed in 4% paraformaldehyde over night at 4°C, embedded in paraffin and cut into 7 μm sections. Immunohistochemistry on paraformaldehyde fixed paraffin sections was performed as follows. Sections were deparaffinized by two 10 minutes incubations in BioClear (a synthetic form of Xylene), followed by rehydratation in ethanol series, beginning at 100% ethanol and ending in 50% ethanol. This was followed by heat mediated antigen retrieval in 0.01 M citrate buffer, pH 6.0, for 5 minutes at 100% microwave power followed by 15 minutes at 70% power. Antigen retrieval methods serve to break the methylene bridges formed during fixation which cross-links proteins and therefore mask antigen sites. After antigen retrieval, sections were blocked in 3% bovine serum albumin (BSA), 5% newborn calf serum (NBCS), 20mM $MgCl_2$, 0.3% Tween-20, 1% milk for 1hr and then incubated with primary antibody, anti phospho-Histone H3 (Ser10), diluted 1:200 in blocking solution over night at 4°C. Sections were washed in PBS and incubated for 1 hour in horseradish peroxidase (HRP)-conjugated anti-rabbit IgG (Vector Laboratories) diluted 1:200 in blocking solution. Finally, samples were stained with DAB (Vector Laboratories). I counted Phospho-Histone H3 (PH3) positive and negative cells in the SHF (at least 2000 cells per embryo) of three somite-matched embryos per genotype.

3.9 Western blotting

Total proteins were extracted after cell lysis with the RIPA buffer (1% NP40, 0.5% NaDoc, 150 mM NaCl, 0.1% SDS, 50mM Tris HCl pH8.0, 1 X protease inhibitor (Roche)). Nuclear and cytoplasmic proteic extracts were prepared using the NE- PER Nuclear and Cytoplasmic Extraction Reagents (Thermo Scientific). Lysates were incubated for 3 min at 95°C to allow protein denaturation. The concentration of protein was determined using a Bredford Protein Assay kit (Biorad) according to the manufacturer's instructions. Equal amount of proteins were loaded on gel and separated by SDS-PAGE, transferred to a Protran Nitrocellulose Hybridization Transfer Membrane 0.2 µm pore size (Amersham), and blocked for 1 h at room temperature in TBST (150 mM NaCl, 10 mM Tris- HCl, pH 7.4, and 0.05% Tween)-powdered milk. The membranes were incubated overnight at 4°C in primary antibodies diluted in TBST-5% milk. The primary antibodies were rabbit anti-TBX1 (Abcam, 1:500), rabbit anti-p53 (Santa Cruz Biotechnology, 1:1000), monoclonal anti-Smarcd1 antibody (BD Bioscience, 1:1000), and rabbit-anti-beta-Actin (Sigma-Aldrich, 1:10000). Next, membranes were rinsed 3 times with TBST for 5 min each, and then they were incubated for 1 h at RT with horseradish peroxidase (HRP)-linked secondary antibodies (diluted in TBST-5% milk). The secondary antibodies were: HRP-conjugated anti-rabbit and anti-mouse antibodies (GE Healthcare, 1:5000 and 1:10.000). Membranes were rinsed 3 times with TBST for 5 min each, and the HRP-derived signal was detected using the Amersham ECL and ECL Plus Western Blotting Detection Reagents (GE Healthcare).

3.10 Co-immunoprecipitation

P19CL6 cells ($2x10^5$) were plated on a 100 mm culture dish. The next day, cells were transfected with a *Trp53* expression vector or with empty vector. Cells were collected after

48h, and 200 μg of nuclear extracts were immunoprecipitated with 2 μg of an anti TBX1 antibody (Abcam, #ab18530), or with 2 μg of rabbit IgG (Santa Cruz Biotechnology, #2027) as a negative control and then incubated with 20 μl of Protein A/G PLUS Agarose (Santa Cruz Biotechnology, #sc-2003) at 4°C over night. The samples were washed 7 times with IPP150 buffer (10 mmol/L Tris-HCl, pH 8.0, 150 mmol/L NaCl, 0.1% NP-40) and resuspended in SDS sample buffer. 10% of input and immunoprecipitated samples were used for Western blot analysis. We used an anti p53 antibody (Santa Cruz Biotechnology, #sc-6243) and an anti Smarcd1 antibody (BD Bioscience, #611728).

3.11 Chromatin Immunoprecipitation

For ChIP assay, P19CL6 cells were collected at day 2 of differentiation. Cells were fixed with 1% formaldehyde diluted in PBS and Buffer A (Transcription Factor ChIP Kit reagent, Diagenode, #Kch-redTBP-012) at room temperature for 10 min. The cross-linking reaction was stopped using 0.125 mol/L glycine at room temperature. Cells were collected by scraping with cold PBS, cells were then lysed and chromatin was sonicated to obtain 150-350 bp fragments using S2 Covaris System (Duty Cycle: 5%, Intensity: 3, Cycles/Burst: 200, Cycles: 5, Cycles time: 60 sec, Temperature: 4°C). 6 μg of sonicated chromatin was immunoprecipitated with 5 μg of a TBX1 antibody (Abcam, #ab18530), 5 μg of a p53 antibody (Santa Cruz Biotechnology, #sc-6243 X), or 5 μg of Rabbit Control IgG (Abcam, #ab46540). Samples were then incubated with 30 μl of Pre-blocked protein A/G coated beads at 4°C over night. After incubation, the samples were washed and DNA-protein-antibody complexes were eluted in Buffer F of the above mentioned kit, at room temperature for 25 min. To reverse cross-linking, samples were incubated at 65°C over night. Phenol/chloroform-purified and ethanol-precipitated DNA was resuspended in 200 μl of H_2O and equal DNA amounts of input and immunoprecipitated DNA were subjected to qPCR

amplification. ChIP signals were normalized to that of an internal control amplimer selected from an ORF-free region of mouse chromosome 14 (Chen, Fulcoli et al. 2012).

The following primer sequences were used:

Gbx2TBE1-F: CTAGGAGGTGCCTCTGAGTTCT

Gbx2TBE1-R: ACCACCATGGAGAGGCCCTAA

Gbx2TBE2-F: TCACAGCACTAAAGTTAGAGAGG

Gbx2TBE2-R: GCCTTGGAAGAGCGACCTGTA

Gbx2TBE3-F: GAGAGCGTTGAGTTCTGAGTGC

Gbx2TBE3-R: GGACCGTGAAAAGAGTCCAGC

Gbx2TBE4-F: CAGGGAGGACGGGATGGAATAA

Gbx2TBE4-R: GCTGATTAATGAGACCCACGAG

Gbx2p53BE1-F: ATTGCGGCGAAAGGAAAGT

Gbx2p53BE1-R: CCACGAAAGGATCCCATTTT

Gbx2p53BE2-F: GTCCTGCAGTCCGTCGTC

Gbx2p53BE2-R: GAGGAGCGCGATTTAAAGGT

Gbx2p53BE3-F: TCGGGGATACGCAGTCTTAG

Gbx2p53BE3-R: TTTAGTGCTGTGACCGAAGC

Gbx2p53BE4-F: GCACCCATGCATTCCATC

Gbx2p53BE4-R: GCCGATGCCGAAAATTCTA

INT-XIV-1F: TTCTTGTCCACAGCCCTCTT

INT-XIV-1R: TGGTGGAAGAGGAGACATCC

3.12 ChIP and Western blotting

For ChIP-WB, sonicated chromatin (obtained as described above) was immunoprecipitated with 10 μg of the TBX1 antibody, 10 μg of the p53 antibody, or 10 μg of Control Rabbit IgG; all antibodies were conjugated with Dynabeads Protein G (Novex by Life Technologies, #10004D). To avoid co-elution of antibodies, they were then cross-linked to the Dynabeads using 20 mmol/L Dimethyl pimelimidate dihydrochloride (Sigma Aldrich, D8388), before continuing with immunoprecipitation. Approximately 50 μg of sonicated chromatin was immunoprecipitated at 4°C over night. Samples were then washed 6 times with cold PBS-0.01% Tween-20 and DNA-protein complexes were eluted in 50 μl of 0.1 mol/L Glycine, pH 2.6 at room temperature, for a total of 3 elutions. Reverse cross-linking was done at 95°C for 30 min in SDS sample buffer. 10% of input and immunoprecipitated samples were detected using Western blot analysis.

3.13 Cloning, plasmids

We have previously described the pCDNA-*Tbx1*-3xHA expression vector (Chen, Fulcoli et al. 2012). pCAG-*Trp53* expression vector was kindly provided by Prof. A. Fusco (University Federico II, Naples).

For luciferase assay, I cloned a 1500 bp fragment of *Gbx2* 3' gene into pGL3 promoter vector (Promega). Briefly, I amplify this fragment with the following primers:

Gbx2Luc-F: 5'-CCCCCATCAGAATTAATCATTG-3'

Gbx2Luc-R: 5'-GAAGAGCGACCTGTAAAGCG-3'

The fragment was cloned into pCRII-TOPO and plasmid was purified from positive DH5α bacterial colonies and digested with KpnI and XhoI restriction enzymes. The same restriction enzymes were used to digest pGL3-Promoter Vector, in which the insert was cloned. Ligation reaction was performed by using T4 DNA ligase enzyme (New England Biolabs) and samples were incubated over night at 16°C.

3.14 Luciferase assay

For luciferase assay, human JEG3 choriocarcinoma celFls were plated in 24-wells and transfected with X-tremeGENE DNA Transfection Reagent (Roche) according to the manufacturer's instructions. Increasing amount of *Trp53* expression vector and equal amount of Gbx2Luc reporter construct were always co-trasfected with a pCMV-β-Gal expression vector (Clonotech). 24 h after transfection, cell extracts were prepared and activities of β-galactosidase and firefly luciferase were measured using the Luciferase Assay System (Promega) and the Beta-Glo Assay System (Promega) respectively, on a Sirius Single Tube Luminometer (Titertek Berthold). Relative luciferase activity (firefly luciferase for reporter and b-galactosidase for normalization of transfection efficiency) was measured following manufacturer's instructions (Promega); to correct for transfection efficiency, the luciferase activity was divided by the β-galactosidase activity in every case. The data represent the means and standard deviations of six independent experiments.

4.1 *Tbx1-enhanced cell proliferation is associated with down regulation of p21 and p27 expression in cultured cells.*

Tbx1 alters cell proliferation through different pathways, for example, by positive regulation of the FGF-MAPK pathway (Vitelli, Lania et al. 2010) or negative regulation of BMP-SMAD1 signaling (Fulcoli, Huynh et al. 2009). Increased proliferation in response to increased *Tbx1* dosage occurs in several cell types in culture, for example differentiating mouse ES cells (Chen, Fulcoli et al. 2009), or undifferentiated mouse ES cells overexpressing *Tbx1*. I performed cell cycle analysis using an inducible (*Tbx1*-TetOFF) system previously established in our laboratory using the ROSA-TET system described by Masui et al. (Masui, Shimosato et al. 2005). The Tet-off system is based on a Tc-regulatable transactivator (tTA), which induces transcription in the absence of Tc or its analog doxycycline (Dox) through binding to the hCMV-1 promoter. This promoter is composed of a Tc-responsive element (TRE) followed by a minimal promoter of the human cytomegalovirus (hCMV) immediate early gene. The tTA protein is a fusion protein composed of the TRE-binding domain of Tc repressor protein and the herpes simplex virus VP16 activation domain (Gossen and Bujard 1992). The ROSA-TET system allows researchers to establish ES cell lines carrying a Tc-regulatable transgene at the ROSA26 locus. This locus was first described as a gene-trapped locus on chromosome 6 (Zambrowicz, Imamoto et al. 1997). This locus is now regarded as one from which proteins can be expressed ubiquitously at a moderate level. A knock-in strategy into the *ROSA26* locus, however, still requires homologous recombination. The ROSA-TET system is based on a knock-in step of a construct carrying both loxP and its mutant sequences (loxPV) into the ROSA26 locus, followed by a subsequent exchange step that introduces a cDNA to be Tc-regulated to the locus, using the recombinase-mediated cassette exchange reaction (Fig. 15A).

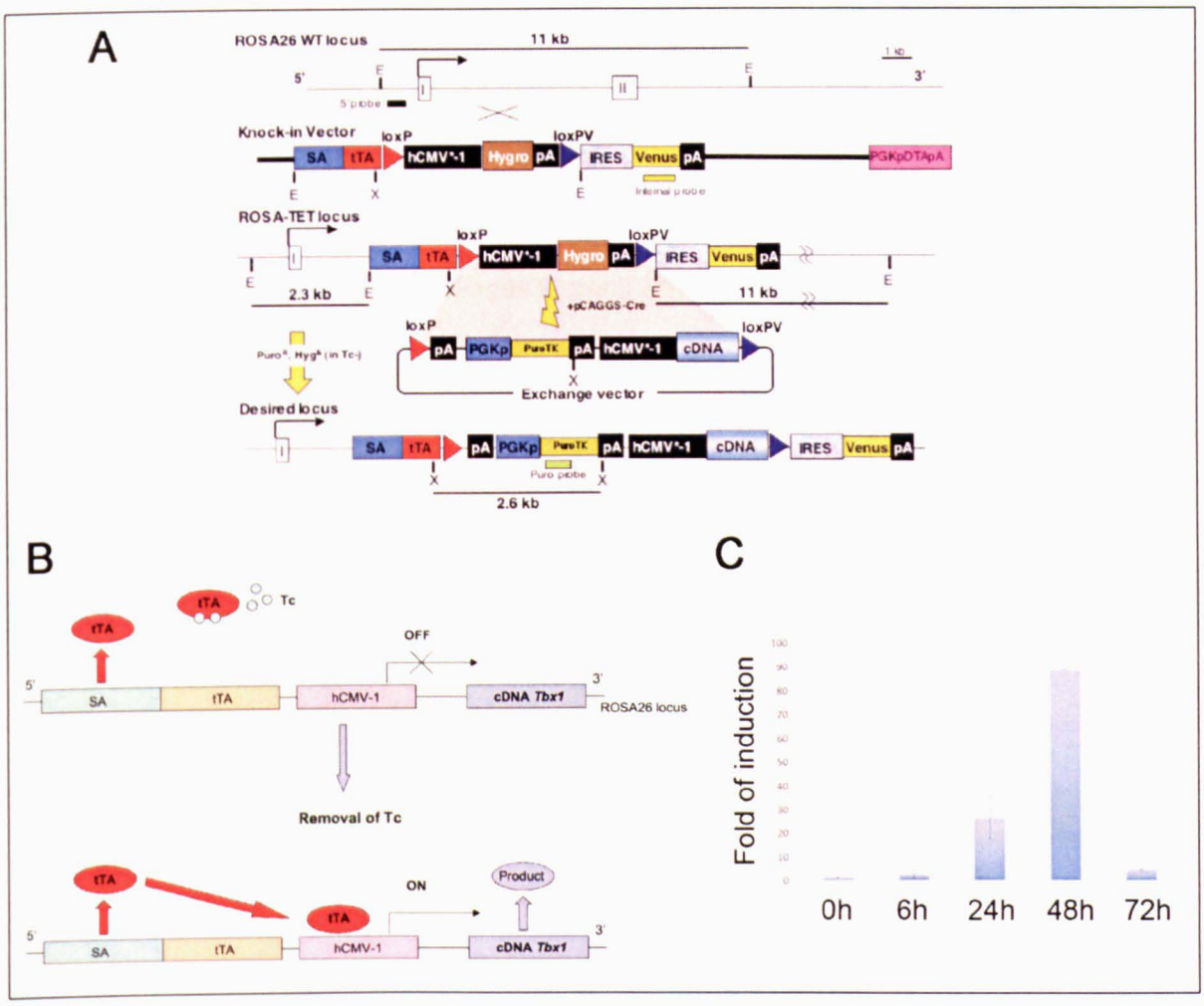

Figure 15: ***Development of the ROSA-TET system and induction of expression in that.*** (A) Experimental strategy to generate the ROSA-TET locus and the desired locus (Masui, Shimosato et al. 2005). (B) Schematic representation of the induction of *Tbx1* expression. (C) qRT-PCR on mRNA from EBRTcTbx1 cells grown in ES medium with and without Tc.

In our laboratory, an exchange vector carrying the *Tbx1* cDNA was cotransfected along with a Cre-expression vector into EBRTcH3 cells which had been derived from EB3 cells by the knock-in step, to establish an ES cell line (named EBRTcTbx1) expressing *Tbx1* under the control of the ROSA26 promoter in a Tc-dependent manner (Fig. 15B). In the absence of Tc in culture medium, tTA binds to the hCMV-1 promoter, inducing expression of *Tbx1*.

By qRT-PCR on mRNA from cells cultured for 6h, 24h, 48h and 72h in the absence of Tc, we observed a *Tbx1* mRNA level increased during time course, confirming the efficiency of the system (Fig. 15C).

Cell cycle analysis on this inducible system was performed after 5h and 24h of *Tbx1* expression. Results showed that *Tbx1* overexpression is associated with an increase of the percentage of cells in S and G2/M phases, compared to control cells (Fig. 16).

Figure 16: ***Tbx1 enhances cell cycle.*** 5h and 24h of *Tbx1* expression increases the percentage of mES cells in S and G2/M phases.

Similar results were obtained on mouse myoblastoid C2C12 cells analyzed by cell proliferation assay. Cells were stained at the moment of culture with Carboxyfluorescein Succinimidyl Ester (CFSE), a fluorescent cell staining dye capable to bind to the intracellular and membrane bound proteins. This dye can be used to monitor cell proliferation, due to the progressive halving of CFSE fluorescence within daughter cells following each cell division.

In my experiment, *Tbx1* was transiently over-expressed in C2C12 cells and after 24h from transfection, cells were analyzed by flow cytometry. Results showed that *Tbx1* over-expressing cells were in the fifth generation compared to the control cells that were in the fourth generation (Fig. 17A).

Then, I performed molecular analysis of cell cycle regulators. The expression levels of the positive regulators, *Cyclin A1*, *Cyclin D1*, *Cyclin D2*, *Cyclin D3* and *Cyclin E1* was not changed, while the expression analysis of negative cell cycle regulators, such as *Cdkn1a*, *Cdkn1b*, *Cdkn2a*, *Cdkn2b*, *Cdkn1c* showed that genes *Cdkn1a* and *Cdkn1b*, which encode the cell cycle inhibitors p21 and p27, respectively, are down regulated after transfection of *Tbx1* (Fig. 17B-D). Up regulation of p21 in response to loss of *Tbx1* was also noted during tooth bud development (Cao, Florez et al. 2010). These findings suggest that the positive regulation of cell cycle by Tbx1 may function through negative regulation (direct or indirect) of cell cycle inhibitors.

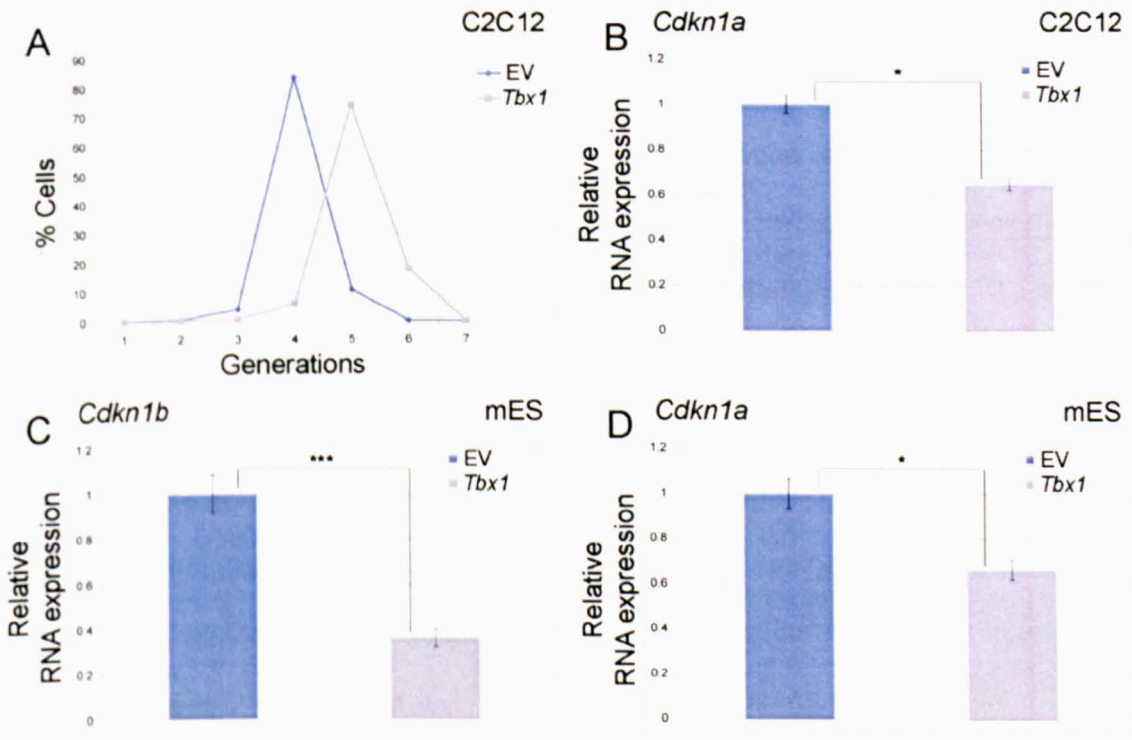

Figure 17: ***Tbx1 enhances cell proliferation and suppresses cell cycle inhibitors expression in cultured cells.*** (A) Cell cycle analysis of C2C12 cells control (EV) and

transfected with a Tbx1 expression vector (*Tbx1*). Transfected cells proliferate faster than control cells.
(B-D) Quantitative real time PCR evaluation of expression of the genes indicated with and without Tbx1 overexpression in C2C12 cells (B) and in mouse embryonic stem (mES) cells. In all cases, the expression is significantly reduced after transfection of a *Tbx1*-expressing vector. *: P= 0.039; **: P= 0.018. Error bars indicate SEM of experiments done in triplicate.

4.2 *Epistatic genetic interaction between Trp53 and Tbx1.*

Tbx1 regulates the homeostasis of cardiac progenitor cells (Chen, Fulcoli et al. 2009), self renewal of stem cells of the hair bulb (Chen, Fulcoli et al. 2012), and stem cells of the tooth bud (Cao, Florez et al. 2010), suggesting that the gene plays a role in the maintenance of a pool of stem/progenitor cells through promotion of cell proliferation and inhibition of differentiation in different tissues. We reasoned that p53 suppression might ameliorate the negative effects of reduced *Tbx1* dosage because it suppresses self renewal and promotes differentiation of stem cells (Jain, Allton et al. 2012; Meletis, Wirta et al. 2006). In addition, because *Cdkn1a* is negatively regulated by Tbx1 and positively regulated by p53, reduced dosage of the latter protein may buffer the effect of Tbx1 on *Cdkn1a* expression.

We crossed *Trp53*$^{+/-}$ and *Tbx1*$^{+/-}$ mice and harvested embryos at E10.5 in order to test whether there is a genetic interaction between *Tbx1* and *Trp53*, and to check if suppression of p53 is sufficient to rescue or ameliorate defects observed in *Tbx1*$^{+/-}$ mutant embryos, and test its effects on the typical haploinsufficiency phenotype, i.e. hypoplasia or aplasia of the 4th pharyngeal arch arteries (4th PAAs) (Jerome and Papaioannou 2001; Lindsay, Vitelli et al. 2001; Merscher, Funke et al. 2001). We analyzed, by intracardiac ink injection, a total of 56 embryos and the results are summarized on Tab. 1A.

A

Genotype (E10.5)	Normal	4th PAA defects
$Tbx1^{+/+}$	16	0
$Tbx1^{+/-}$	1	12 (92%)
$Trp53^{+/-}$; $Tbx1^{+/-}$	10	1 (9%) *
$Trp53^{+/-}$	16	0

* P=0.00004

B

Genotype (E10.5)	Pifithrin-α	Normal	4th PAA defects
$Tbx1^{+/+}$	Untreated	10	0
	Treated	7	0
$Tbx1^{+/-}$	Untreated	0	10 (100%)
	Treated	14	5 (36%) *

* P=0.00016

Table 1: *Rescue of fourth pharyngeal arch artery defects by genetic or pharmacological suppression of p53.* (A) Genetic experiment. (B) Treatment with Pifithrin-α.
PAA: pharyngeal arch artery. "Normal" refers to the pattern of the PAA system.

WT and *Trp53*$^{+/-}$ embryos were all normal (n=32) while *Tbx1*$^{+/-}$ where mostly abnormal (12 out of 13 embryos or 92%). Double heterozygous *Trp53*$^{+/-}$;*Tbx1*$^{+/-}$ embryos, however, were mostly normal (10 out of 11 embryos, or 91%, P=0.00004). Examples of ink injection data are shown on Fig. 18. As shown, in WT embryos (Fig. 18A) all three PAAs (the 3rd, the 4th and the 6th) are developed, in *Tbx1*$^{+/-}$ embryos (Fig. 18B) there is aplasia of the 4th PAA, that is rescued in *Trp53*$^{+/-}$;*Tbx1*$^{+/-}$ embryos (Fig. 18C). Therefore, *Trp53* deletion almost completely rescues this particular phenotype.

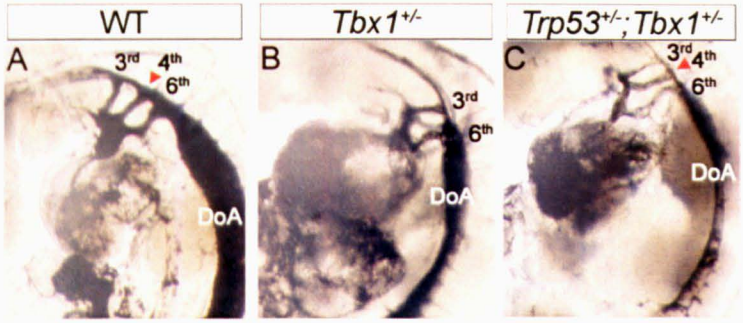

Figure 18: ***Trp53 deletion rescues the 4th PAA defects in Tbx1$^{+/-}$ embryos.***
Examples of ink injections assays for the visualization of the pharyngeal arch arteries in E10.5 embryos. (A) Ink-injected, WT E10.5 embryo showing the normal anatomy of the 3rd, 4th and 6th pharyngeal arch arteries on the left. (B) Ink-injected, *Tbx1*$^{+/-}$; *Trp53*$^{+/+}$ E10.5 embryo. Note the absence of the left 4th PAA. (C) Ink-injected, *Tbx1*$^{+/-}$; *Trp53*$^{+/-}$ E10.5 embryo. Note the presence and normal anatomy of the 4th PAA.
Arrowheads indicate the 4th PAA.

4.3 *p53 transient pharmacological inhibition rescues the Tbx1 haploinsufficiency phenotype*

To exclude that in *Trp53*$^{+/-}$;*Tbx1*$^{+/-}$ embryos, *Tbx1* haploinsufficiency phenotype rescue was due to a gene mutation linked to the mutant *Trp53* allele or to genetic background, we used an alternative approach to inhibit *Trp53*, therefore we repeated the

experiment using pharmacological suppression of p53 with a specific inhibitor of p53, Pifithrin-α, (Komarov, Komarova et al. 1999) and the effect of this drug was examined. Timing of drug administration to pregnant females was based upon our previous findings showing that *Tbx1* is required for 4th PAA development as early as E7.5 but it is not longer required after E9.5 (Xu, Cerrato et al. 2005). Therefore, we injected Pifithrin-α into pregnant females at E7.5, E8.5 and E9.5, and harvested embryos at E10.5 to score the 4th PAA phenotype. Results (Tab. 1B) showed again a significant suppression of the 4th PAA defect (P=0.00016). Thus, reduced dosage of p53, either provided by permanent deletion of the gene or by temporary restricted pharmacological inhibition, has a significant suppressing effect upon the *Tbx1* haploinsufficiency phenotype.

4.4 *Trp53 mutation modifies the hypomorphic but not the null Tbx1 phenotype.*

Reduced p53 dosage may suppress the *Tbx1* mutant phenotype indirectly, e.g. through a compensatory mechanism that buffers the consequences of loss of *Tbx1*, or it may act more specifically by interacting with the normal transcriptional functions of Tbx1. While these hypotheses are not mutually exclusive, if the second mechanism is significant, the Tbx1 protein must be present for the rescue to occur. Therefore, we first tested whether *Trp53* mutation can modify the intracardiac phenotype of $Tbx1^{-/-}$ embryos. To this end, we crossed $Tbx1^{+/-}$; $Trp53^{+/-}$ and $Tbx1^{+/-}$; $Trp53^{+/+}$ mice and harvested embryos at E18.5, when the cardiac phenotype can be fully assessed morphologically. Results, summarized on Fig. 19A, confirmed the rescue of the haploinsufficiency phenotype also at this developmental stage, but revealed that $Tbx1^{-/-}$;$Trp53^{+/+}$ and $Tbx1^{-/-}$; $Trp53^{+/-}$ embryos were phenotypically indistinguishable (Fig. 19) presented with TAC, that communicates exclusively with the right ventricle, and VSD.

A

Genotype		E18.5	
Tbx1	*Trp53*	Normal	CV defects
+/+	+/+	13	0
+/+	+/-	9	0
+/-	+/+	5	11 (a)
+/-	+/-	19 *	3 (a)
-/-	+/+	0	10 (b)
-/-	+/-	0	6 (b)

* 0.00051

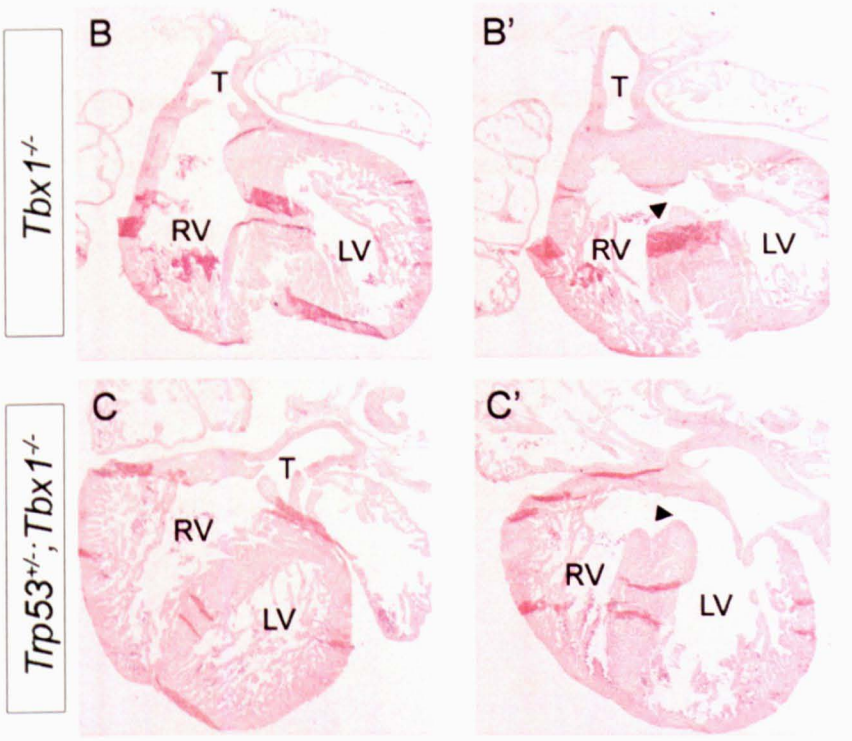

Figure 19: ***Trp53 ablation in a Tbx1 null background causes severe cardiovascular abnormalities as in Tbx1$^{-/-}$ embryos.*** (A) Tabulated summary of cardiovascular phenotype in E18.5 *Tbx1* mutants with and without *Trp53* deletion. Normal: refers to heart phenotype; CV defects: refers to cardiovascular defects observed in *Tbx1* $^{+/-}$ and *Tbx1*$^{-/-}$ embryos. Rescue of the aortic arch haploinsufficiency phenotype was confirmed at E18.5 (asterisk). (B-C') Histological section of E15.5 embryo hearts showing essentially the same phenotype with or without *Trp53* ablation. (B-B') Two different sections of the same heart of a *Tbx1*$^{-/-}$ embryo, showing truncus arteriosus communis (T) communicating with the right ventricle and ventricular septal defects (arrowhead). (C-C') Two different sections of the same heart of a *Tbx1*$^{-/-}$;*Trp53*$^{+/-}$ embryo showing the same phenotype an in *Tbx1* null embryo.
T: truncus arteriosus communis; RV: right ventricle; LV: left ventricle.

Next, we used the hypomorphic allele *Tbx1*^{neo2}, which expresses approximately 15% of the *Tbx1* mRNA compared to the WT allele (Zhang and Baldini 2008). We crossed *Tbx1*$^{+/-}$;*Trp53*$^{+/-}$ and *Tbx1*$^{+/neo2}$;*Trp53*$^{+/+}$ mice and harvested embryos at E18.5. A tabulated summary of cardiac phenotyping data is shown in Fig. 20A. The external appearance of *Tbx1*$^{-/neo2}$;*Trp53*$^{+/+}$ and *Tbx1*$^{-/neo2}$;*Trp53*$^{+/-}$ embryos was indistinguishable and embryo dissection showed that both genotypes had absence or severely hypoplastic thymus. However, cardiac phenotyping revealed some important differences. Most notably, 3 of the 18 *Tbx1*$^{-/neo2}$;*Trp53*$^{+/-}$ embryos examined (17%) showed a normally septated heart (Fig. 20B-C'), while all the 17 *Tbx1*$^{-/neo2}$;*Trp53*$^{+/+}$ embryos examined had a complex septation defect (see for examples Fig. 21 panels A, B, E, F).

A

Genotype (E18.5)	n	Normal	VSD	DORV	Incomplete TA	TA
Tbx1$^{-/Neo2}$	17	0	0	13	3	1
Trp53$^{+/-}$; *Tbx1*$^{-/Neo2}$	18	3	1	6 + 2(ovAo)	4 + 1(ovTA)	1

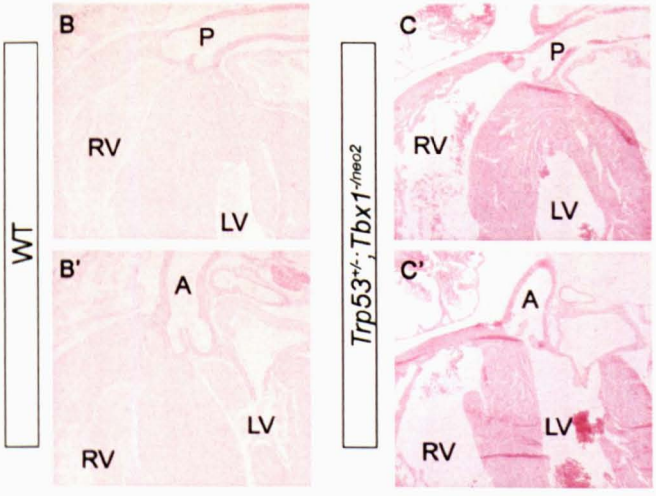

Figure 20: ***Trp53 deletion ameliorates the outflow tract phenotype in Tbx1 hypomorphic mutants.*** (A) Tabulated summary of cardiovascular phenotype in hypomorphic mutants with and without *Trp53* deletion.
n: total number of embryos examined with the genotype indicated. Normal: refers to heart phenotype; VSD: ventricular septal defects; DORV: double outlet right ventricle; TA: Truncus

arteriosus communis; ovAo: overriding aorta; ovTA: overriding of (unseptated) truncus arteriosus.
Histological sections of E18.5 embryo hearts showing complete rescue of ventricular and conotruncal septation. (B-B') Two different sections of the same heart of a WT littermate of the embryo shown in C-C'. (C-C') Two different sections of the same heart of a *Tbx1*$^{-/neo2}$;*Trp53*$^{+/-}$ embryo. Note the normal septation of the great arteries and ventricles, similar to WT embryos.
A: Aorta; P: Pulmonary trunk; RV: right ventricle; LV: left ventricle.

In addition, 3 *Tbx1*$^{-/neo2}$;*Trp53*$^{+/-}$ embryos presented with a milder form of double outlet right ventricle (DORV) or incomplete truncus arteriosus (TA). In these cases, the aorta or the truncus arteriosus were overriding the ventricular septum, while in *Tbx1*$^{-/neo2}$;*Trp53*$^{+/+}$ embryos they originated from the right ventricle (Fig. 21). This indicates that *Trp53* mutation improves the alignment between the outflow tract and the ventricles. Furthermore, we found a single case of isolated VSD among the *Tbx1*$^{-/neo2}$;*Trp53*$^{+/-}$ embryos (Fig. 21F-H). In contrast, all of the *Tbx1*$^{-/neo2}$;*Trp53*$^{+/+}$ embryos examined presented with VSD associated with conotruncal septation defects or DORV (Fig. 20A).

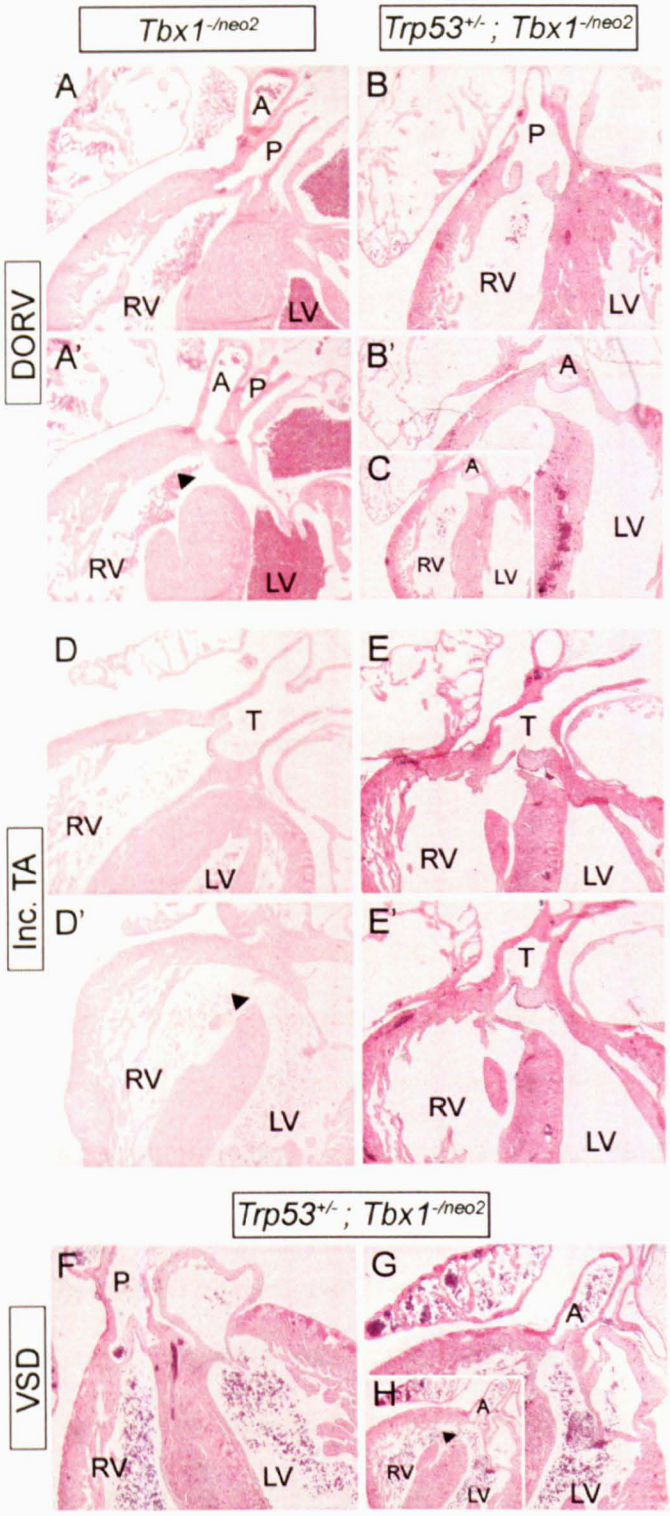

Figure 21: ***Trp53 deletion ameliorates the outflow tract phenotype in Tbx1 hypomorphic mutants at E18.5.*** (A-A') Two sections of the same heart of a *Tbx1*$^{-/neo2}$;*Trp53*$^{+/+}$ embryo. Note that both the aorta and the pulmonary trunk originate from the right ventricle. This is an arrangement observed in all the embryos with this genotype. (B-B'-C) Three sections of the same heart of a *Tbx1*$^{-/neo2}$;*Trp53*$^{+/-}$ embryo. The pulmonary trunk communicates with the right ventricle, while the aorta communicates with both ventricles, indicating a better alignment between the outflow and the heart chambers, compared with the embryo shown in A-A'.

In C, the section is shown at a lower magnification to fit the panel. (D-D') Two sections of the same heart of a *Tbx1*$^{-/neo2}$;*Trp53*$^{+/+}$ embryo. Note that the truncus arteriosus communis (T) is positioned directly above the RV. (E-E') Two sections of the same heart of a *Tbx1*$^{-/neo2}$;*Trp53*$^{+/-}$ embryo. The truncus arteriosus communis communicates with both the RV and LV, above the interventricular septum. (F-G-H) Three sections of the same heart of a *Tbx1*$^{-/neo2}$;*Trp53*$^{+/-}$ embryo. The pulmonary trunk is connected to the RV and the aorta to the LV. Although the latter is located above the septum, it does not directly communicate with the RV.
In H, the section is shown at a lower magnification to fit the panel.

DORV: Double outlet right ventricle; Inc. TA: incomplete truncus arteriosus (there is truncal septation but not conal septation). VSD: ventricular septal defect. A: Aorta; P: Pulmonary trunk; T: truncus arteriosus (unseptated); RV: right ventricle; LV: left ventricle. Arrowhead: interventricular communication (VSD).

4.5 *Trp53* ablation rescues the proliferation defect in a *Tbx1*$^{-/neo2}$ background

It has been demonstrated that Tbx1 cell-autonomously maintains the cardiac progenitor population within the SHF by enhancing the proliferation of cardiac precursor cells. Cell proliferation and apoptosis analysis in mesodermal specific conditional *Tbx1* mutants revealed an obvious reduction of mitotic cell number in the splanchnic mesoderm, by contrast, no changes in apoptotic activity was observed (Zhang, Huynh et al. 2006).
Because the OFT phenotype of *Tbx1* mutants is associated with reduced cell proliferation in the SHF, we tested whether *Trp53* ablation can rescue the proliferation defect in a *Tbx1*$^{-/neo2}$ background, thus providing a possible explanation of the partial rescue of the OFT phenotype. To this end, we immunostained histological sections of WT, *Tbx1*$^{-/neo2}$;*Trp53*$^{+/+}$ and *Tbx1*$^{-/neo2}$;*Trp53*$^{+/-}$ E9.5 embryos with an anti phosphorylated histone 3 (PH3) antibody and evaluated the percentage of PH3+ cells in the SHF area (operatively defined as the posterior pericardial wall excluding inflow and outflow proper) (Fig. 22). Results showed that 65.1% of the SHF cells were PH3+ in WT embryos, 43.5% in *Tbx1*$^{-/neo2}$;*Trp53*$^{+/+}$ embryos, confirming the reduction of cardiac precursors in *Tbx1* hypomorphic mutants, and 53.3% in *Tbx1*$^{-/neo2}$;*Trp53*$^{+/-}$, significantly more than in *Tbx1*$^{-/neo2}$;*Trp53*$^{+/+}$ littermates ($P<<0.001$). Thus,

Trp53 ablation had a significant impact on SHF cell proliferation in a *Tbx1* mutant background.

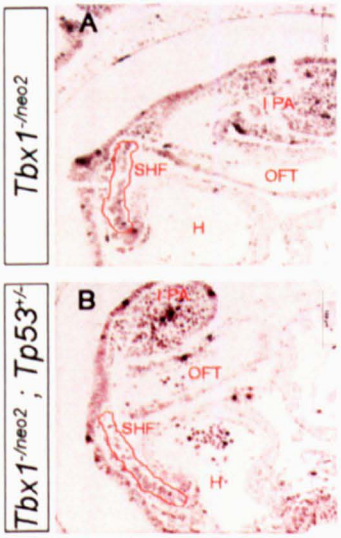

C

Genotype (E9.5)	MI (%)
Tbx1+/+;Tp53+/+ n=3 (2000cells/genotype)	65
Tbx1-/Neo2 n=3 (2000cells/genotype)	43
Tbx1-/Neo2;Tp53+/- n=3 (2000cells/genotype)	53

Figure 22: ***Trp53 ablation rescues cardiac precursors proliferation defects in Tbx1$^{-/neo2}$ background.*** (A, B) E9.5. sagittal sections immunostained with an anti-phospho-Histone H3 antibody to evaluate cell proliferation; the area where cell proliferation quantification were performed is indicated by the red boxes . (C) Mitotic index (M.I.) in the SHF area at E9.5 mutant embryos. P values were calculated using the Chi-squared test.
I PA: first pharyngeal arch; OFT: outflow tract; SHF: second heart field; H: heart.

4.6 *Tbx1 and p53 proteins co-occupy chromatin segments.*

To gain insights into the nature of the Tbx1-p53 interaction, we first tested whether p53 and Tbx1 regulate each other (Fig. 23A-B). We analyzed *Tbx1* and *Trp53* expression in WT, *Tbx1*$^{+/-}$, *Trp53*$^{+/-}$ and double heterozygous *Trp53*$^{+/-}$;*Tbx1*$^{+/-}$ E8.5 embryos. Results excluded that *Trp53* is a negative regulator of *Tbx1* expression in mouse embryos, and vice-versa. Next, we tested whether the two proteins interact directly. However, co-immunoprecipitation did not reveal any interaction (Fig. 23C). Next, we asked whether the

two proteins, albeit not interacting directly, occupy the same chromatin regions. To this end, we used chromatin immunoprecipitation combined with western blotting (ChIP-WB). Chromatin was extracted from cross-linked differentiated P19Cl6 cells, fragmented to a range of 150-350 bp and immunoprecipitated using anti-Tbx1 or anti-p53 antibodies. Captured complexes were released, de-cross-linked, and proteins were subjected to western blot analyses. Results showed that the p53 protein was present in the Tbx1-captured complexes (Fig. 23D), and vice-versa (Fig. 23E). Thus, there are chromatin segments that are occupied by both Tbx1 and p53, suggesting that the two transcription factors co-regulate shared targets.

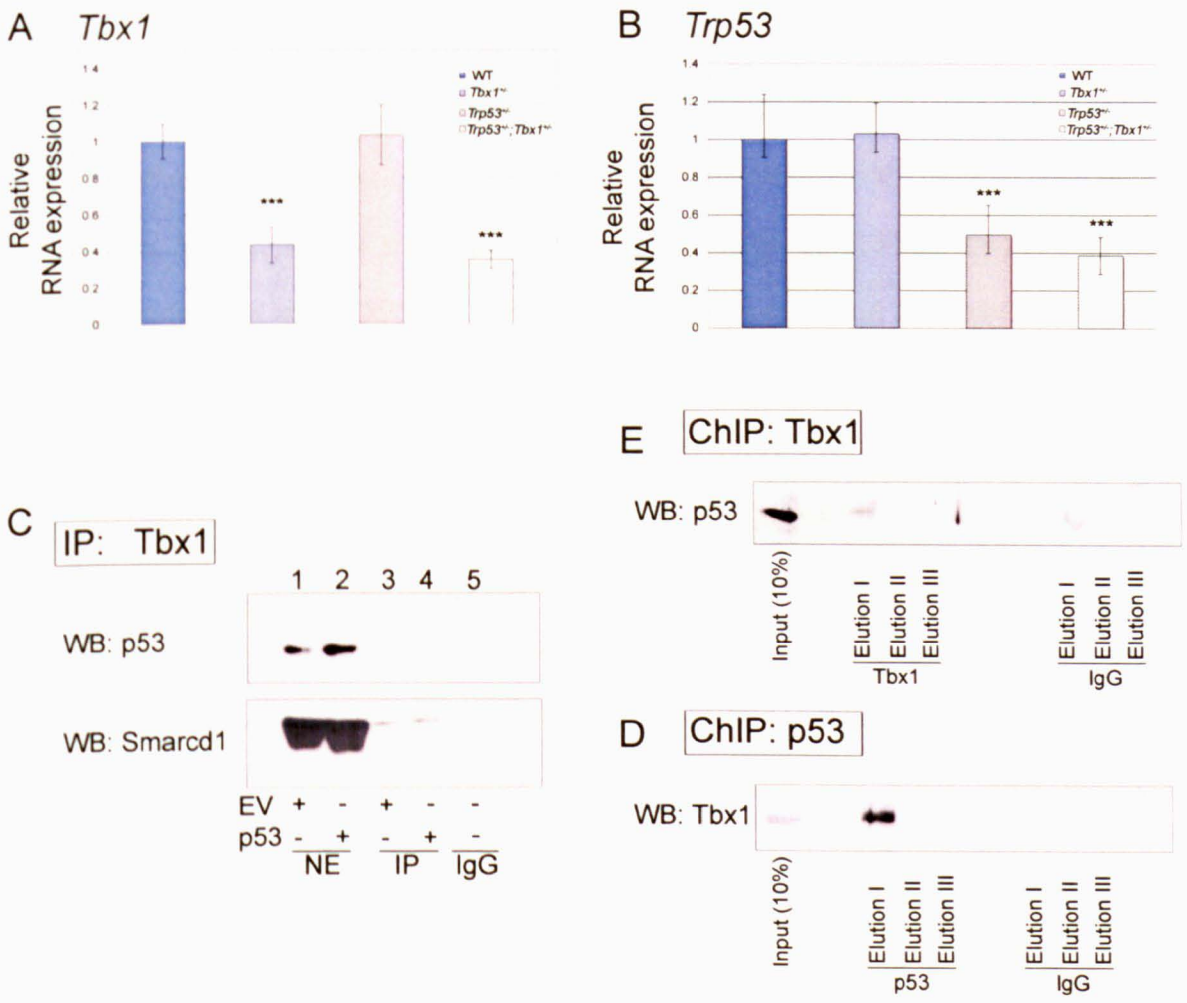

Figure 23: ***Molecular analyses of Trp53-Tbx1 interaction.*** (A-B) Quantitative real time PCR evaluation of *Tbx1* and *Trp53* expression in E8.5 embryos with the genotypes indicated.

Tbx1 expression is associated with heterozygous deletion, as expected, but is not affected by the presence of *Trp53* deletion. Similarly, *Trp53* expression is halved in *Trp53*$^{+/-}$ embryos, as expected, but is not affected by the presence of *Tbx1* deletion ***: P=0.001. Error bars indicate standard error of the mean (SEM) of five independent experiments. (C) Immunoprecipitation experiment using nuclear extracts from differentiated (48hrs) P19Cl6 cells and an antibody anti Tbx1. In parallel we used also cells transfected with a *Trp53* expression vector (lane 2 and lane 4). We carried out western blotting using an antibody against p53 and Smarcd1/Baf60a (positive control). The p53 protein is not co-immunoprecipitated. (D) ChIP-western blot experiment using an anti Tbx1 antibody. The p53 protein is readily detected. (E) ChIP-western blot experiment using an anti p53 antibody. The Tbx1 protein is present in the eluate.

4.7 The Gbx2 gene is down regulated in Tbx1$^{+/-}$ *embryos and rescued by Trp53 mutation*

To identify putative shared targets, we followed a candidate gene approach. We considered three Tbx1 target genes that are known to interact with *Tbx1* during 4th PAA development, *Wnt5a*, *Smad7* and *Gbx2* (Chen, Fulcoli et al. 2012; Papangeli and Scambler 2013; Calmont, Ivins et al. 2009). We first tested the expression of these genes in WT, *Tbx1*$^{+/-}$, *Trp53*$^{+/-}$, and *Tbx1*$^{+/-}$;*Trp53*$^{+/-}$ E8.5 embryos using quantitative reverse transcription PCR (qRT-PCR). Results showed *Gbx2* to be the most interesting target because its expression was the most affected by heterozygous *Tbx1* deletion (Fig. 24A-C). Both *Gbx2* and *Tbx1* are strongly expressed in the pharyngeal region of E8.5 embryos (Fig. 24D,E). Section analysis showed that *Gbx2* is expressed predominantly in the pharyngeal surface ectoderm (PSE), although some staining could also be detected in the pharyngeal endodermal (P.endo) layer (Fig. 24D',E'). Therefore, *Tbx1* and *Gbx2* show overlapping expression domains at the time of 4th PAA specification. *Gbx2* expression in *Tbx1*$^{-/-}$ embryos at E8.5 was lost from both the PSE and the P.endo, and when *Gbx2* expression was examined in *Tbx1* PSE conditional mutants, its expression was lost in the PSE, whereas it was maintained in the P.endo (compare Fig. 24G with 24H, and Fig. 24A' with 24H'). Therefore, decreased *Gbx2* expression is more likely to be due to gene dowregulation than

to a lack of development/survival of *Gbx2* expressing cells in the PSE. Thus, it has been demonstrated that *Gbx2* expression was lost in some regions of E8.5 *Tbx1* null embryos (Calmont, Ivins et al. 2009), but differential expression of *Gbx2* was never seen in *Tbx1*$^{+/-}$ mutants.

Our qRT-PCR analysis on E8.5 embryos showed these results; *Gbx2* expression was reduced in *Tbx1*$^{+/-}$ mutants, but it was not affected by *Trp53* deletion and, strikingly, expression returned to WT levels in *Tbx1*$^{+/-}$;*Trp53*$^{+/-}$ embryos (Fig. 24C). Homozygous deletion of *Gbx2* causes similar 4th PAA abnormalities to those in *Tbx1*$^{+/-}$ embryos, and *Gbx2* heterozygous deletion strongly enhances the *Tbx1* haploinsufficiency phenotype (Calmont, Ivins et al. 2009). Therefore, it is likely that at least part of the gene haploinsufficiency rescue in *Tbx1*$^{+/-}$;*Trp53*$^{+/-}$ embryos is due to rescue of *Gbx2* expression.

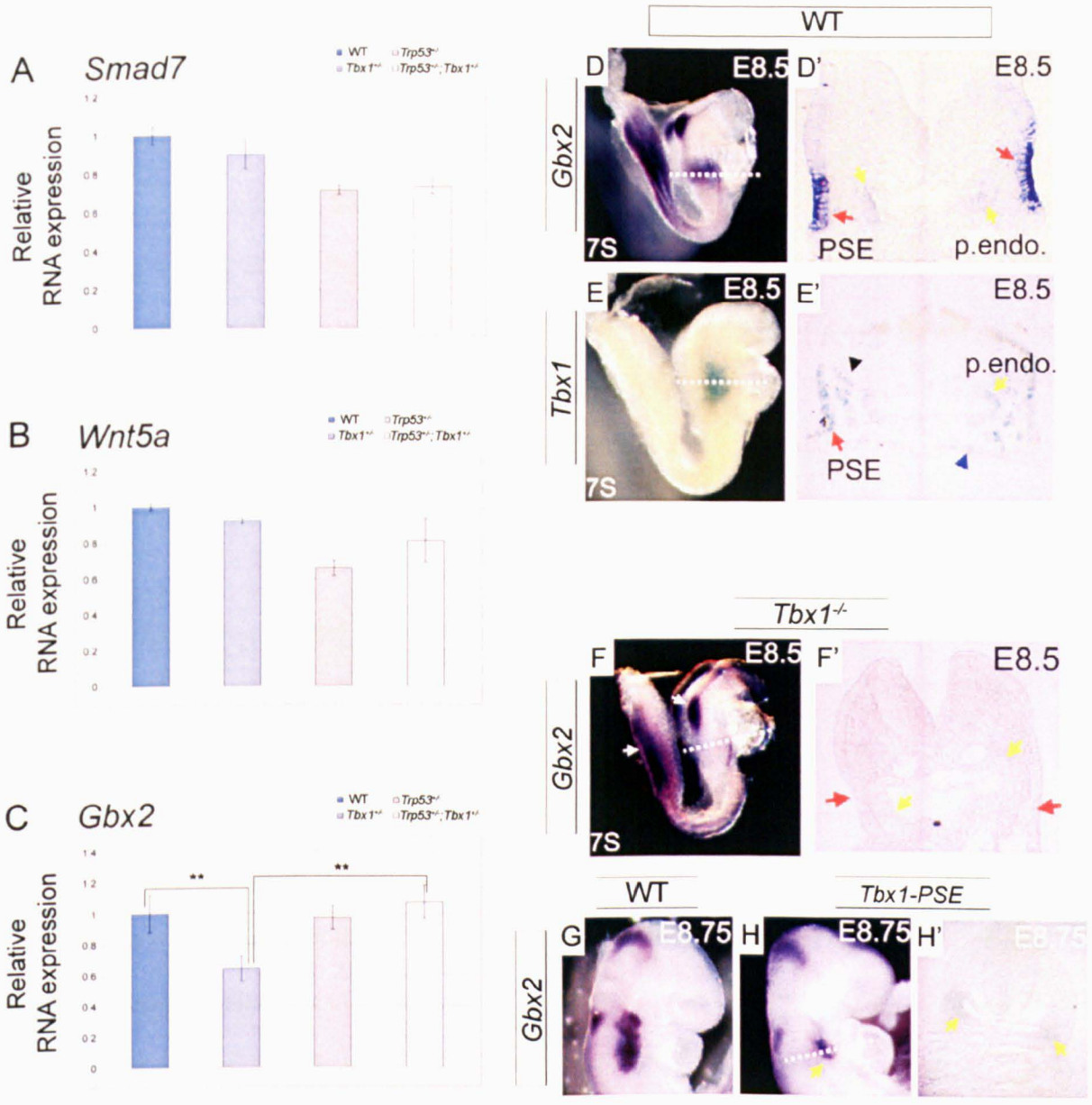

Figure 24: ***Trp53 deletion rescues the Gbx2 expression down regulation in Tbx1$^{+/-}$ E8.5 embryos.*** (A-B) Quantitative real time PCR (qPCR) evaluation of the *Smad7* (A) and *Wnt5a* (B) gene expression in E8.5 embryos (2 embryos/genotype). None of the variation observed are statistically significant. (C) qPCR evaluation of the *Gbx2* gene expression in E8.5 embryos (5 embryos/genotype). The expression is significantly reduced in *Tbx1*$^{+/-}$ embryos and significantly enhanced in double heterozygous embryos. There is not significant difference between WT and double heterozygous embryos. **: P= 0.004. Error bars indicate SEM of five independent experiments. (D-H') In situ hybridization (ISH) for *Gbx2* on WT embryos (D-D', G), *Tbx1*$^{-/-}$ embryos (F, F'), *Tbx1-PSE* (*AP2α*$^{Cre/+}$;*Tbx1*$^{flox/flox}$) embryos (H, H') and β-galactosidase staining of *Tbx1*$^{+/-}$ embryos (E, E'). Dotted lines in D, E, F, H show section plane in D', E', F', H', respectively. Red and yellow arrows indicate regions of *Gbx2* and *Tbx1* staining in the PSE and in the P.endo, respectively. Black arrowhead indicates *Tbx1* expression in the head mesoderm; blue arrowhead indicates *Tbx1* in the SHF mesoderm (Calmont, Ivins et al. 2009).

4.8 *A DNA fragment adjacent to the Gbx2 gene is occupied by both Tbx1 and p53 transcription factors*

Our results demonstrated that *Trp53* ablation rescues *Gbx2* expression *in vivo*. *In vitro* experiments demonstrated that Tbx1 and p53 could be part of the same chromatin complex. Therefore, based on these evidences, we asked whether the *Gbx2* gene may be occupied by both Tbx1 and p53 proteins, explaining the regulation of *Gbx2* expression either after Tbx1 haploinsufficiency or after *Trp53* ablation in a *Tbx1*$^{+/-}$ background. To this end, we computationally searched for T-box binding elements (TBEs) and p53 binding elements (p53BEs).

No direct Tbx1 binding sites have been identified so far, anyway Agarwal and colleagues (Agarwal, Wylie et al. 2003) have shown in vivo that *Fgf10* requires Tbx5 for initiation of its expression. This is supported by their in vitro transactivation data, which show powerful activation of the *Fgf10* promoter by TBX5, through an evolutionary conserved T-box binding element (TBE) located in the 5' region of the *Fgf10* gene. It has been demonstrated that Tbx1 can directly activate the *Fgf10* promoter through that TBE in a tissue culture assay (Xu H. et al., 2004), raising the intriguing possibility that different T-box transcription factors may share target genes. So we used the Tbx5 consensus DNA sequence, loosely defined as A/G/TG/AGTGNNA using a position weight matrix (PWM) based on all published T-box binding sites, to look for evolutionary conserved T-box binding elements into the *Gbx2* gene. The rVISTA program was used to align *Gbx2* and 3kb of upstream and downstream human and mouse genomic regions, in order to search putative TBEs and p53BEs. From this computational analysis we found 4 candidate sites for each of these transcription factors (Fig. 25A). The 4 TBEs were found in the downstream region of the *Gbx2* gene, while of the 4 p53BEs, 2 were found in the upstream region and other 2 are positioned in the downstream region of the *Gbx2* gene. Moreover, more recently, in our laboratory a genome-wide ChIP-seq assay has carried out to map binding sites of Tbx1. Results have shown Tbx1

enrichment in the downstream region of the *Gbx2* gene, therefore we focused on this region to test a direct bind of Tbx1 to the gene.

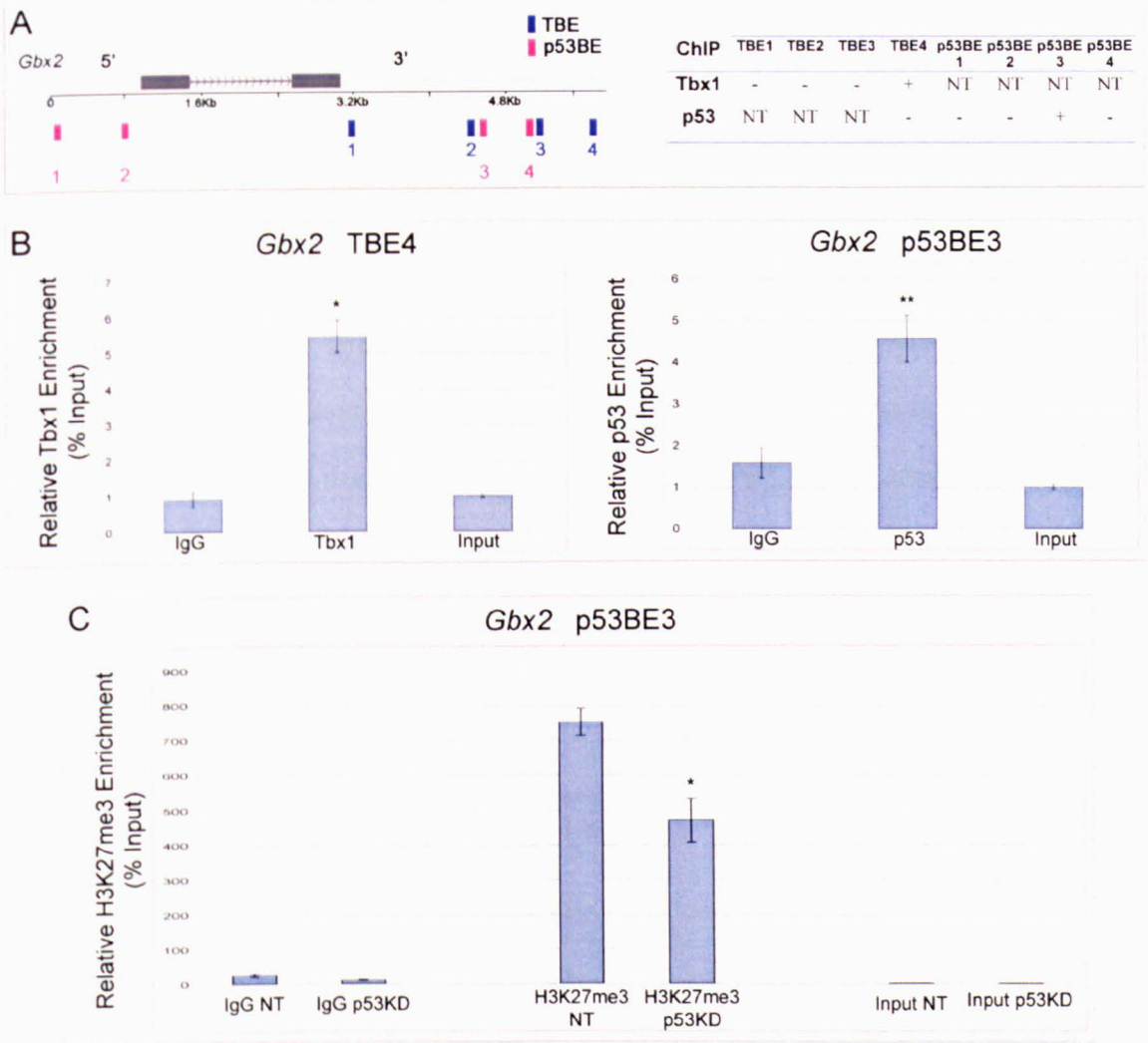

Figure 25: ***p53 and Tbx1 occupy a DNA segment adjacent to the Gbx2 gene.*** (A) Left: schematic representation of the *Gbx2* gene showing the position of computationally-detected T-box (blue) and p53 (red) binding sites. Right: summary of results of ChIP experiments. +: enriched; -: not enriched; NT: not tested. The genomic coordinates (mm10) of TBE4 and p53BE3 are chr1:89925759-89925824 and chr1:89927115-89927206, respectively. (B) Quantitative ChIP results for the two enriched sites. Left: ChIP using an anti Tbx1 antibody; Right: ChIP using an anti p53 antibody. *: P=0.04 **: P= 0.009. Error bars indicate mean ± standard deviation of 4 independent experiments. (C) Quantitative ChIP with an anti H3K27me3 antibody at the p53BE3 site. The experiment was carried out from P19CL6 transfected with a control siRNA (NT) or with an anti-p53 siRNA (p53KD). The immunoprecipitation was carried out with an anti Trimethyl-Histone H3 (Lys27) antibody. Note that the level of H3K27me3 at the p53BE3 site is significantly lower in the p53 knock

down sample. *: P= 0.05. Error bars indicate mean ± standard deviation of 2 independent experiments.

To test whether these TBEs and p53BEs are occupied by each of the transcription factors, we performed ChIP of cardiomyocyte differentiated P19Cl6 cells (48 hrs. after induction of differentiation). We chose this *in vitro* system because under these conditions all three endogenous genes (*Tbx1*, *Trp53* and *Gbx2*) are expressed and, interestingly, *Gbx2* gene is not expressed in undifferentiated P19CL6 cells, its expression starts after induction of differentiation, reaching its maximal expression at day 2 and day 3 of differentiation (Fig. 26).

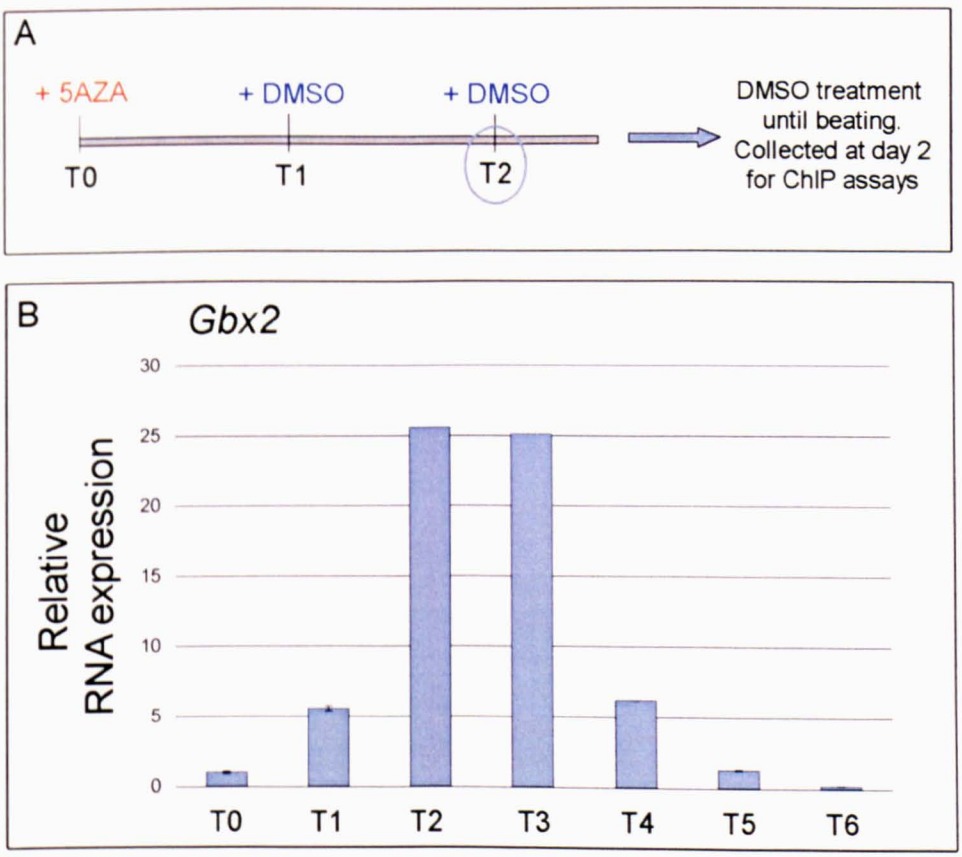

Figure 26: ***Gbx2 expression during cardiomyocyte differentiation of P19CL6 cells.*** (A) Schematic representation of cardiomyocyte differentiation of P19CL6 cells. (B) qRT-PCR results showed the maximal *Gbx2* expression at day 2-3 of differentiation.

Quantitative ChIP using an anti-Tbx1 antibody revealed the occupation of TBE4 (Fig. 25B, left panel), while ChIP with an anti-p53 antibody revealed occupation of p53BE3 (Fig. 25B, right panel), in four independent experiments per antibody.

The gene expression data shown above suggest that p53 alone does not have a direct effect on *Gbx2* expression, but its deletion buffers the effect of the *Tbx1* deletion. Therefore, considering that p53 has been shown to interact with a component of the Polycomb repressive complex 2 (Yang, Wang et al. 2013), we asked whether p53 suppression may alter the chromatin state of the *Gbx2* genetic element occupied by p53 and Tbx1. To this end, we knocked down *Trp53* during differentiation of P19CL6 cells (Fig. 27), and we performed qChIP (48 hrs. after induction of differentiation) with an anti H3K27me3 antibody and found that the DNA segment is highly enriched for this histone modification, but after p53 suppression by siRNA, the levels of H3K27me3 are substantially reduced (Fig. 25C).

Overall, these results indicate that *Gbx2* is regulated by both transcription factors.

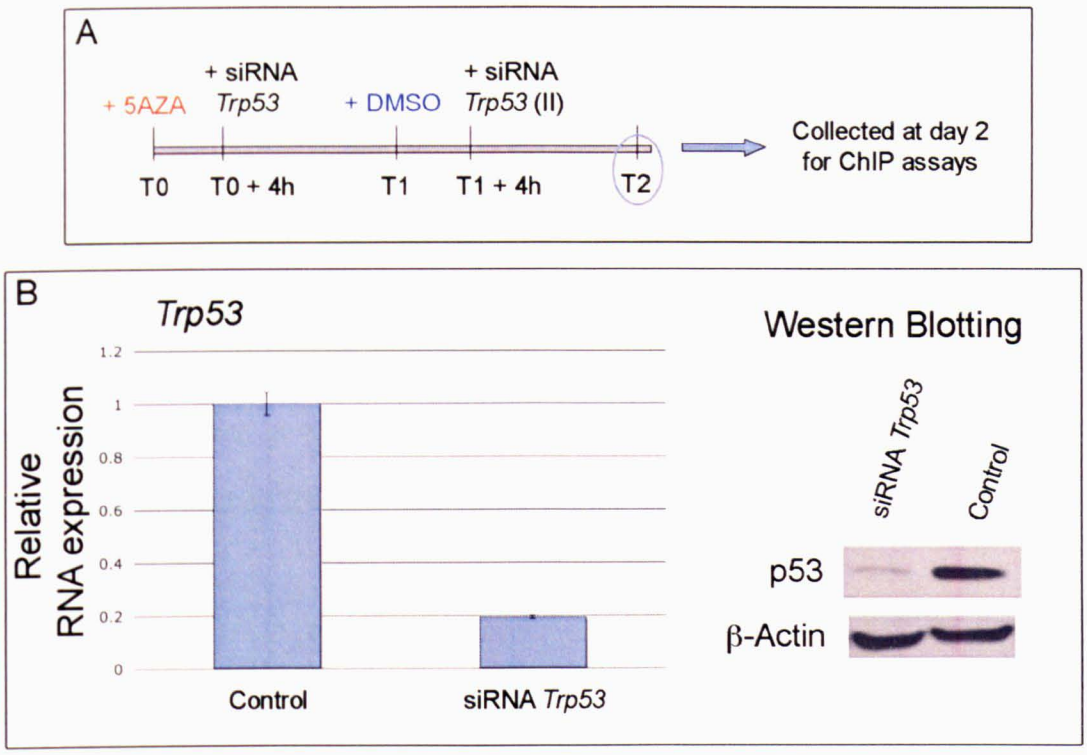

Figure 27: ***Trp53 knockdown during cardiomyocyte differentiation of P19CL6 cells.*** (A) Schematic representation of siRNA transfection during differentiation of P19CL6 cells. (B) 80% reduction of mRNA (left panel) and reduction of the protein (right panel) was achieved after 48 hrs from transfection.

4.9 *The DNA fragment occupied by Tbx1 and p53 is sensitive to p53 dosage in a luciferase reporter assay*

Gene expression analysis showed that *Gbx2* expression is restored in *Tbx1*$^{+/-}$ E8.5 embryos after ablation of *Trp53*, but its expression is not modified in *Trp53*$^{+/-}$ embryos, and ChIP experiments demonstrated that p53 binds to *Gbx2*. To understand whether the identified site bound by p53 is really negatively regulated by this transcription factor, we cloned an evolutionarily conserved (in human and mouse) DNA segment containing the p53BE identified by ChIP analysis, into a luciferase reporter plasmid with a basic promoter (Fig.

28A). We then carried out luciferase assays on human JEG3 choriocarcinoma cells transfected with increasing amount of a *Trp53* expression vector together with equal amount of the luciferase reporter construct. Due to the quite strong activity of the basal promoter in the construct, the basal luciferase activity was not too low to appreciate a decrease in the presence of p53. Results showed that the DNA segment responded well to transfected p53. Increasing amount of the p53 protein results in a reduction of the relative luciferase activity compared to the control, in a dose dependent manner (Fig. 28B). Thus, our results showed that this p53BE is required for p53-induced inactivation in this assay.

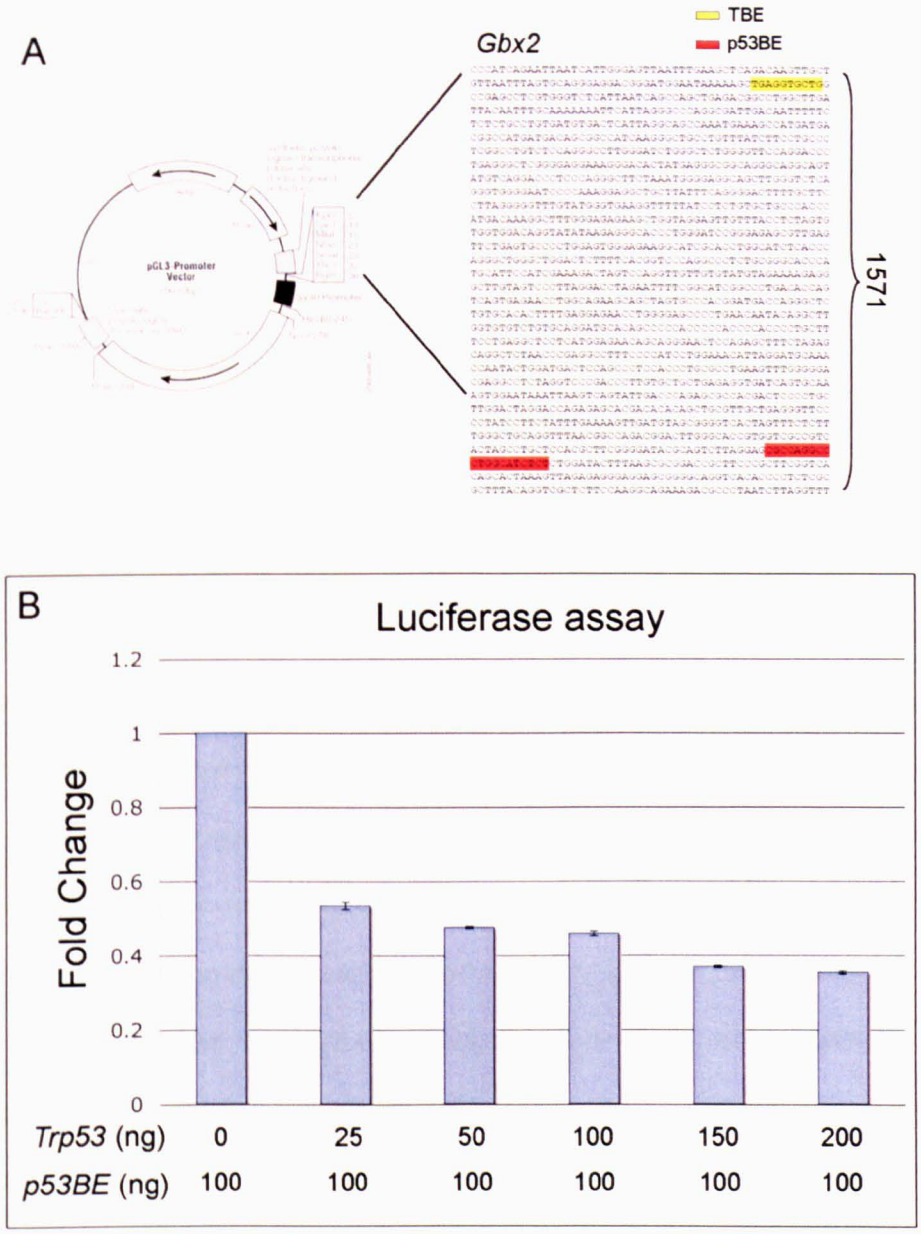

Figure 28: ***Gbx2 has a conserved p53 binding element (p53BE) that is required for response to p53 in luciferase assays.*** (A) Schematic illustration of the luciferase reporter construct containing a *Gbx2* DNA fragment with a TBE and a p53BE. (B) Luciferase assays on transfected human JEG3 cells. *Gbx2* luciferase reporter activity is sensitive to p53 dosage. Error bars indicate standard error of the mean (SEM) of six independent experiments.

Gene haploinsufficiency is a situation in which a single functional copy of a gene, in a diploid organism, is insufficient to support a normal phenotype. Loss of a functional copy of a gene may be due to a chromosomal deletion, a mutation that causes loss of the RNA message or of its stability, or that causes an altered, non functional protein product. Gene haploinsufficiency is transmited as a dominant trait. Most genes are not haploinsufficient, therefore, a loss-of-function allele often has no discernible phenotype. This phenomenon has been attributed to the metabolic theory of dominance described over 30 years ago. Briefly, this model states that the phenotypic consequences of heterozygous loss-of-function alleles are masked by the presence of one wild-type allele due to the redundancy of cellular physiology (Kacser and Burns, 1981). There are, however, exceptions to this rule where deletion of a single gene copy leads to an abnormal phenotype. Such haploinsufficiency is observed in all eukaryotes from yeast to humans. The relevance of haploinsufficiency in human disease has become increasingly apparent. Many of the haploinsufficient mutations in humans are observed in transcription factors, and it is not surprising that such haploinsufficiencies are detrimental, as they should result in multiple transcription defects of diverse downstream targets (reviewed in Seidman and Seidman, 2002). Haploinsufficiency has also been implicated in cancer; heterozygous mutations in both *Trp53* (Venkatachalam, Stuart et al., 2001) and *ATM* (Spring, Ahangari et al., 2002) result in increased cancer susceptibility.

Gene haploinsufficiency is often a cause of genetic disease and indicates absence or insufficiency of genetic buffering system(s) to compensate for the loss of one copy of the gene. Comparison of known haplo*insufficient Vs.* haplo*sufficient* genes indicated that haploinsufficient genes tend to have, i) developmental or morphogenetic importance, ii) more interactions with other genes and iii) interact with other haploinsufficient genes (Huang, Lee et al. 2010).

Hemizygous deletion of 22q11 affects approximately 1:4000 live births and may give rise to many different malformations but classically results in a constellation of phenotypes that receive a diagnosis of DiGeorge syndrome, velocardiofacial syndrome, or, now more commonly, 22q11.2 deletion syndrome (22q11.2DS). Particularly affected are the heart and great vessels, the endocrine glands of the neck, the face, the soft palate, and cognitive development. Although up to 30 genes may be deleted, it is haploinsufficiency of the transcription factor *TBX1* that is thought to make the greatest contribution to the disorder. Chromosome engineering, transgenic complementation, and gene targeting experiments revealed that haploinsufficiency of the T-box transcription factor Tbx1 produces a partial phenocopy of the syndrome. Mouse embryos are exquisitely sensitive to varying levels of *Tbx1* mRNA; thus *Tbx1* is a dosage-sensitive gene, and its haploinsufficiency affects a number of morphogenetic and developmental processes. *Tbx1* gene, when haploid results in fourth PAA abnormalities, while loss of function of *Tbx1*, as tested in $Tbx1^{-/-}$ embryos, leads to disruption of PAAs 3–6, possibly secondary to lack of segmentation of the distal pharyngeal arches and pouches. Great artery defects involving third and sixth PAA derivatives are almost never seen in 22q11.2DS patients, suggesting that the haploinsufficiency model reflects more closely the aortic arch defects than do the homozygous mutations. Phenotypic anomalies also extend into adult life, patients reaching adolescence and adulthood have a predisposition to neuropsychiatric disease, for which there is no specific treatment. Thus, understanding gene haploinsufficiency mechanisms is not only important from a biological point of view, but it is also potentially important for the development of future treatments.

In this work I searched for genetic and pharmacological strategies to rescue the *Tbx1* mutant phenotype and I considered cell proliferation as a potential target. It is known that Tbx1 has a positive role to control cell proliferation in different cell types and through different pathways (Vitelli et al., 2003; Vitelli, Lania et al. 2010; Fulcoli, Huynh et al. 2009). From *in vitro* studies I found that Tbx1 enhanced cell proliferation and this effect could be a

consequence of down-regulation of two cell cycle inhibitors, *Cdkn1a* and *Cdkn1b*. It has been demonstrated that *Cdkn1a* expression is up-regulated in *Tbx1*$^{-/-}$ mouse dental epithelium (Cao, Florez et al. 2010) and it has been proposed that this up-regulation is due to the interaction of Tbx1 with the C-terminal tail of PITX2, leading to inhibition of PITX2 transcriptional activation of *Cdkn1a* promoter. Thus, proposing a new mechanism by which Tbx1 promotes cell proliferation. Therefore, one possibility is that *Cdkn1a* down-regulation by Tbx1 could be done by inhibition of p53-dependent transcriptional activation of this gene. Using program rVista, I searched for TBEs within the *Cdkn1a* promoter, near two p53BEs known to be responsible for *Cdkn1a* transcriptional activation (Laptenko, Beckerman et al., 2011). I found 2 TBEs, but none was occupied by Tbx1, as determined by ChIP assay in my tissue culture model (P19CL6). However, another possibility is that *Cdkn1a* activation by p53 requires the binding of cofactors, such as a component of the SWI/SNF chromatin remodeling complex, Baf60a (Oh, Sohn et al., 2008). This protein interacts with both Tbx1 (Chen, Fulcoli et al. 2012) and p53 (Oh, Sohn et al., 2008), therefore it is possible that Tbx1 and p53 proteins compete with each other in binding to Baf60a, and if there is a relative excess of Tbx1, there may be less Baf60a available for p53, leading to reduced activation of *Cdkn1a* expression.

Thus, Tbx1 may be facilitating cell proliferation through negative regulation (direct or indirect) of cell cycle inhibitors.

In this work, I followed a rationale that was based on the contrasting effects of Tbx1 and a *Cdkn1a-Cdkn1b* activator, p53, on cell differentiation and proliferation, for devising a genetic and pharmacological rescue strategy. First of all I focused my study on the *Tbx1* haploinsufficiency phenotype. Of particular note, heterozygotes show 4th PAAs hypo/aplasia, hypoplasia of the parathyroid and thyroid glands and behavioral abnormalities. The detection of the 4th PAA hypo/aplasia was very important, because normal growth and remodeling of this structure is necessary for final patterning of the mature aortic arch, and its loss causes the interruption observed in IAA-B. The penetrance of 4th PAA and other defects is greatly

affected by genetic background (Taddei, Morishima, et al. 2001). The genetic background affects the extent of "recovery" of arterial growth of the 4th PAA during development (Lindsay and Baldini, 2001) as well as the penetrance of initial abnormalities. I found that *Trp53* heterozygous deletion was effective in rescuing the *Tbx1* haploinsufficient phenotype in early embryos, during the formation of the arteries, as demonstrated by the analysis of the 4th PAA phenotype in E10.5 mutant embryos. Analysis of the 4th PAAs derivatives in E18.5 embryos, confirmed the rescue of the haploinsufficiency phenotype also at this developmental stage. I excluded that rescue is due to regulation of *Tbx1* gene expression by p53 because *Trp53* deletion does not affect *Tbx1* expression in embryos. Similarly, I excluded that rescue is due to regulation of *Trp53* gene expression by Tbx1 because, also in this case, *Tbx1* heterozygous deletion does not affect *Trp53* expression in embryos as well as in tissue culture systems. It is also unlikely that rescue may be due to the anti-apoptotic effects of loss of p53. Indeed, abnormal apoptosis is not part of the *Tbx1* mutant phenotype (Vitelli, Morishima et al. 2002; Calmont, Ivins et al. 2009). I propose an alternative explanation, I speculate that Tbx1 and p53 cooperate in regulating specific targets relevant for the development of the structures rescued by *Trp53* mutation. This view is supported by the specificity of rescue and by the co-immunoprecipitation of p53 and Tbx1 in ChIP assays. Indeed, the gene *Gbx2*, encoding a homeobox protein required for normal development of the 4th PAAs, is occupied by both Tbx1 and p53 and its expression is affected by *Tbx1* heterozygosity, but not by *Trp53* heterozygosity, and it is rescued by combined mutation of *Tbx1* and *Trp53*. *Gbx2* and *Tbx1* are co-expressed in the pharyngeal surface ectoderm and in the pharyngeal endoderm (Calmont, Ivins et al. 2009), tissues that have been linked to the 4th PAA phenotype (Zhang, Cerrato et al. 2005; Calmont, Ivins et al. 2009; Randall, McCue et al. 2009). *Gbx2* haploinsufficiency alone shows normal PAAs development, while *Gbx2* haploinsufficiency in a *Tbx1* heterozygous background enhances the 4th PAA phenotype in *Tbx1* mutants.

Therefore, *Gbx2* is a strong candidate for being a shared target, and the rescue of its expression in double mutants could explain the rescue of the 4th PAA phenotype.

Then, I focused my study on the *Tbx1* null phenotype. Homozygous null mutation of *Tbx1* causes more severe defects including failure of the outflow tract (OFT) septation, and absence of the caudal pharyngeal arches. Tbx1 is a transcriptional modulator, and deregulation of this activity has been linked to alterations in the expression of various genes involved in cardiovascular morphogenesis. OFT septation requires *Tbx1* between E8.5 and E9.5. Using a $Tbx1^{mcm}$ (tamoxifen-inducible Cre knocked into the *Tbx1* locus), it has been shown that induction of Cre activity at E8.5 reveals contribution to the OFT endothelium and myocardium of cells derived from *Tbx1*-expressing progenitors (Xu, Cerrato et al., 2005). *Tbx1* is required in all three germ layers of the embryonic pharyngeal region for normal development. *Mesp1Cre* was used to ablate *Tbx1* activity in mesodermal derivatives. By late gestation, mesodermal mutants strongly resembled $Tbx1^{-/-}$ embryos, with severe thymic defects, persistent truncus arteriosus, VSDs, and aortic arch defects as well as hypoplastic ears. At E10.5, the conditional mutants had lost the 2nd, 4th and 6th branchial arches, and had hypoplastic second arches, again reminiscent of *Tbx1* nulls (Zhang, Huynh et al., 2006). These data suggest that mesodermal expression of *Tbx1* has a critical role in pharyngeal segmentation. Loss of the arch arteries in mesodermal mutants might be explained by the lack of the arches themselves. The OFT phenotype observed in $Tbx1^{-/-}$ mutants are associated with decreased cardiac precursors proliferation and their premature differentiation, and it has been reported that Tbx1 controls cell proliferation and affects cellular differentiation in a cell autonomous fashion, but it also directs non-cell autonomous effects (Vitelli, Morishima et al., 2002)

As I mentioned above, the mouse embryo is sensitive to *Tbx1* expression level. Intronic insertion of a selection cassette has been used to generate hypomorphic alleles of *Tbx1* (Zhang and Baldini, 2008). Systematic analysis of the phenotype associated with a hypomorphic series revealed differing sensitivities to reduced *Tbx1* dosage in different

organs and structures. PAA development was particularly sensitive to reduced *Tbx1* dosage, 4th PAA hypoplasia appearing already at 70% wild-type levels of mRNA. Outflow tract septation defects were observed at 20% and alignment defects at 15%. Therefore *Tbx1* dosage manipulations using hypomorphic alleles revealed that different tissues have different sensitivity to *Tbx1* dosage.

I found that *Trp53* heterozygous deletion was partially effective in rescuing the cardiac outflow tract phenotype in hypomorphic mutants, and ineffective in null mutants. This differential response to *Trp53* deletion can be interpreted in different ways. For example, it might be necessary to have a particular balance between dosage of *Tbx1* and dosage of *Trp53*, therefore to have an effective rescue in a *Tbx1* null background and to maintain this balance, I should completely delete *Trp53*. This hypothesis, however, does not explain well the apparent lack of rescue in the null, considering that a partial rescue can readily be detected in embryos with only ~15% of the *Tbx1* mRNA. Another possibility is that in the null, the anatomical structures or tissues sensitive to p53-dependent rescue are severely disrupted or even absent and thus a rescue cannot occur. This may be the case for the posterior pharyngeal arch artery system, which is absent in the null, but is unlikely to be the case for the OFT, which is formed in the null but not modified by *Trp53* deletion. In contrast, increased cell proliferation associated with *Trp53* deletion may explain the improvement of the OFT phenotype observed in *Tbx1* hypomorphic mutants, as reduced cell proliferation in the SHF is associated with OFT abnormalities (Vincent and Buckingham 2010; Xu, Morishima et al. 2004; Prall, Menon et al. 2007).

I propose that *Gbx2* is a strong candidate gene, whose rescued expression in combined *Tbx1* and *Trp53* mutants could explain the rescue of the 4th PAA phenotype. *Gbx2* has been studied mostly as a regulator of midbrain development (Joyner, Liu et al., 2000). It has been reported that *Gbx2* homozygous null embryos exhibit cerebellar defects and die soon after birth (Wassarman, Lewandoski et al., 1997). Mutants pups were cyanotic at birth, suggesting that neonatal lethality may be attributable to cardiovascular defects, in fact, approximately

39% of *Gbx2* mutants exhibit cardiovascular defects that are not limited to the remodeling of the PAAs, but they also exhibit VSDs and OFT malformations (Byrd and Meyers, 2005). *Gbx2* is not expressed in the SHF, therefore it cannot explain the partial rescue of the OFT phenotype, which is due to loss of *Tbx1* in the mesoderm (Zhang, Huynh et al. 2006). Moreover, *Gbx2* has been identified as a downstream target of signal transducer and activator of transcription 3 (Stat3), a transcription factor that forms a homodimer upon induction by leukemia inhibitor factor (LIF) and subsequently translocates into the nucleus, where it regulates transcription of its downstream targets to maintain embryonic stem cell (ESC) identity. *Gbx2*, as a novel target of Stat3, seems to have a role in maintaining the undifferentiated state of mESC and in sustaining mESC self-renewal in the absence of LIF; and it functions also as a reprogramming factor, cooperating synergistically with Oct4, Sox2, Klf4 and c-Myc (Tai and Ying, 2013). Therefore, it is possible that *Gbx2* has a role also in promoting proliferation and in inhibiting differentiation. Because *Gbx2* is not expressed in the SHF, its role in OFT development is indirect. Whether or not Tbx1-dependent expression of *Gbx2* is critical to OFT development is not clear. However, we cannot exclude that *Trp53* deletion improved the OFT phenotype by buffering the effects of the loss of Tbx1 on *Gbx2* regulation.

In summary, I propose that p53 and Tbx1 co-regulate, in a contrasting manner, a set of common target genes. Consequently, the reduced dosage of p53 enhances the transcriptional functions of Tbx1 on those targets. The evidence in support of this view is based upon our chromatin co-immunoprecipitation data, co-occupation and co-regulation of the *Gbx2* gene. In addition, both Tbx1 and p53 interact with the same component of the SWI-SNF chromatin remodeling complex Smarcd1/Baf60a (Chen, Fulcoli et al.; Oh, Sohn et al. 2008), suggesting that the two transcription factors may interact with the same machinery at a chromatin level. It has also been shown that p53 interacts with a component of the Polycomb repressive complex 2 (Yang, Wang et al. 2013) and, by doing so it could add repressive marks (H3K27me3) on a set of targets, including some of the Tbx1 targets, thus

making them less likely to be activated by Tbx1. Our finding that p53 dosage affects negatively the enrichment of H3K27me3 at the genetic element occupied by Tbx1 and p53 supports the hypothesis that reduced expression of p53 reduces repressive marks on the *Gbx2* gene and thereby "facilitates" its regulation by Tbx1. This rescue mechanism requires the presence of the Tbx1 protein, thus explaining why p53 suppression has no effect on the null *Tbx1* phenotype. A schematic representation of a proposed model by which Tbx1-p53 regulate *Gbx2* expression is shown in Fig. 29.

Finally, my data suggest, for the first time, that p53 plays a role in the biology of cardiac progenitors. While the loss of *Trp53* has no effect on cardiac development, it is known that p53 occupies a large set of developmentally critical genes, including genes involved in cardiac development (Akdemir, Jain et al. 2013). While its exact role on cardiac differentiation remains to be defined, I speculate that part of this role would be to keep genes involved in cardiac differentiation open for transcriptions (and/or suppress genes important to maintain the progenitor state) and thus facilitate the switch from progenitor state to differentiated state.

In view of the complexities of p53 functions in the context of embryonic development and cell differentiation (Rivlin, Kolfman et al., 2014; Danilova, Sakamoto et al., 2008; Armstrong, Kaufman et al., 1995; Sah, Attardi et al., 1995), it is possible that *Gbx2* is not the only player in phenotypic rescue. Nevertheless, our data about the *Gbx2* gene illustrate an intriguing mechanism of interaction that might function also on other shared target genes yet to be identified. Therefore, further work is required to address my hypothesis. For example, it would be interesting to carry out sequential ChIP assays followed by deep sequencing (re-Chip-seq) to have a genome-wide analysis of co-occupied enhancers. Parallel gene expression analysis (RNA-seq) will identify neighboring target genes sensitive to *Tbx1/Trp53* dosage balance. Furthermore, genome-wide ChIP-seq assays in *Tbx1-Trp53* combined mutants should provide gene features and chromatin profiling compared to the control mutants. Another experimental would test whether there is competition between the two

transcription factors in binding Baf60a. Indeed, the SWI-SNF-like subunit Baf60a binds p53 and Tbx1 and is very important, if not essential, for the function of both transcription factors (Chen, Fulcoli et al., 2012; Oh, Sohn et al., 2008).

Last but not least, my data provide a proof of concept that the *Tbx1* mutant phenotype can be significantly ameliorated using pharmacological approaches, thus encouraging further studies into the functional mechanisms and interactions of *Tbx1* with the aim of identifying potential drug targets.

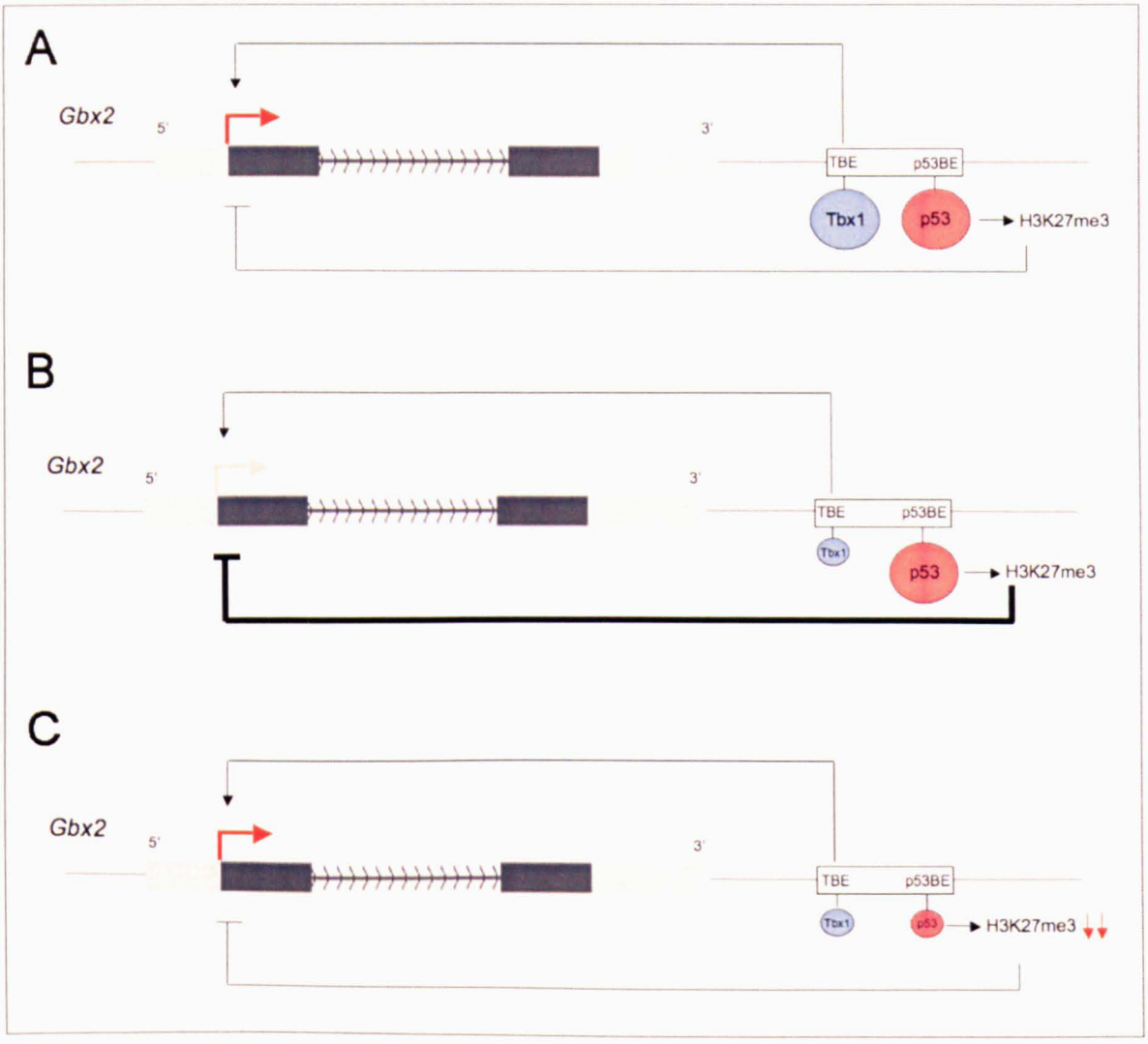

Figure 29: **Schematic model of *Gbx2* regulation.** My data suggest that when there is a balance between Tbx1 and p53, Tbx1 directly regulate *Gbx2* causing a massive expression of the gene (A). When Tbx1 is reduced, there is an unbalance between the two transcription factors causing a reduction of *Gbx2* expression (B). The restoration of the balance between Tbx1 and p53 results in a rescue of the *Gbx2* expression, due to the reduction of the repressive mark H3K27me3 (C).

REFERENCES

Agarwal, P., J. N. Wylie, et al. (2003). "Tbx5 is essential for forelimb bud initiation following patterning of the limb field in the mouse embryo." Development **130**(3): 623-33.

Akdemir, K. C., A. K. Jain, et al. (2013) "Genome-wide profiling reveals stimulus-specific functions of p53 during differentiation and DNA damage of human embryonic stem cells." Nucleic Acids Res **42**(1): 205-23.

Armstrong, J. F., M. H. Kaufman, et al. (1995). "High-frequency developmental abnormalities in p53-deficient mice." Curr Biol **5**(8): 931-6.

Barlow, C., M. Liyanage, et al. (1997). "Partial rescue of the prophase I defects of Atm-deficient mice by p53 and p21 null alleles." Nat Genet **17**(4): 462-6.

Bollag, R. J., Z. Siegfried, et al. (1994). "An ancient family of embryonically expressed mouse genes sharing a conserved protein motif with the T locus." Nat Genet **7**(3): 383-9.

Bondue, A., S. Tannler, et al. (2011) "Defining the earliest step of cardiovascular progenitor specification during embryonic stem cell differentiation." J Cell Biol **192**(5): 751-65.

Bruneau, B. G., G. Nemer, et al. (2001). "A murine model of Holt-Oram syndrome defines roles of the T-box transcription factor Tbx5 in cardiogenesis and disease." Cell **106**(6): 709-21.

Buckingham, M., S. Meilhac, et al. (2005). "Building the mammalian heart from two sources of myocardial cells." Nat Rev Genet **6**(11): 826-35.

Burn, J., A. Takao, et al. (1993). "Conotruncal anomaly face syndrome is associated with a deletion within chromosome 22q11." J Med Genet **30**(10): 822-4.

Byrd, N. A. and E. N. Meyers (2005). "Loss of Gbx2 results in neural crest cell patterning and pharyngeal arch artery defects in the mouse embryo." Dev Biol **284**(1): 233-45.

Cai, C. L., X. Liang, et al. (2003). "Isl1 identifies a cardiac progenitor population that proliferates prior to differentiation and contributes a majority of cells to the heart." Dev Cell **5**(6): 877-89.

Calmont, A., S. Ivins, et al. (2009). "Tbx1 controls cardiac neural crest cell migration during arch artery development by regulating Gbx2 expression in the pharyngeal ectoderm." Development **136**(18): 3173-83.

Cao, H., S. Florez, et al. (2010) "Tbx1 regulates progenitor cell proliferation in the dental epithelium by modulating Pitx2 activation of p21." Dev Biol **347**(2): 289-300.

Chapman, D. L., N. Garvey, et al. (1996). "Expression of the T-box family genes, Tbx1-Tbx5, during early mouse development." Dev Dyn **206**(4): 379-90.

Chen, L., F. G. Fulcoli, et al. (2012) "Transcriptional control in cardiac progenitors: Tbx1 interacts with the BAF chromatin remodeling complex and regulates Wnt5a." PLoS Genet **8**(3): e1002571.

Chen, L., F. G. Fulcoli, et al. (2009). "Tbx1 regulates proliferation and differentiation of multipotent heart progenitors." Circ Res **105**(9): 842-51.

Chow, E. W., A. S. Bassett, et al. (1994). "Velo-cardio-facial syndrome and psychotic disorders: implications for psychiatric genetics." Am J Med Genet **54**(2): 107-12.

Cicalese, A., G. Bonizzi, et al. (2009). "The tumor suppressor p53 regulates polarity of self-renewing divisions in mammary stem cells." Cell **138**(6): 1083-95.

Conlon, F. L., L. Fairclough, et al. (2001). "Determinants of T box protein specificity." Development **128**(19): 3749-58.

Danilova, N, Sakamoto, KM, Lis, S (2008). "p53 family in development." Mech Dev **125**: 919-931

de la Chapelle, A., R. Herva, et al. (1981). "A deletion in chromosome 22 can cause DiGeorge syndrome." Hum Genet **57**(3): 253-6.

de la Cruz, M. V., C. Sanchez Gomez, et al. (1977). "Experimental study of the development of the truncus and the conus in the chick embryo." J Anat **123**(Pt 3): 661-86.

DiGeorge, AM (1968). "Congenital absence of the thymus and its immunologic consequences: concurrence with congenital hypoparathyroidism." Birth Defects Original Article Series **4**(1): 116-21

Dodou, E., M. P. Verzi, et al. (2004). "Mef2c is a direct transcriptional target of ISL1 and GATA factors in the anterior heart field during mouse embryonic development." Development **131**(16): 3931-42.

Donehower, L. A., M. Harvey, et al. (1992). "Mice deficient for p53 are developmentally normal but susceptible to spontaneous tumours." Nature **356**(6366): 215-21.

Driscoll, D. A., M. L. Budarf, et al. (1992). "A genetic etiology for DiGeorge syndrome: consistent deletions and microdeletions of 22q11." Am J Hum Genet **50**(5): 924-33.

Driscoll, D. A., J. Salvin, et al. (1993). "Prevalence of 22q11 microdeletions in DiGeorge and velocardiofacial syndromes: implications for genetic counselling and prenatal diagnosis." J Med Genet **30**(10): 813-7.

Driscoll, D. A., N. B. Spinner, et al. (1992). "Deletions and microdeletions of 22q11.2 in velo-cardio-facial syndrome." Am J Med Genet **44**(2): 261-8.

Edelmann, L., R. K. Pandita, et al. (1999). "Low-copy repeats mediate the common 3-Mb deletion in patients with velo-cardio-facial syndrome." Am J Hum Genet **64**(4): 1076-86.

Evans, S. M., D. Yelon, et al. (2010) "Myocardial lineage development." Circ Res **107**(12): 1428-44.

Fulcoli, F. G., T. Huynh, et al. (2009). "Tbx1 regulates the BMP-Smad1 pathway in a transcription independent manner." PLoS One **4**(6): e6049.

Gogos, J. A., M. Morgan, et al. (1998). "Catechol-O-methyltransferase-deficient mice exhibit sexually dimorphic changes in catecholamine levels and behavior." Proc Natl Acad Sci U S A **95**(17): 9991-6.

Gossen, M. and H. Bujard (1992). "Tight control of gene expression in mammalian cells by tetracycline-responsive promoters." Proc Natl Acad Sci U S A **89**(12): 5547-51.

Gottlieb, T. M. and M. Oren (1996). "p53 in growth control and neoplasia." Biochim Biophys Acta **1287**(2-3): 77-102.

Guo, C., Y. Sun, et al. (2011) "A Tbx1-Six1/Eya1-Fgf8 genetic pathway controls mammalian cardiovascular and craniofacial morphogenesis." J Clin Invest **121**(4): 1585-95.

Hakem, R., J. L. de la Pompa, et al. (1997). "Partial rescue of Brca1 (5-6) early embryonic lethality by p53 or p21 null mutation." Nat Genet **16**(3): 298-302.

Hayashi, S. and A. P. McMahon (2002). "Efficient recombination in diverse tissues by a tamoxifen-inducible form of Cre: a tool for temporally regulated gene activation/inactivation in the mouse." Dev Biol **244**(2): 305-18.

Hiruma, T., Y. Nakajima, et al. (2002). "Development of pharyngeal arch arteries in early mouse embryo." J Anat **201**(1): 15-29.

Hu, T., H. Yamagishi, et al. (2004). "Tbx1 regulates fibroblast growth factors in the anterior heart field through a reinforcing autoregulatory loop involving forkhead transcription factors." Development **131**(21): 5491-502.

Hu, W., Z. Feng, et al. (2007). "p53 regulates maternal reproduction through LIF." Nature **450**(7170): 721-4.

Huang, N., I. Lee, et al. (2010) "Characterising and predicting haploinsufficiency in the human genome." PLoS Genet **6**(10): e1001154.

Hutson, M. R. and M. L. Kirby (2007). "Model systems for the study of heart development and disease. Cardiac neural crest and conotruncal malformations." Semin Cell Dev Biol **18**(1): 101-10.

Hutson, M. R., X. L. Zeng, et al. (2010) "Arterial pole progenitors interpret opposing FGF/BMP signals to proliferate or differentiate." Development **137**(18): 3001-11.

Hutson, M. R., P. Zhang, et al. (2006). "Cardiac arterial pole alignment is sensitive to FGF8 signaling in the pharynx." Dev Biol **295**(2): 486-97.

Huynh, T., L. Chen, et al. (2007). "A fate map of Tbx1 expressing cells reveals heterogeneity in the second cardiac field." Genesis **45**(7): 470-5.

Jacks, T., L. Remington, et al. (1994). "Tumor spectrum analysis in p53-mutant mice." Curr Biol **4**(1): 1-7.

Jain, A. K., K. Allton, et al. (2012) "p53 regulates cell cycle and microRNAs to promote differentiation of human embryonic stem cells." PLoS Biol **10**(2): e1001268.

Jerome, L. A. and V. E. Papaioannou (2001). "DiGeorge syndrome phenotype in mice mutant for the T-box gene, Tbx1." Nat Genet **27**(3): 286-91.

Jones, N. C., M. L. Lynn, et al. (2008). "Prevention of the neurocristopathy Treacher Collins syndrome through inhibition of p53 function." Nat Med **14**(2): 125-33.

Jones, S. N., A. E. Roe, et al. (1995). "Rescue of embryonic lethality in Mdm2-deficient mice by absence of p53." Nature **378**(6553): 206-8.

Joyner, AL, Liu, A and Millet, S (2000). "Otx2, Gbx2 and Fgf8 interact to position and maintain a mid-hindbrain organizer." Curr. Opin. Cell Biol. **12**(6): 736-41

Kacser, H., and J. A. Burns (1981). "The molecular basis of dominance." Genetics **97**: 639–666.

Kang, J., E. Nathan, et al. (2009). "Isl1 is a direct transcriptional target of Forkhead transcription factors in second-heart-field-derived mesoderm." Dev Biol **334**(2): 513-22.

Kelley, R. I., E. H. Zackai, et al. (1982). "The association of the DiGeorge anomalad with partial monosomy of chromosome 22." J Pediatr **101**(2): 197-200.

Kelly, R. G. (2012) "The second heart field." Curr Top Dev Biol **100**: 33-65.

Kelly, R. G., N. A. Brown, et al. (2001). "The arterial pole of the mouse heart forms from Fgf10-expressing cells in pharyngeal mesoderm." Dev Cell **1**(3): 435-40.

Kenzelmann Broz, D. and L. D. Attardi (2010) "In vivo analysis of p53 tumor suppressor function using genetically engineered mouse models." Carcinogenesis **31**(8): 1311-8.

Kimber, W. L., P. Hsieh, et al. (1999). "Deletion of 150 kb in the minimal DiGeorge/velocardiofacial syndrome critical region in mouse." Hum Mol Genet **8**(12): 2229-37.

Ko, L. J. and C. Prives (1996). "p53: puzzle and paradigm." Genes Dev **10**(9): 1054-72.

Komarov, P. G., E. A. Komarova, et al. (1999). "A chemical inhibitor of p53 that protects mice from the side effects of cancer therapy." Science **285**(5434): 1733-7.

Krizhanovsky, V. and S. W. Lowe (2009). "Stem cells: The promises and perils of p53." Nature **460**(7259): 1085-6.

Laptenko, O., Beckerman, R., et al. (2011). "p53 binding to nucleosomes within the p21 promoter in vivo leads to nucleosome loss and transcriptional activation." Proc Natl Acad Sci USA **108**(26): 10385-90.

Levine, A. J. (1997). "p53, the cellular gatekeeper for growth and division." Cell **88**(3): 323-31.

Levine, A. J. and M. Oren (2009). "The first 30 years of p53: growing ever more complex." Nat Rev Cancer **9**(10): 749-58.

Lim, D. S. and P. Hasty (1996). "A mutation in mouse rad51 results in an early embryonic lethal that is suppressed by a mutation in p53." Mol Cell Biol **16**(12): 7133-43.

Lindsay, E. A. (2001). "Chromosomal microdeletions: dissecting del22q11 syndrome." Nat Rev Genet **2**(11): 858-68.

Lindsay, E. A. and A. Baldini (2001). "Recovery from arterial growth delay reduces penetrance of cardiovascular defects in mice deleted for the DiGeorge syndrome region." Hum Mol Genet **10**(9): 997-1002.

Lindsay, E. A., A. Botta, et al. (1999). "Congenital heart disease in mice deficient for the DiGeorge syndrome region." Nature **401**(6751): 379-83.

Lindsay, E. A., R. Goldberg, et al. (1995). "Velo-cardio-facial syndrome: frequency and extent of 22q11 deletions." Am J Med Genet **57**(3): 514-22.

Lindsay, E. A., F. Vitelli, et al. (2001). "Tbx1 haploinsufficieny in the DiGeorge syndrome region causes aortic arch defects in mice." Nature **410**(6824): 97-101.

Ludwig, T., D. L. Chapman, et al. (1997). "Targeted mutations of breast cancer susceptibility gene homologs in mice: lethal phenotypes of Brca1, Brca2, Brca1/Brca2, Brca1/p53, and Brca2/p53 nullizygous embryos." Genes Dev **11**(10): 1226-41.

Lupski, J. R. (1998). "Genomic disorders: structural features of the genome can lead to DNA rearrangements and human disease traits." Trends Genet **14**(10): 417-22.

Macatee, T. L., B. P. Hammond, et al. (2003). "Ablation of specific expression domains reveals discrete functions of ectoderm- and endoderm-derived FGF8 during cardiovascular and pharyngeal development." Development **130**(25): 6361-74.

Masui, S., D. Shimosato, et al. (2005). "An efficient system to establish multiple embryonic stem cell lines carrying an inducible expression unit." Nucleic Acids Res **33**(4): e43.

Matsuoka, R., A. Takao, et al. (1994). "Confirmation that the conotruncal anomaly face syndrome is associated with a deletion within 22q11.2." Am J Med Genet **53**(3): 285-9.

McDonald-McGinn, D. M., B. S. Emanuel, et al. (1996). "Autosomal dominant "Opitz" GBBB syndrome due to a 22q11.2 deletion." Am J Med Genet **64**(3): 525-6.

McDonald-McGinn, D. M. and K. E. Sullivan (2011) "Chromosome 22q11.2 deletion syndrome (DiGeorge syndrome/velocardiofacial syndrome)." Medicine (Baltimore) **90**(1): 1-18.

Meletis, K., V. Wirta, et al. (2006). "p53 suppresses the self-renewal of adult neural stem cells." Development **133**(2): 363-9.

Merscher, S., B. Funke, et al. (2001). "TBX1 is responsible for cardiovascular defects in velo-cardio-facial/DiGeorge syndrome." Cell **104**(4): 619-29.

Mic, F.A., Molotkov, A. et al. (2000). Mech. Dev. **97**, 227-230.

Minguillon, C. and Logan, M. (2003). "The comparative genomics of T-box genes." Brief Funct Genomic Proteomic **2**(3): 224-33

Montes de Oca Luna, R., L. L. Amelse, et al. (1997). "Deletion of p21 cannot substitute for p53 loss in rescue of mdm2 null lethality." Nat Genet **16**(4): 336-7.

Montes de Oca Luna, R., D. S. Wagner, et al. (1995). "Rescue of early embryonic lethality in mdm2-deficient mice by deletion of p53." Nature **378**(6553): 203-6.

Moon, A. M., D. L. Guris, et al. (2006). "Crkl deficiency disrupts Fgf8 signaling in a mouse model of 22q11 deletion syndromes." Dev Cell **10**(1): 71-80.

Morgan, S. C., H. Y. Lee, et al. (2008). "Cardiac outflow tract septation failure in Pax3-deficient embryos is due to p53-dependent regulation of migrating cardiac neural crest." Mech Dev **125**(9-10): 757-67.

Mueller, I., R. Kobayashi, et al. (2010) "Effective and steady differentiation of a clonal derivative of P19CL6 embryonal carcinoma cell line into beating cardiomyocytes." J Biomed Biotechnol **2010**: 380561.

Murphy, K. C., L. A. Jones, et al. (1999). "High rates of schizophrenia in adults with velo-cardio-facial syndrome." Arch Gen Psychiatry **56**(10): 940-5.

Murphy, K. C. and M. J. Owen (2001). "Velo-cardio-facial syndrome: a model for understanding the genetics and pathogenesis of schizophrenia." Br J Psychiatry **179**: 397-402.

Niederreither, K., Vermot, J., et al. (2001) *Development (Cambridge, U.K.)* **128**, 1019-1031

Oh, J., D. H. Sohn, et al. (2008). "BAF60a interacts with p53 to recruit the SWI/SNF complex." J Biol Chem **283**(18): 11924-34.

Pane, L. S., Z. Zhang, et al. (2012) "Tbx1 is a negative modulator of Mef2c." Hum Mol Genet **21**(11): 2485-96.

Pani, L., M. Horal, et al. (2002). "Rescue of neural tube defects in Pax-3-deficient embryos by p53 loss of function: implications for Pax-3- dependent development and tumorigenesis." Genes Dev **16**(6): 676-80.

Papaioannou, V. E. (2001). "T-box genes in development: from hydra to humans." Int Rev Cytol **207**: 1-70.

Papangeli, I. and P. Scambler (2013) "The 22q11 deletion: DiGeorge and velocardiofacial syndromes and the role of TBX1." Wiley Interdiscip Rev Dev Biol **2**(3): 393-403.

Papolos, D. F., G. L. Faedda, et al. (1996). "Bipolar spectrum disorders in patients diagnosed with velo-cardio-facial syndrome: does a hemizygous deletion of chromosome 22q11 result in bipolar affective disorder?" Am J Psychiatry **153**(12): 1541-7.

Parisot, P., K. Mesbah, et al. (2011) "Tbx1, subpulmonary myocardium and conotruncal congenital heart defects." Birth Defects Res A Clin Mol Teratol **91**(6): 477-84.

Park, E. J., L. A. Ogden, et al. (2006). "Required, tissue-specific roles for Fgf8 in outflow tract formation and remodeling." Development **133**(12): 2419-33.

Park, E. J., Y. Watanabe, et al. (2008). "An FGF autocrine loop initiated in second heart field mesoderm regulates morphogenesis at the arterial pole of the heart." Development **135**(21): 3599-610.

Paylor, R., B. Glaser, et al. (2006). "Tbx1 haploinsufficiency is linked to behavioral disorders in mice and humans: implications for 22q11 deletion syndrome." Proc Natl Acad Sci U S A **103**(20): 7729-34.

Prall, O. W., M. K. Menon, et al. (2007). "An Nkx2-5/Bmp2/Smad1 negative feedback loop controls heart progenitor specification and proliferation." Cell **128**(5): 947-59.

Puech, A., B. Saint-Jore, et al. (2000). "Normal cardiovascular development in mice deficient for 16 genes in 550 kb of the velocardiofacial/DiGeorge syndrome region." Proc Natl Acad Sci U S A **97**(18): 10090-5.

Pulver, A. E., G. Nestadt, et al. (1994). "Psychotic illness in patients diagnosed with velo-cardio-facial syndrome and their relatives." J Nerv Ment Dis **182**(8): 476-8.

Randall, V., K. McCue, et al. (2009). "Great vessel development requires biallelic expression of Chd7 and Tbx1 in pharyngeal ectoderm in mice." J Clin Invest **119**(11): 3301-10.

Rivlin, N, Koifman, G, Rotter, V (2014). "p53 orchestrates between normal differentiation and cancer." Semin Cancer Biol. (Epub ahead of print)

Roberts, C., S. M. Ivins, et al. (2005). "Retinoic acid down-regulates Tbx1 expression in vivo and in vitro." Dev Dyn **232**(4): 928-38.

Rochais, F., K. Mesbah, et al. (2009). "Signaling pathways controlling second heart field development." Circ Res **104**(8): 933-42.

Ryckebusch, L., N. Bertrand, et al. (2010) "Decreased levels of embryonic retinoic acid synthesis accelerate recovery from arterial growth delay in a mouse model of DiGeorge syndrome." Circ Res **106**(4): 686-94.

Ryan AK, Goodship JA, et al. (1997) "Spectrum of clinical features associated with interstitial chromosome 22q11 deletions: a European collaborative study". J Med Genet. **34**(10):798-804.

Saga, Y., N. Hata, et al. (1996). "MesP1: a novel basic helix-loop-helix protein expressed in the nascent mesodermal cells during mouse gastrulation." Development **122**(9): 2769-78.

Sah, V. P., L. D. Attardi, et al. (1995). "A subset of p53-deficient embryos exhibit exencephaly." Nat Genet **10**(2): 175-80.

Scambler, P. J. (2000). "The 22q11 deletion syndromes." Hum Mol Genet **9**(16): 2421-2426.

Scambler, P. J. (2000). "The 22q11 deletion syndromes." Hum Mol Genet **9**(16): 2421-6.

Scambler, P. J., A. H. Carey, et al. (1991). "Microdeletions within 22q11 associated with sporadic and familial DiGeorge syndrome." Genomics **10**(1): 201-6.

Schmid, P., A. Lorenz, et al. (1991). "Expression of p53 during mouse embryogenesis." Development **113**(3): 857-65.

Schoenwolf, GC, Bleyl, SB et al. (2009) Francis-West: Larsen's human embryology. 4th ed.

Seidman, J. G., and C. Seidman (2002) "Transcription factor haploinsufficiency: when half a loaf is not enough." J. Clin. Invest. **109**: 451–455.

Shaikh, T. H., H. Kurahashi, et al. (2000). "Chromosome 22-specific low copy repeats and the 22q11.2 deletion syndrome: genomic organization and deletion endpoint analysis." Hum Mol Genet 9(4): 489-501.

Shprintzen, R. J. (2000). "Velo-cardio-facial syndrome: a distinctive behavioral phenotype." Ment Retard Dev Disabil Res Rev 6(2): 142-7.

Smith, J. (1997). "Brachyury and the T-box genes." Curr. Opin. Genet. Dev. 7(4): 474-80

Snider, P., M. Olaopa, et al. (2007). "Cardiovascular development and the colonizing cardiac neural crest lineage." ScientificWorldJournal 7: 1090-113.

Spring, K., F. Ahangari, S. P. Scott, P. Waring, D. M. Purdie et al. (2002). "Mice heterozygous for mutation in Atm, the gene involved in ataxia-telangiectasia, have heightened susceptibility to cancer." Nat. Genet. 32: 185–190.

Stoller JZ, et al. (2005). "Identification of a novel nuclear localization signal in Tbx1 that is deleted in DiGeorge syndrome patients harboring the 1223delC mutation." Hum Mol Genet 14:885–892

Swillen, A., K. Devriendt, et al. (1999). "The behavioural phenotype in velo-cardio-facial syndrome (VCFS): from infancy to adolescence." Genet Couns 10(1): 79-88.

Taddei, I., Morishima, M., et al. (2001). "Genetic factors are major determinants of phenotypic variability in a mouse model of the DiGeorge/del22q11 syndromes." Proc Natl Acad Sci USA 98(20): 11428-31

Tai, C.I. and Ying, Q.L. (2013). " Gbx2, a LIF/Stat3 target, promotes reprogramming to and retention of the pluripotent ground state." J Cell Sci 126(5): 1093-8

van den Hoff, M. J., A. F. Moorman, et al. (1999). "Myocardialization of the cardiac outflow tract." Dev Biol 212(2): 477-90.

van Weerd, J. H., K. Koshiba-Takeuchi, et al. (2011) "Epigenetic factors and cardiac development." Cardiovasc Res 91(2): 203-11.

Venkatachalam, S., Stuart, DT et al. (2001). " Is *p53* Haploinsufficient for Tumor Suppression? Implications for the $p53^{+/-}$ Mouse Model in Carcinogenicity Testing." Toxicol Pathol 29: 147-154

Vermot, J., K. Niederreither, et al. (2003). "Decreased embryonic retinoic acid synthesis results in a DiGeorge syndrome phenotype in newborn mice." Proc Natl Acad Sci U S A 100(4): 1763-8.

Vincent, S. D. and M. E. Buckingham (2010) "How to make a heart: the origin and regulation of cardiac progenitor cells." Curr Top Dev Biol 90: 1-41.

Vitelli, F., G. Lania, et al. (2010) "Partial rescue of the Tbx1 mutant heart phenotype by Fgf8: genetic evidence of impaired tissue response to Fgf8." J Mol Cell Cardiol 49(5): 836-40.

Vitelli, F., M. Morishima, et al. (2002). "Tbx1 mutation causes multiple cardiovascular defects and disrupts neural crest and cranial nerve migratory pathways." Hum Mol Genet 11(8): 915-22.

Vitelli, F., I. Taddei, et al. (2002). "A genetic link between Tbx1 and fibroblast growth factor signaling." Development 129(19): 4605-11.

Vitelli, F., Viola, A., Morishima, M. et al. (2003). " TBX1 is required for inner ear morphogenesis." Hum Mol Genet. 12(16): 2041-8

Vousden, K. H. and D. P. Lane (2007). "p53 in health and disease." Nat Rev Mol Cell Biol 8(4): 275-83.

Waldo, K. L., D. H. Kumiski, et al. (2001). "Conotruncal myocardium arises from a secondary heart field." Development 128(16): 3179-88.

Wang, J., S. B. Greene, et al. (2010) "Bmp signaling regulates myocardial differentiation from cardiac progenitors through a MicroRNA-mediated mechanism." Dev Cell 19(6): 903-12.

Wassarman, KM, Lewandoski, M et al., 1997. "Specification of the anterior hindbrain and establishment of a normal mid/ hindbrain organizer is dependent on Gbx2 gene function." Development 124(15): 2923-34

Watanabe, Y., S. Zaffran, et al. (2012) "Fibroblast growth factor 10 gene regulation in the second heart field by Tbx1, Nkx2-5, and Islet1 reveals a genetic switch for down-regulation in the myocardium." Proc Natl Acad Sci U S A 109(45): 18273-80.

Xu, H., F. Cerrato, et al. (2005). "Timed mutation and cell-fate mapping reveal reiterated roles of Tbx1 during embryogenesis, and a crucial function during segmentation of the pharyngeal system via regulation of endoderm expansion." Development 132(19): 4387-95.

Xu, H., M. Morishima, et al. (2004). "Tbx1 has a dual role in the morphogenesis of the cardiac outflow tract." Development **131**(13): 3217-27.

Yagi, H, et al. (2003). "Role of TBX1 in human del22q11.2 syndrome." Lancet. Oct 25;362(9393):1366-73.

Yang, Y., C. Wang, et al. (2013) "Polycomb group protein PHF1 regulates p53-dependent cell growth arrest and apoptosis." J Biol Chem **288**(1): 529-39.

Zambrowicz, B. P., A. Imamoto, et al. (1997). "Disruption of overlapping transcripts in the ROSA beta geo 26 gene trap strain leads to widespread expression of beta-galactosidase in mouse embryos and hematopoietic cells." Proc Natl Acad Sci U S A **94**(8): 3789-94.

Zhang, Z. and A. Baldini (2010) "Manipulation of endogenous regulatory elements and transgenic analyses of the Tbx1 gene." Mamm Genome **21**(11-12): 556-64.

Zhang, Z. and A. Baldini (2008). "In vivo response to high-resolution variation of Tbx1 mRNA dosage." Hum Mol Genet **17**(1): 150-7.

Zhang, Z., F. Cerrato, et al. (2005). "Tbx1 expression in pharyngeal epithelia is necessary for pharyngeal arch artery development." Development **132**(23): 5307-15.

Zhang, Z., T. Huynh, et al. (2006). "Mesodermal expression of Tbx1 is necessary and sufficient for pharyngeal arch and cardiac outflow tract development." Development **133**(18): 3587-95.

Zweier C, et al. (2007). "Human TBX1 missense mutations cause gain of function resulting in the same phenotype as 22q11.2 deletions." Am J Hum Genet. Mar;80(3):510-7.

ACKNOWLEDGMENTS

Eccomi qui, ancora una volta, alle prese con i ringraziamenti dopo la stesura di una tesi che, nonostante tutto, ho avuto il piacere di portare a termine. Senza la possibilità che mi è stata data di svolgere il mio PhD, di portare avanti il mio progetto nel migliore dei modi, con le migliori risorse e con la totale fiducia, non sarei mai giunta a questo punto, quindi il mio primo ringraziamento va ad Antonio Baldini. Grazie per aver sempre avuto fiducia in me, nel mio lavoro, nelle mie potenzialità, nella mia passione, nata prima di cominciare la tesi di laurea nel tuo lab, ma cresciuta in maniera esponenziale durante tutto il mio percorso.

Gabry (mamylab), un grandissimo e sentito GRAZIE va a te, alla mi amica, alla mia sorella, alla mia collega, alla mia guida scientifica...grazie per le innumerevoli discussioni scientifiche e non (servono spesso anche quelle), grazie per i tuoi insegnamenti, per i tuoi consigli, per i dubbi che spesso mi hai fatto nascere, per avermi spinto a volte a fare di piu' per convincerti dei miei risultati...e' stato piacevole trascorrere lo scorso 1 Novembre con te in lab e vedere quel risultato a cui non credevi! E' stato piacevole trascorrere ogni singolo giorno, di questi 8 anni, con te accanto!

Compagna di sventure, Pia, collega di PhD, amica, sorella, quante ne abbiamo passate questi 4 anni dietro questo dottorato!?! Siamo state dal primo momento unite, nel bene e nel male (specialmente nel male!), dal giorno in cui ti vidi fuori lo studio di Elizabeth, e da li' e' nata la nostra grande amicizia. Grazie per avermi molto spesso sopportato, supportato ed ascoltato...parlavo sempre io del mio lavoro, trascurando a volte il tuo, ma poi ho recuperato...finalmente ho visto i tuoi ottimi risultati dal vivo ☺ !

Marca, un particolare grazie va anche a te...non mi sopporti piu', lo so! Tranquilla, ho finito di scrivere! Che bello pero' quest'ultimo periodo...il caffe' preso la mattina insieme a te ha tutto un altro sapore! Le ramanzine prese insieme a te hanno tutto un altro valore! Grazie per

avermi sopportato in questi ultimi mesi, tra il lavoro da pubblicare e la tesi da scrivere sono arrivata al punto di non sopportarmi neanch' io! Sara' piacevole averti accanto a me quando ritornero' al mio adorato banco (mi manchi!).

Chi c'e' ancora...ma quante siamo?? Mi sto dilungando troppo.

Rosa, Saretta, Gemma, Gabriellina, Vale, Elizabeth, grazie anche a voi, al vostro aiuto tecnico, Rosa e Gabriellina, grazie a tutte voi per l'aiuto scientifico, per le discussioni, domande, perplessita'. Quanti bei congressi abbiamo condiviso, Sara e Gabriellina, sono state esperienze che portero' sempre con me!

Non posso non ringraziare te, questa volta un uomo che non fa parte del lab, ovviamente, perche', oltre Antonio, il nostro lab e' composto da sole DONNE!! Grazie Ciro. Lo so che e' stata dura condividere questi 5 anni con me ed il mio amante (il lab!), specialmente in quest'ultimo periodo; lo so che mi sono sempre giustificata dicendo "questo e' un momento particolare", ma ti prometto che ce la mettero' tutta per organizzare il mio tempo, il mio lavoro, la mia vita nel migliore dei modi. Grazie per la tua tolleranza, per la tua comprensione, per ascoltare sempre tutto quello che ti racconto sul lab, gli esperimenti, i risultati, grazie per le discussioni scientifiche che spesso ho anche con te.

Infine, ma non per ultima, ringrazio la mia adorata famiglia, grazie mamma e papa', grazie Aldo e Sergio per aver sempre creduto in me e per essere fieri della vostra figlia e sorella!

Dimenticavo, ringrazio ancora, tanto, quegli animaletti innocenti, pelosi, con la codina lunga ed il visino dolce...i miei topini! Grazie per aver sacrificato la vostra vita per la scienza!